THE EFFECTS OF GLUCOSE IN TRANSIENT FOREBRAIN ISCHEMIA AS STUDIED USING *IN VIVO* NUCLEAR MAGNETIC RESONANCE SPECTROSCOPY

BY

RANDY LEE TYSON

A thesis
Submitted to the Faculty of Graduate Studies
in Partial Fulfillment of the Requirements
for the Degree of

Doctor of Philosophy

Department of Chemistry
University of Manitoba
Winnipeg, Manitoba

ISBN 0-612-16346-6

Name _____

Dissertation Abstracts International and *Masters Abstracts International* are arranged by broad, general subject categories. Please select the one subject which most nearly describes the content of your dissertation or thesis. Enter the corresponding four-digit code in the spaces provided.

BIOLOGICAL SCIENCES - BIOLOGY; NEUROSCIENCE
SUBJECT TERM

0317
SUBJECT CODE

UMI

Subject Categories

THE HUMANITIES AND SOCIAL SCIENCES

COMMUNICATIONS AND THE ARTS
Architecture 0729
Art History 0377
Cinema 0900
Dance 0378
Fine Arts 0357
Information Science 0723
Journalism 0391
Library Science 0399
Mass Communications 0708
Music 0413
Speech Communication 0459
Theater 0465

EDUCATION
General 0515
Administration 0514
Adult and Continuing 0516
Agricultural 0517
Art 0273
Bilingual and Multicultural 0282
Business 0688
Community College 0275
Curriculum and Instruction 0727
Early Childhood 0518
Elementary 0524
Finance 0277
Guidance and Counseling 0519
Health 0680
Higher 0745
History of 0520
Home Economics 0278
Industrial 0521
Language and Literature 0279
Mathematics 0280
Music 0522
Philosophy of 0998
Physical 0523
Psychology 0525
Reading 0535
Religious 0527
Sciences 0714
Secondary 0533
Social Sciences 0534
Sociology of 0340
Special 0529
Teacher Training 0530
Technology 0710
Tests and Measurements 0288
Vocational 0747

LANGUAGE, LITERATURE AND LINGUISTICS
Language
- General 0679
- Ancient 0289
- Linguistics 0290
- Modern 0291

Literature
- General 0401
- Classical 0294
- Comparative 0295
- Medieval 0297
- Modern 0298
- African 0316
- American 0591
- Asian 0305
- Canadian (English) 0352
- Canadian (French) 0355
- English 0593
- Germanic 0311
- Latin American 0312
- Middle Eastern 0315
- Romance 0313
- Slavic and East European 0314

PHILOSOPHY, RELIGION AND THEOLOGY
Philosophy 0422
Religion
- General 0318
- Biblical Studies 0321
- Clergy 0319
- History of 0320
- Philosophy of 0322

Theology 0469

SOCIAL SCIENCES
American Studies 0323
Anthropology
- Archaeology 0324
- Cultural 0326
- Physical 0327

Business Administration
- General 0310
- Accounting 0272
- Banking 0770
- Management 0454
- Marketing 0338

Canadian Studies 0385
Economics
- General 0501
- Agricultural 0503
- Commerce-Business 0505
- Finance 0508
- History 0509
- Labor 0510
- Theory 0511

Folklore 0358
Geography 0366
Gerontology 0351
History
- General 0578
- Ancient 0579
- Medieval 0581
- Modern 0582
- Black 0328
- African 0331
- Asia, Australia and Oceania 0332
- Canadian 0334
- European 0335
- Latin American 0336
- Middle Eastern 0333
- United States 0337

History of Science 0585
Law 0398
Political Science
- General 0615
- International Law and Relations 0616
- Public Administration 0617

Recreation 0814
Social Work 0452
Sociology
- General 0626
- Criminology and Penology 0627
- Demography 0938
- Ethnic and Racial Studies 0631
- Individual and Family Studies 0628
- Industrial and Labor Relations 0629
- Public and Social Welfare 0630
- Social Structure and Development 0700
- Theory and Methods 0344

Transportation 0709
Urban and Regional Planning 0999
Women's Studies 0453

THE SCIENCES AND ENGINEERING

BIOLOGICAL SCIENCES
Agriculture
- General 0473
- Agronomy 0285
- Animal Culture and Nutrition 0475
- Animal Pathology 0476
- Food Science and Technology 0359
- Forestry and Wildlife 0478
- Plant Culture 0479
- Plant Pathology 0480
- Plant Physiology 0817
- Range Management 0777
- Wood Technology 0746

Biology
- General 0306
- Anatomy 0287
- Biostatistics 0308
- Botany 0309
- Cell 0379
- Ecology 0329
- Entomology 0353
- Genetics 0369
- Limnology 0793
- Microbiology 0410
- Molecular 0307
- Neuroscience 0317
- Oceanography 0416
- Physiology 0433
- Radiation 0821
- Veterinary Science 0778
- Zoology 0472

Biophysics
- General 0786
- Medical 0760

EARTH SCIENCES
Biogeochemistry 0425
Geochemistry 0996
Geodesy 0370
Geology 0372
Geophysics 0373
Hydrology 0388
Mineralogy 0411
Paleobotany 0345
Paleoecology 0426
Paleontology 0418
Paleozoology 0985
Palynology 0427
Physical Geography 0368
Physical Oceanography 0415

HEALTH AND ENVIRONMENTAL SCIENCES
Environmental Sciences 0768
Health Sciences
- General 0566
- Audiology 0300
- Chemotherapy 0992
- Dentistry 0567
- Education 0350
- Hospital Management 0769
- Human Development 0758
- Immunology 0982
- Medicine and Surgery 0564
- Mental Health 0347
- Nursing 0569
- Nutrition 0570
- Obstetrics and Gynecology 0380
- Occupational Health and Therapy 0354
- Ophthalmology 0381
- Pathology 0571
- Pharmacology 0419
- Pharmacy 0572
- Physical Therapy 0382
- Public Health 0573
- Radiology 0574
- Recreation 0575
- Speech Pathology 0460
- Toxicology 0383

Home Economics 0386

PHYSICAL SCIENCES
Pure Sciences
Chemistry
- General 0485
- Agricultural 0749
- Analytical 0486
- Biochemistry 0487
- Inorganic 0488
- Nuclear 0738
- Organic 0490
- Pharmaceutical 0491
- Physical 0494
- Polymer 0495
- Radiation 0754

Mathematics 0405
Physics
- General 0605
- Acoustics 0986
- Astronomy and Astrophysics 0606
- Atmospheric Science 0608
- Atomic 0748
- Electronics and Electricity 0607
- Elementary Particles and High Energy 0798
- Fluid and Plasma 0759
- Molecular 0609
- Nuclear 0610
- Optics 0752
- Radiation 0756
- Solid State 0611

Statistics 0463

Applied Sciences
Applied Mechanics 0346
Computer Science 0984
Engineering
- General 0537
- Aerospace 0538
- Agricultural 0539
- Automotive 0540
- Biomedical 0541
- Chemical 0542
- Civil 0543
- Electronics and Electrical 0544
- Heat and Thermodynamics 0348
- Hydraulic 0545
- Industrial 0546
- Marine 0547
- Materials Science 0794
- Mechanical 0548
- Metallurgy 0743
- Mining 0551
- Nuclear 0552
- Packaging 0549
- Petroleum 0765
- Sanitary and Municipal 0554
- System Science 0790

Geotechnology 0428
Operations Research 0796
Plastics Technology 0795
Textile Technology 0994

PSYCHOLOGY
General 0621
Behavioral 0384
Clinical 0622
Developmental 0620
Experimental 0623
Industrial 0624
Personality 0625
Physiological 0989
Psychobiology 0349
Psychometrics 0632
Social 0451

THE UNIVERSITY OF MANITOBA

FACULTY OF GRADUATE STUDIES

COPYRIGHT PERMISSION

THE EFFECTS OF GLUCOSE IN TRANSIENT FOREBRAIN ISCHEMIA AS STUDIED USING IN VIVO NUCLEAR MAGNETIC RESONANCE SPECTROSCOPY

BY

RANDY LEE TYSON

A Thesis/Practicum submitted to the Faculty of Graduate Studies of the University of Manitoba in partial fulfillment of the requirements for the degree of

DOCTOR OF PHILOSOPHY

pI hereby declare that I am the sole author of this thesis.

I authorize the University of Manitoba to lend this thesis to other institutions or individuals for the purpose of scholarly research.

Randy Lee Tyson

I further authorize the University of Manitoba to reproduce this thesis by photocopying or other means, in total or in part, at the request of other institutions or individuals for the purpose of scholarly research.

Randy Lee Tyson

The University of Manitoba requires the signatures of all persons using or photocopying this thesis. Please sign below, and give address and date.

ABSTRACT

Damage due to cerebral ischemia is known to be increased by hyperglycemia and decreased with mild hypoglycemia. *In vivo* ^{31}P, ^{23}Na and ^{1}H NMR spectroscopy was used to explore various aspects of metabolic disturbances caused by transient global ischemia (10 min duration, bilateral carotid artery occlusion with concurrent hypotension).

^{31}P nuclear magnetic resonance spectroscopy was used to follow changes in cerebral pH and high-energy phosphate metabolites during forebrain ischemia in hypo-, normo- and hyperglycemic rats, and during reperfusion in animals in which the blood glucose level was altered post-ischemia. During ischemia, the decrease in tissue pH was found to be dependent on the pre-ischemia blood glucose concentration, being greatest in hyperglycemic and least in hypoglycemic animals. The increase of P_i, a consequence of the hydrolysis of high-energy phosphate metabolites, also depended on the blood glucose concentration, being greatest in hypoglycemic and least in hyperglycemic animals. ATP and PCr decreased more rapidly in hypoglycemic rats compared to normo- or hyperglycemic animals, which showed no differences in the rates of depletion. Post-ischemia hyperglycemia resulted in delayed recovery of tissue pH in all groups and of PCr and ATP in animals hyperglycemic throughout the experiment. Insulin administration immediately following ischemia increased the rate of recovery of pH, ATP and PCr in hyperglycemic animals. ATP remained significantly below pre-ischemia level in all subgroups at 1 hr post-ischemia, while PCr was lower than it was pre-ischemia only in those subgroups hyperglycemic prior to and/or following ischemia.

Intracellular sodium $[Na^+]_i$, as measured using double-quantum ^{23}Na NMR spectroscopy, increased during ischemia to 210% of pre-ischemia level in all rats, but a delay in this increase was observed in normo- and hyperglycemic animals. The rate of $[Na^+]_i$ increase was fastest in hypo- and slowest in hyperglycemic rats. During reperfusion, $[Na^+]_i$ recovered rapidly in hypo- and normoglycemic rats, while in hyperglycemic animals recovery was slow. Tissue sodium content, measured using single-quantum ^{23}Na NMR spectroscopy, increased to 117% of pre-ischemia level in hypo- and to 107% in normo- and hyperglycemic animals during reperfusion. The slower increase in $[Na^+]_i$ during forebrain ischemia in rats with higher blood glucose levels suggests that Na^+ homeostasis is maintained longer in

these animals. On reperfusion, the slower recovery of sodium homeostasis may contribute to the increased neuronal injury following cerebral ischemia in hyperglycemic animals.

The level of glycemia during ischemia also has long term effects on tissue metabolism. The times following ischemia when a depression in both ATP turnover rate (given by the forward creatine kinase rate constant, measured using saturation transfer ^{31}P NMR spectroscopy) and glycolytic capacity (given by the agonal glycolytic rate constant, measured using STEAM localized ^{1}H NMR spectroscopy) is dependent on the blood glucose level during ischemia. The post-ischemia depression in the cerebral metabolic rate of glucose seen elsewhere [Pulsinelli, 1982b; Kozuka, 1989; Triolo, 1990; Katsura, 1994] is not due to damage to enzymes in the glycolytic pathway, nor are its effects observed in ATP turnover within the first 24 hr of reperfusion. The further depression in post-ischemia cerebral metabolic rate of glucose caused by hyperglycemia may be due to the decrease in glycolytic capacity, either through damage to enzymes in the pathway or in glucose transport.

TABLE OF CONTENTS

TABLE OF FIGURES

TABLE OF TABLES

TABLE OF ABBREVIATIONS

ABP = arterial blood pressure

ADP = adenosine diphosphate

AGR = agonal glycolytic rate

3',5'-cyclic AMP = 3',5'-cyclic adenosine monophosphate

5'-AMP = adenosine-5'- monophosphate

ATP = adenosine triphosphate

BBB = blood-brain barrier

CBF = cerebral blood flow

CCA = common carotid artery

CK = creatine kinase

CMR_g = cerebral metabolic rate of glucose consumption

CSF = cerebral-spinal fluid

DQ = double quantum

EEG = electroencephalogram

hypo = hypoglycemia

hyper = hyperglycemia

I_∞^i = intensity of the double quantum signal at infinity during ischemia

I_∞^p = intensity of the double quantum signal at infinity following reperfusion

I_0^p = intensity of the double quantum signal at the beginning of reperfusion

I_{rec}^p = intensity of the overshoot recovery of the double quantum signal following reperfusion

k_{AGR} = agonal glycolytic rate constant

k_{DQ}^p = rate constant for the decrease in the double quantum signal after reperfusion

k_{DQ}^i = rate constant for the increase of the double quantum signal during ischemia

k_{for} = rate constant for the forward creatine kinase reaction

k_{DQ}^p = rate constant for the overshoot recovery the double quantum in signal

$\mathbf{M}_{0,PCr}$ = magnetization of the PCr resonance at steady-state

$\mathbf{M}_{PCr}(\tau)$ = magnetization of the PCr at γ-ATP saturation time τ

Mi-CK = mitochondrial creatine kinase

NAA = N-acetyl aspartate

$NADP^+$, NADPH = nicotinamide adenine dinucleotide phosphate

$[Na^+]_i$ = intracellular sodium concentration

$[Na^+]_t$ = tissue sodium concentration

NGF = nerve growth factor

NMR = nuclear magnetic resonance

P_i = inorganic phosphate

PCr = phosphocreatine

SQ = single quantum

τ = γ-ATP saturation time

$T_{1,PCr}$ = PCr longitudinal relaxation time

ACKNOWLEDGEMENTS

I would like to thank the many people who aided me in performing the experiments described herein, including Dr. Richard Buist (who helped run the experiments at the spectrometer end), Maureen Donnelly, Mark Campbell, Drs. Fang Wei Yang and Yan Fan Yang (who helped in animal preparation). Thanks also goes to Drs. Jim Peeling and Garnette Sutherland for their guidance when direction was lacking and keeping my nose pointed towards the light at the end of the tunnel. My personal thanks also to the Manitoba Health Research Council and the Canadian Heart and Stroke Society for their financial support.

INTRODUCTION

Cerebrovascular disease is a major medical problem, affecting 15,000 people in Canada (7% of all deaths), 67,000 hospital discharges and 3.2 million hospitalization days in 1991 [Petrasovits, 1994]. The mechanisms of damage resulting from temporary loss of blood flow to regions of the brain, as in stroke, or the whole brain, resulting from cardiac arrest, are not clearly understood. In particular, following short-duration global ischemia (5-20 min), resulting from a complete stoppage of blood flow to the whole brain, only certain selectively vulnerable populations of neurons die. These neurons do not die immediately, but only after 2-7 days following the event, a phenomenon known as delayed neuronal death. Again, the mechanisms of damage in these selectively vulnerable regions is not clearly understood, but these regions tend to have high densities of excitatory neurotransmitter receptors.

Increased blood glucose at the time of ischemia increases damage to these regions and as well increases the number of regions affected and depresses an already low cerebral metabolic rate further than does normoglycemic ischemia [De Courten-Meyers, 1988; Nedergaard, 1987a; Pulsinelli, 1982a; Vazquez-Cruz, 1990; Yip, 1991]. On the other hand, the lowering of blood glucose decreases the amount of damage due to ischemia [Le May, 1988; Nedergaard, 1987b; Strong, 1990; Voll, 1989, 1991a].

Cerebral metabolic recovery following short-duration forebrain ischemia is also strongly mediated by blood glucose level, affecting, among other cellular processes, high-energy phosphate metabolism, maintenance of membrane ion gradients [Hansen, 1978] and energy-producing enzyme systems [Katsura, 1989; Kozuka, 1989; Pulsinelli, 1982b; Triolo, 1990]. Herein, a number of NMR spectroscopic techniques were used to observe the early recovery of high-energy phosphate metabolism and membrane ion gradients and the long term effects on glycolysis and ATP turnover rate.

A. Brain Metabolism

1. *Transport of glucose from blood*

The brain uses 80% of glucose taken in by the body [Schienberg, 1965]. For neurons and glia to have ready access to glucose, glucose must first be transported from blood across the endothelial cells lining brain capillaries. These cells in brain are unique in that they form very tight junctions, lacking fenestrae and vesicles. This so-called 'blood-brain barrier' (BBB) was hypothesized at the end of the 1800's, it being noted that the transfer of acid dyes into brain was strongly impeded [Ehrlich, 1885]. Transport of glucose is facilitated by a sodium-independent transporter known as Glut-1 [Thorens, 1990]. Essentially 100% of glucose in brain crosses the blood-brain barrier via the Glut-1 transporter [Pardridge, 1990]. Other carriers exist for various classes of compounds, examples of which are given in table 1.

Once glucose has crossed the BBB, it must pass through the cell membranes of glia and neurons into the cytosol. In astrocytes the transporters which accomplish this are the Glut-1 and Glut-3 transporters [Medings, 1990]. The activity of the Glut-3 transporter is unaffected by insulin, unlike the Glut-1 transporter, in which activity is increased with insulin administration. Interestingly, an increase in Glut-1 mRNA levels is not associated with an increase in glucose uptake, as measured using 2-deoxyglucose.

Table 1. Blood-brain barrier nutrient and thyroid hormone carriers [Pardridge, 1988].

Carrier	Representative Substrate	K_m (μM)	V_{max} (nmol/min/g)
Hexose	Glucose	11000±1400	1420±140
Monocarboxylic acid	Lactic acid	1800±600	91±35
Neutral amino acid	Phenylalanine	26±6	22±4
Amine	Choline	340±70	11±1
Basic amino acid	Arginine	40±24	5±3
Nucleoside	Adenosine	25±3	0.75±0.08
Purine base	Adenine	11±3	0.50±0.09
Thyroid hormone	Triiodothyronine	1.7±0.7	0.19±0.08

Also, Glut-1 exists in two forms with molecular masses of 55 kDa and 45 kDa. These two forms are encoded by the same gene, but differ in their extent of glycosylation [Birnbaum, 1986; Kasaniki, 1987]. The reasons for these differences and the difference in function of these two types of the same transporter remain unclear. The transporter for glucose in neuronal membranes is not known. *In vitro* experiments have shown that the Glut-1 protein is present in glial cells but is not expressed in neurons [Weimer, 1989; Sadiq, 1990]. Pronounced changes in Glut-1 expression during rat brain development occurs [Pardridge, 1990], pointing to the possibility that another glucose transporter is present. This unknown transporter may be Glut-3, since it occurs at high levels in brain [Bell, 1990] and is localized primarily in neurons [Mantych, 1992]. While it cannot be ruled out that another glucose transporter may be present in brain which causes these developemental changes, the other known glucose transporters (Glut-2, Glut-4 and Glut-5) are essentially non-existent in brain [Bell, 1990].

2. *Glucose and Normal Brain Metabolism*

The brain accounts for 20% of all oxygen used in the body, despite being only 2% of the total body weight. To meet this high metabolic demand, normal, non-hypoglycemic brain uses almost to exclusion glucose as the precursor for all of its energy demands. This contrasts with other organs which can use a variety of compounds for energy production. From measurements in the arteriovenous differences of various compounds in adult humans, only glucose and oxygen [Sokoloff, 1960] significantly change. Further evidence for the importance of glucose is indicated from the finding that the only product released in large amounts is carbon dioxide.

Hypoglycemia, induced by either hepatectomy or the administration of insulin, results in cerebral dysfunction ranging from mild behavioral impairment to coma. These effects can be reversed by the administration of glucose, maltose (which is hydrolyzed to glucose) and mannose (which is phosphorylated and converted to fructose-6-phosphate, an intermediate in the glycolysis pathway).

In contrast to glucose, not all oxygen consumed is used for energy production in brain. Various oxidases and hydroxylases require oxygen for the synthesis and metabolism of neurotransmitters, neuromodulators and other compounds.

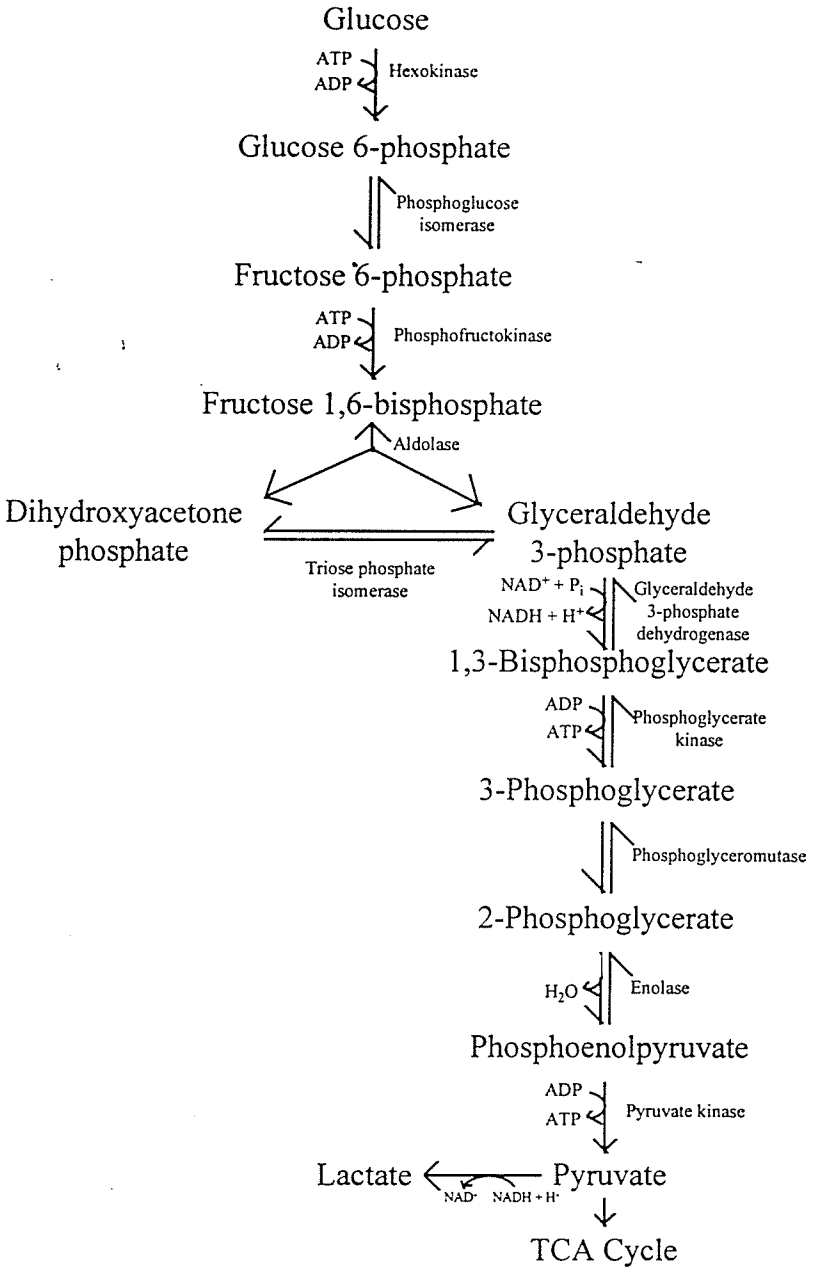

Figure 1. Reactions of the Embden-Meyerhoff pathway. From [Voet, 1990].

The effects of hypoglycema can be reversed by the administration of glucose, maltose (which is hydrolyzed to glucose) or mannose (which phosphorylated and enters the glycolytic pathway as fructose-6-phosphate) [Sokoloff, 1960]. The administration of lactate, pyruvate or glutamate does not reverse the effects of hypoglycemia on the central nervous system [Sokoloff, 1960]. These data show that only aerobic utilization of glucose provides sufficient energy for maintenance of neuronal function, and that glucose is an obligatory (not just a preferred) substrate.

Figure 1 shows a schematic overview of the glycolytic pathway (the following discussion of glycolysis is taken from [Voet, 1990; Siegel, 1994]). Glucose is first converted to glucose 6-phosphate through phosphorylation by hexokinase. This reaction is essentially irreversible and is a key point in the regulation of carbohydrate metabolism in brain. The hexokinase in brain is mostly the electrophoretically slow-moving (type 1) isoenzyme and exists both in the cytosol (soluble) and firmly attached to mitochondria, the relative amounts of each pool being in equilibrium. Binding to mitochondria alters the kinetics of phosphorylation and its inhibition by the product glucose 6-phosphate in such a way that the bound-type is more active. The extent of binding is dependent on the [ATP]/[ADP] ratio, so that metabolic demand regulates the bound fraction of hexokinase. Thus, ATP functions both as a substrate of the enzyme and, at another site, as a regulator to decrease ATP production through its influence on the fraction of bound hexokinase.

In addition to its influence on inhibiting hexokinase, glucose 6-phosphate aids in solubilizing hexokinase, further reducing the efficiency of phosphorylation. Thus, a number of mechanisms are available for fine-tuning the activity of the initial step of glycolysis in response to changes in the cellular environment. Glucose 6-phosphate is also a substrate for the pentose phosphate and glycogen-forming pathways.

Approximately 5-8% of the glucose 6-phosphate produced by the initial reaction of the glycolytic pathway is used as the substrate for the pentose phosphate pathway in adult monkey brain and 2-3% in rat brain [Gaintonde, 1983]. The pentose phosphate pathway provides NADPH for reductive biosynthesis and ribose-5-phosphate for nucleotide and nucleic acid biosynthesis [Siegel, 1983]. Two reaction sequences in this pathway form a cycle in which the first metabolizes three molecules of glucose-6-phosphate to three

molecules of CO_2, six molecules of NADPH and one molecule of glyceraldehyde-3-phosphate. The second sequence regenerates two molecules of glucose-6-phosphate or fructose-6-phosphate. The energy produced in this pathway is not ATP, as in glycolysis or the TCA cycle, but in the reducing power of NADPH. The pentose phosphate pathway also provides pentose for nucleotide synthesis. The flux of the pentose phosphate pathway is regulated by glucose 6-phosphate, NADP, glyceraldehyde 3-phosphate and fructose 6-phosphate.

The next step in glycolysis is the conversion of glucose 6-phosphate to fructose 6-phosphate in a reversible fashion by phosphohexose isomerase, maintaining a [glucose 6-phosphate]/[fructose 6-phosphate] ratio of 5:1. Fructose 6-phosphate, along with ATP, serve as the substrates for phosphofructokinase to form fructose 1,6-diphosphate. This is an irreversible reaction, a characteristic of regulatory reactions. The activity of phosphofructokinase is modulated by a large number of metabolites and cofactors, the concentrations of which under different metabolic conditions greatly influence the glycolytic flux. Most important of these is the availability of inorganic phosphate (P_i) and citrate. This enzyme is inhibited by ATP, Mg^{+2} and citrate and is stimulated by NH_4^+, K^+, P_i, 5'-AMP, 3',5'-cyclic AMP, ADP and fructose 1,6-diphosphate. The effects of NH_4^+, P_i and AMP are additive, acting at several different allosteric sites on the enzyme. The inhibition by citrate implies an end-product inhibition of glycolysis. NH_4^+, a product of amino acid and amine metabolism, is controlled by transamination reactions (coupled to TCA cycle intermediates, glutamic dehydrogenase and glutamine synthase) by causing stimulation of glycolysis. This raises the pyruvate and α-ketoglutarate levels, thereby reducing NH_4^+ levels.

Fructose 1,6-diphosphate is then split by brain aldolase to glyceraldehyde 3-phosphate and dihydroxyacetone phosphate. Dihydroxyacetone phosphate is the substrate for both glycerophosphate dehydrogenase, used in NADH oxidation and lipid pathways, and triose phosphate isomerase, which maintains the equilibrium between glyceraldehyde 3-phosphate and dihydroxyacetone phosphate. While the equilibrium in the triose phosphate isomerase strongly favors accumulation of dihydroxyacetone phosphate, the effective removal of glyceraldehyde 3-phosphate cause the conversion of dihydroxyacetone

phosphate to glyceraldehyde 3-phosphate. Hence, one molecule of fructose 1,6-diphosphate yields two molecules of glyceraldehyde 3- phosphate.

Brain enolase catalyzes the dehydration of 2-phosphoglycerate to phosphoenolpyruvate. This enzyme is present as two related dimers, one of which, the γ type, is typically found in neurons and the other, the α type, is localized to glia. Phosphoenolpyruvate kinase requires not only Mg^{+2}, as in other regulatory enzymes, but also Na^{+} or K^{+} as well.

Glycolysis in brain produces lactate even at rest and when well-oxygenated. Lactate is then transported to blood. The amount of lactate produced corresponds to about 13% of the pyruvate produced by glycolysis. Five isoenzymes of lactate dehydrogenase are present in adult brain, with the one that moves electrophoretically fastest (toward the anode) being the most predominant. The activities of the various isoenzymes and their distribution in various brain regions may be controlled by oxygen levels in tissues. This enzyme serves in the cytoplasm to oxidize NADH, which accumulates through the action of glyceraldehyde phosphate dehydrogenase. This permits the continued production of ATP even in the absence of oxygen, since NADH cannot penetrate the mitochondrial membrane easily. The oxidation of NADH in the cytoplasm depends on this reaction and on the activity of shuttle mechanisms transferring reducing equivalents to the mitochondria. Glycerol phosphate dehydrogenase also participates in the oxidation of NADH by reducing dihydroxyacetone phosphate to glycerol 3-phosphate. Under conditions of hypoxia, the levels of α-ketoglutarate and lactate increase at similar rates, though the amount of lactate is much higher.

3. *Agonal Glycolysis*

Under the condition of complete blood flow stoppage, a sharp increase (by approximately an order of magnitude) occurs in the rate of glycolysis as brain tissue attempts to meet its metabolic demands in the absence of oxidative phosphorylation [Petroff, 1988]. The rate-controlling enzymes are strongly stimulated by rapidly decreasing ATP and increasing ADP and P_i. Glycolysis in brain can be considered to be a closed system under these conditions, since neither O_2 nor glucose can enter, lactate cannot be cleared and the lack of O_2 ensures that glycolytic intermediates are not used by, for instance, the TCA

cycle. The maximum rate of lactate accumulation yields an estimate of the agonal glycolytic rate (AGR). AGR gives an indication of the metabolic conditions at the time of circulatory arrest.

The amount of lactate accumulation is dependent on the glucose available at circulatory arrest and the time course of this increase follows first-order kinetics [Nilsson, 1975]. The first-order rate constant, k_{AGR}, gives an overall measure of ability of glycolysis to produce lactate from glucose. The measured rate constant can be influenced by a number of factors, and has been shown to be sensitive to the type of anesthesia [Nilsson, 1975]. If transient ischemia has been induced, then, since the cerebral metabolic rate is altered following ischemia, ischemia-induced changes in k_{AGR} may be observed.

The AGR constant k_{AGR} has been measured in several studies through sequential ^{1}H NMR spectroscopy. In rabbit brain, k_{AGR} is 0.46 min^{-1} and is independent of the terminal blood glucose concentration [Petroff, 1988]. In contrast, under normoglycemic conditions in neonatal piglets k_{AGR} is sensitive to both blood glucose level and to age [Corbett, 1991; Corbett, 1993b], k_{AGR} ranging from 0.20 min^{-1} at 17.4 mM blood glucose to 0.39 min^{-1} at 1.0 mM blood glucose in 120-day old piglets.

4. *Creatine Kinase System*

The creatine kinase/phosphocreatine (CK/PCr) system is thought to have several functions [Hemmer, 1993; Wallimann, 1994]: First, it serves as a temporal energy buffer, keeping ATP and ADP concentrations steady and buffering H^+ produced by hydrolysis of ATP. The pH buffering mechanism was proposed in order to explain the dissociation between the production of lactate (*ca.* 5 mM/kg) early during ischemia without a concurrent pH drop [Kraig, 1986]. Second, by keeping ADP concentrations low (and therefore keeping the ATP/ADP ratio high) at sites where CK is functionally coupled to ATP-requiring processes (*e.g.*, ion channels), the thermodynamic efficiency of ATP hydrolysis is improved. Third, the CK reaction allows the release of P_i, an important regulator in glycolysis, from PCr. P_i stimulates phosphorylase and phosphofructokinase and relieves the inhibition of hexokinase by glucose-6-phosphate. Fourth, PCr can act as an energy carrier, moving a phosphate group from mitochondrial oxidative phosphorylation sites to energy-requiring sites coupled to CK.

Cytosolic creatine kinase is a dimer of 82 kDa composed of two monomers labelled the M and B subunits and exists as MM, BB or MB isoenzymes. Creatine kinase in mitochondria (Mi-CK) is biochemically and immunologically distinct from cytosolic CK [Basson, 1985] with a molecular weight of 80-86 kDa, and exists as an octomer. In brain tissue, 95-99% of cytosolic CK is the so-called brain-type, composed of two B subunits. CK seems to be distributed evenly over all cell types (including neurons and glia) [Kauppinen, 1994].

In normal brain, the forward rate constant for the creatine kinase reaction has been measured using ^{31}P saturation-transfer nmr spectroscopy (see below) with results listed in table 2. In all of these studies, however, surface coils were used for transmission, possibly resulting in incomplete saturation of the γ-ATP resonance. The equation fitted to the saturation transfer data assumes complete saturation and even a small amount of unsaturated γ-ATP can lead to serious errors in the estimation of the unidirectonal rate constant k_{for} and the longitudinal relaxation time of the PCr resonance $T_{1,PCr}$ [Spencer, 1993].

The study of k_{for} under pathophysiological conditions may reflect more accurately changes in ATP turnover, and hence metabolic demand, than do the measurement of ATP and PCr steady-state concentrations [Holtzman, 1993a; Sauter, 1993].

Age-related changes in k_{for} are closely paralleled by changes in Mi-CK activity [Holtzman,

Table 2. Forward rate constants for the creatine kinase reaction and spin-lattice relaxation times of PCr in normal brain obtained by various workers.

k_{for} (s^{-1})	$T_{1,PCr}$ (s)	Source
0.18-0.30	3.0[a]	Holtzman, 1993a
0.25 ± 0.02	3.93 ± 0.27	Sauter, 1993
0.68 ± 0.03	2.2 ± 0.2	Rudin, 1989
0.22 ± 0.05	4.18 ± 0.04	Cox, 1988[b]
0.37 ± 0.07	1.7 ± 0.2	Bittl, 1987
0.53 ± 0.07	1.13 ± 0.12	Degani, 1987
0.22 ± 0.03	3.1 ± 0.2	Morris, 1985[b]
0.26	2.19 ± 0.24	Shoubridge, 1982

[a]Determined from separate ^{31}P progressive saturation nmr experiments.
[b]In vitro study.

1993b]. Over a period of 5 days, k_{for} increases 3-4 fold in rats between the ages of 13 and 17 days. Thus, mitochondrial CK is an important contributor to the overall value of k_{for}. Damage to mitochondria due to ischemia should be observable in changes in k_{for} measured using ^{31}P nmr spectroscopic techniques.

Creatine kinase rates have been measured under the effects of bicucculine injection [Sauter, 1993], where the forward rate constant doubles, cyanide poisoning, where the rate constant increases by 75% at low doses and decreases 50-70% at higher doses [Holtzman, 1993] and after injection with the calcium channel blocker israpidine, which results in a 23% decrease in k_{for} [Rudin, 1989].

During conditions of hypoxia (superfused guinea pig brain slices, pO_2 *ca.* 16 kPa), cerebral PCr concentrations decrease 48% without changes in ATP concentration [Cox, 1988]. Corresponding to the above results, k_{for} increases in an attempt to maintain normal ATP concentration. This increase is not sufficient, however, to maintain the reaction flux, in contrast to severe hypoglycemia (0.1-0.2 mM).

The creatine kinase rate in brain following an ischemic episode has not been measured previously following transient cerebral ischemia. Due to large changes in cerebral metabolic rate following ischemia, changes in CK activity should be expected. The cerebral metabolic rate undergoes a transient increase early in reperfusion, the level of increase depending on brain region, followed by a significant decrease to 50% of pre-ischemia rate [Choki, 1983]. This decrease of CMR is exacerbated by pre-ischemia hyperglycemia [Kozuka, 1989]. Following 15 min of forebrain ischemia in rats, the cerebral metabolic rate for O_2 at 6 hr of recovery decreases to 40-50% of normal (as does cerebral blood flow) [Katsura, 1994]. Seizures induced post-ischemia in these animals, however, causes an increase in metabolic rate [Katsura, 1994]. Thus, while metabolism is depressed, the cerebral metabolic capacity remains intact [Katsura, 1994].

For other kinase systems, changes in activity following ischemia are dependent on at least the duration of ischemia and the brain region. For instance, the effect that ischemia has on the casein kinase rate is dependent on the brain region and on the length of ischemia [Hu, 1993]. In areas easily damaged by ischemia (10 min duration), such as the CA1 region of the hippocampus and the striatum, a 30-50% decrease in casein kinase activity has been observed at 1 hr reperfusion, with a slow recovery to normal. However, areas more resistant to ischemia, such as the CA3 region of the hippocampus and the neocortex,

show a 20-60% increase in casein kinase activity. For longer periods of ischemia, sufficient to damage these regions, this transient increase in casein kinase activity no longer occurs. It is not inconceivable that similar results would be obtained for creatine kinase activity. Most studies of post-ischemia protein synthesis or kinase activity use 30 min ischemia, presumably because changes in metabolism occur on a global scale rather than in specific regions of the brain at this duration without unduly increasing the mortality rate.

5. *Membrane Ion Gradients*

Approximately 40% of aerobic metabolism in resting brain is dedicated to the maintenance of ion homeostasis [Astrup, 1981], which enables the transmission of neuronal impulses, the maintenance of cell volume, substrate transport and other processes. The Na^+ gradient, generated by Na^+/K^+ ATPase, is of particular importance, since this form of potential energy is used to maintain Ca^{+2} homeostasis through the Na^+/Ca^{+2} exchanger, optimal intracellular pH through the Na^+/H^+ antiport, and cotransport of glucose and amino acids across the cell membrane (refer to figure 2). In the text, $[X]_i$ refers to intracellular concentration of species X and $[X]_e$ refers to extracellular concentration.

Table 3. Ion concentrations in normal brain intracellular and extracellular compartments [Hansen, 1985].

Ion	Intracellular concentration	Extracellular concentration
K^+	100 μM	3 μM
Na^+	30 μM	150 μM
Cl^-	5 μM	130 μM
HCO_3^-	12 μM	24 μM
Ca^{+2}	0.0001 μM	1.3 μM
Mg^{+2}	0.8 μM	1 μM
pH	7.00	7.30

The brain maintains a large concentration gradient across cell membranes of various ions, including Na^+, Cl^-, Ca^{+2}, Mg^{+2}, HCO_3^-, and H^+ (large extracellular concentration), as well as K^+ (large intracellular concentration) (table 3). With the onset of ischemia, a slow rise in extracellular K^+ begins, the rate increasing progressively over time. This slow increase is thought to be due to reduced Na^+/K^+ ATPase activity. Following 2 min of ischemia, $[K^+]_e$ increases sharply from ~10 mM to ~80 mM in the span of several seconds, corresponding to depolarization. This is followed by another period of slow increase (table 4). During the early rise in $[K^+]_e$, only a small change in $[Ca^{+2}]_e$ is observed, since a low $[Na^+]_i$ remains for Na^+/Ca^{+2} exchange to maintain the very large Ca^{+2} membrane gradient. Simultaneous with the sharp increase in $[K^+]_e$, $[Ca^{+2}]_e$ drops to 10% of normal, as a large Ca^{+2} flow into the intracellular space occurs. Similar observations have been made with $[Na^+]_e$ and $[Cl^-]_e$. The extracellular space changes markedly during ischemia. Under normal conditions, the extracellular space is ~20%. During the initial slow increase in $[K^+]_e$, the extracellular space decreases to between 16-20%. With depolarization a sharp drop in the extracellular space occurs, dropping to 9-16% [Hansen, 1980]. The available glucose has a

Table 4. Interstitial and intracellular ion concentrations and interstitial volume under normal and ischemic conditions [Hansen, 1985].

	Control	Ischemia
Interstitial space, % volume of brain (cortex)	20%	16-9%
Interstitial ion concentration		
$[Na^+]$	154 mM	63 mM
$[Cl^-]$	129 mM	75 mM
$[K^+]$	3.1 mM	58 mM
Intracellular ion concentrations		
$[Na^+]$	30 mM	61 mM
$[Cl^-]$	10 mM	41 mM
$[K^+]$	100 mM	78 mM

strong bearing on the length of time before membrane depolarization occurs, being shortest with hypoglycemia and longest with hyperglycemia [Hansen, 1978].

With recirculation, $[K^+]_e$ recovers rapidly (in several minutes) in both normo- and hyperglycemic animals [Siemkowicz, 1981b], while $[Ca^{+2}]_i$ takes between 30-60 min of recovery before pre-ischemia levels are attained [Ericinska, 1992]. No data exist for changes in $[Na^+]_i$ either during or following ischemia.

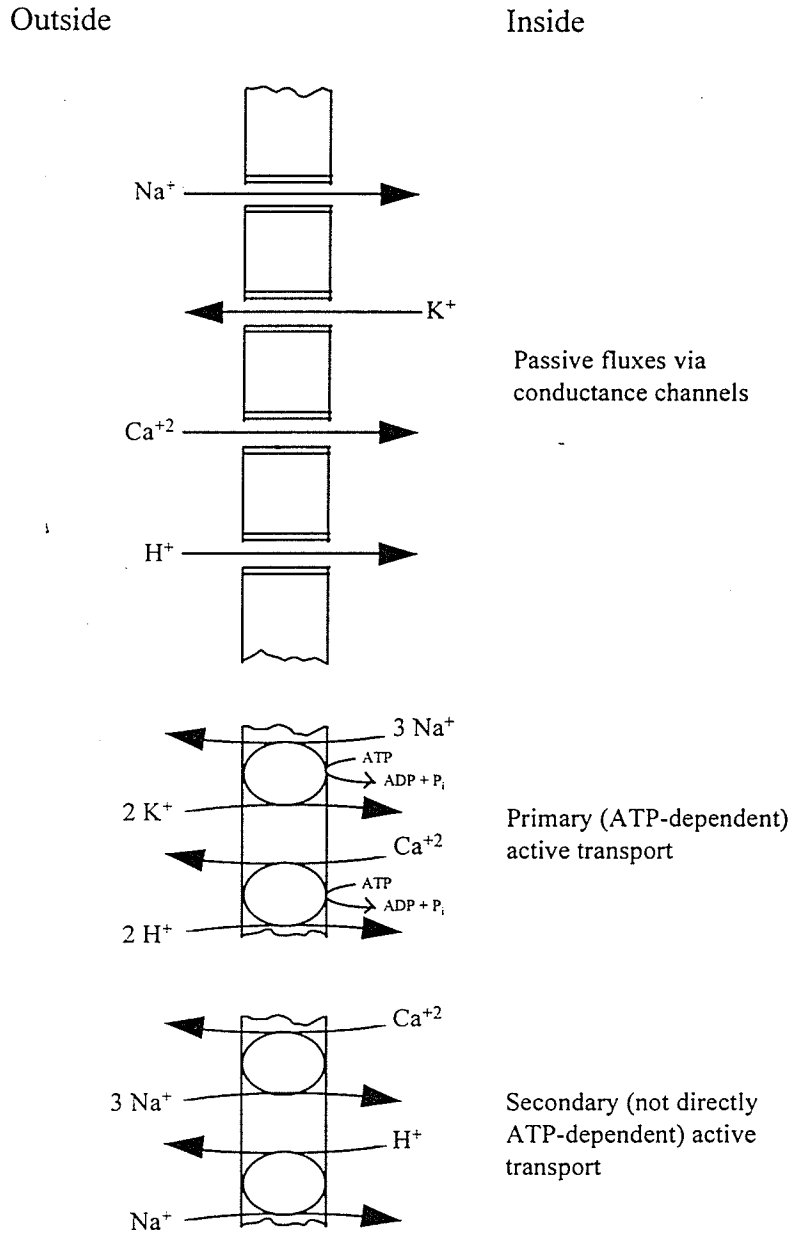

Figure 2. Major mechanisms of passive and energy-dependent ion fluxes across cell membranes (From [Siesjö, 1989a]).

B. Cerebral Ischemia

1. *Pathophysiology of Global Ischemia*

Thirty seconds following decapitation, phosphocreatine (PCr) and glucose levels are essentially depleted, and ATP levels are reduced by 50% [Goldberg, 1966]. Similar effects are seen when the mean arterial blood pressure decreases below 30 mm Hg, when arterial P_{O_2} decreases below 30 mm Hg or when bilateral carotid arterial occlusion is coupled with a 50% reduction in cerebral blood flow.

It has been demonstrated in both experimental [Branston, 1974; Heiss, 1976] and clinical [Sharbrough, 1973; Tamura, 1981] studies that both spontaneous and evoked electrical activity ceases when cerebral blood flow (CBF) decreases to below 16-18 ml/100 g/min, representing the CBF threshold for loss of neuronal activity. The CBF threshold for the loss of ion homeostasis is lower than this, being 10-12 ml/100 g/min [Astrup, 1977; Branston, 1977]. Gross perturbation of cellular energy homeostasis also occurs at this CBF threshold value.

Currently, there are three cascades of events causing ischemic damage that are of interest to researchers: damage due to calcium overload, cytosolic acidosis, and enhanced production of free radicals. It should be noted that none of the three pathways of damage is completely independent of the other, though it is instructive to divide them into separate mechanisms. Each of these sequences of events begins with the loss of sodium homeostasis following the depletion of high-energy phosphates (energy failure) [Cottrell, 1995].

The first cascade involves events triggered by the increase in the cytosolic concentration of intracellular Ca^{+2}, $[Ca^{+2}]_i$. Under normal conditions $[Ca^{+2}]_i$, is maintained at about 10^{-7} M, a 10,000-fold extracellular/intracellular concentration gradient across cell membranes. This gradient is created at the expense of cellular metabolism, either from ATP (for powering Ca^{+2}-ATPase, for instance) or the Na^+ gradient (which drives the Na^+/Ca^{+2} and the Na^+/H^+ exchangers). Calcium is an important cation in neuronal function, being involved in cell-to-cell communication and in second messenger systems. When energy failure occurs, a large influx of Ca^{+2} occurs through both voltage-gated and receptor-gated channels. A portion of this increased Ca^{+2} load is sequestered in mitochondria, endoplasmic reticulum

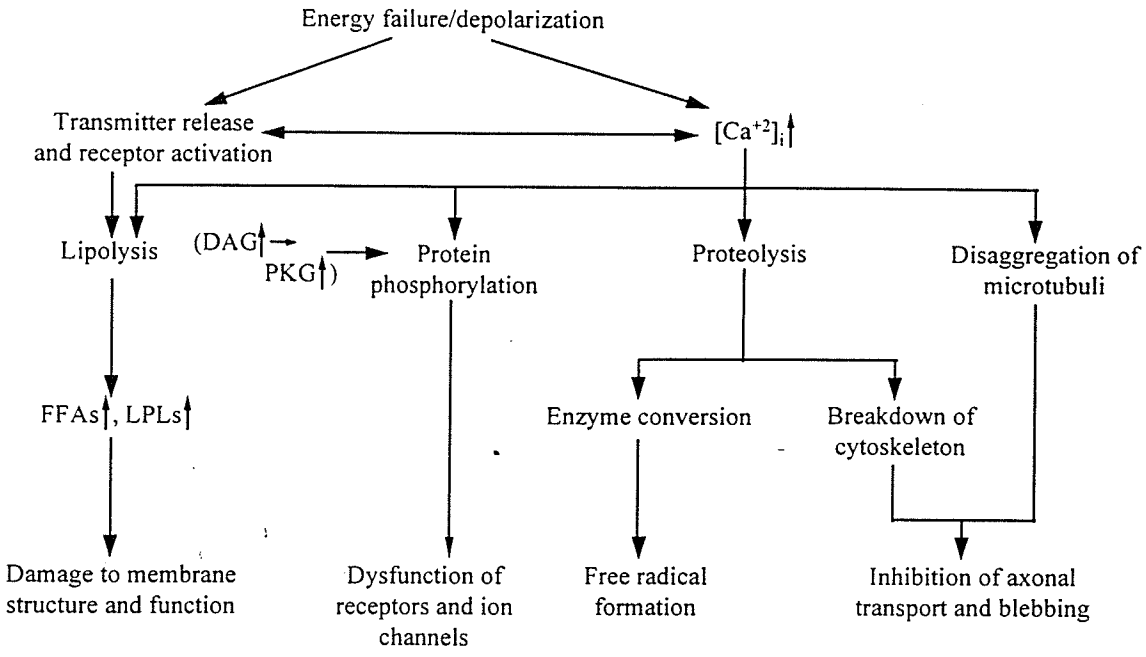

Figure 3. Diagram illustrating the major consequences of calcium overload following energy failure. DAG = diacylglycerides; PKC = protein kinase C, FFA = free fatty acids; LPL = lysophospholipid. From [Siesjö, 1992].

and Ca^{+2}-binding proteins, such as calmodulin. With the onset of energy failure, $[Ca^{+2}]_i$ increases through cell leakage. The increase in $[Ca^{+2}]$ is facilitated by the release of large amounts of neurotransmitters, predominantly glutamate. This excessive rise in $[Ca^{+2}]_i$ causes an overactivation of phospholipase A_2 and other lipases, proteases and endonucleases and, through the activation of protein kinases may alter the function of receptors and membrane channels, as well as release large amounts of neurotransmitters into the extracellular space [Benveniste, 1984; Nakata, 1992] (figure 3). Phospholipase A_2 is exclusively activated by Ca^{+2} and attacks membrane phospholipids, cleaving fatty acyl chains from the beta position of phospholipids, causing the release of lysophospholipids and free fatty acids (including arachidonic acid). The activation of proteases causes a breakdown in the components of the cytoskeleton and severs the anchorage between the plasma membrane and the cytoskeleton. Free fatty acids and lysophospholipids deteriorate cell membranes and act as ionophores [Siesjö, 1992]. In addition, free fatty acids metabolize to produce vasoactive factors (leukotrienes and prostaglandins) which cause constriction of blood vessels,

resulting in the so-called "no flow" phenomenon. Phospholipase A_2 also attacks synaptosomal membranes resulting in the inactivation of important membrane enzymes, and free fatty acids inhibit the exchange of ADP for ATP by mitochondria. Free fatty acids also trigger the mitochondrial calcium translocase pump, which removes cytosolic calcium during early reperfusion. This requires oxidative energy and takes precedence over ATP production. Free fatty acids are also powerful uncouplers of oxidative phosphorylation.

Phospholipase C catalyzes the formation of diacylglycerides when acting on phosphatidylinositol bisphosphate, a further source of arachidonc acid through the action of di- and monoacylglyceride lipases, and inositoltriphosphate, which further leads to increases in $[Ca^{+2}]_i$. This then activates protein kinase C. Protein kinase C may cause changes in membrane function though the phosphorylation of receptors or ion channels. In fact, neuronal damage through exposure to high concentrations of glutamate is greatly reduced in cultures by gangliosides, which act as protein kinase C antagonists [Manev, 1990].

The second cascade of events, that due to acidosis produced during ischemia, is particularly important in the setting of hyperglycemia. It is well established that pre-ischemia hyperglycemia worsens neuronal damage, producing severe edema and post-ischemia seizure activity [Meyers, 1977; Siemkowicz, 1978, 1981a, 1985; Smith, 1987; Pulsinelli, 1982a; Nedergaard, 1987a, 1987b; De Courten-Meyers, 1988, 1989; Prado, 1988; Yip, 1991; Wagner, 1992]. Presumeably, this acidosis occurs through the production of lactic acid through anaerobic glycolysis during ischemia. Once blood flow is returned, the major mechanism for the extrusion of excess H^+ is the Na^+/H^+ exchanger, requiring that the sodium gradient be re-established prior to removal of H^+ from the cytosol. A consequence of this is that if H^+ leaks back into the cell through the Cl^-/HCO_3^- antiport, Na^+ and Cl^- can accumulate in the cytosol, both of these ions cotransporting water and causing cytosolic edema [Siesjö, 1988].

Mitochondria are unable to produce ATP if the pH falls toward 6, since ADP-stimulated oxygen consumption is inhibited [Hillered, 1985]. Thus, for oxidative phosphorylation to resume it is necessary for pH to return normal levels. Two processes facilitate this return of pH: accelerated Na^+/H^+ exchange and oxidation of lactate [Siesjö, 1992]. While the Na^+/H^+ exchanger is stimulated by increased $[H^+]_i$, at low pH levels (< 6.2) it operates only very slowly [Grinstein, 1984]. Thus, if acidosis is particularly

severe, as in the case of hyperglycemic ischemia, tissue pH can remain low even after circulation has been restored.

The third cascade of events is the action of free radicals. It has been suggested that this mechanism is common to a number of physiological problems, including ischemia, hyperoxic stress, aging and cancer [Siesjö. 1992]. Hypoxanthine and xanthine accumulate during ischemia and the rise in $[Ca^{+2}]_i$ following energy failure activates proteases which in turn convert xanthine dehydrogenase to xanthine oxidase. Upon the return of blood flow, free radicals are produced when reduced compounds accumulated during ischemia are re-oxidized. For instance, the action of xanthine oxidase on hypoxanthine and xanthine to form uric acid produces superoxide (O_2^-) and peroxide (H_2O_2). Free radicals are produced in all cells and cells have a number of mechanisms to deal with them. First there are free radical scavengers, such as α-tocopherol and ascorbic acid. There are also enzymatic processes which eliminate free radicals. These enzymes, such as superoxide dismutase, catalase and glutathione peroxidase, metabolize free radicals or their precursors. It has been postulated that the production of free radicals may be enhanced during conditions of hyperthermia and excessive acidosis, the latter occuring during ischemia under hyperglycemic conditions [Siesjö, 1989].

2. *Delayed Neuronal Death*

Neurons are very sensitive to injury from ischemia, hypoxia and severe hypoglycemia. Short-duration global ischemia (5-20 min) causes damage to certain neuronal populations which is not manifest for several days following reperfusion, a phenomenon known as delayed neuronal death. The hippocampal CA1 pyramidal neurons are particularly vulnerable to ischemia, while other populations of neurons (caudate and thalamic nuclei, parietal cortical neurons, hippocampal CA3 neurons) are somewhat less affected [Kirino,1982; Pulsinelli, 1982a]. Figure 4 shows a series of ^1H magnetic resonance images following this delayed damage in several brain regions.

Figure 4. Slide showing the time-dependent damage due to short-duration ischemia in rat brain using T_2-weighted ^1H magnetic resonance imaging: normal brain (top left of each slice); 1 day following ischemia (top right); 2 days following ischemia (bottom left); and 14 days following ischemia (bottom right). Bright areas show regions of increased water mobility and correspond to regions of damage. Courtesy of Dr. Richard Buist.

It is currently thought that glutamate excitotoxicity, and through this the calcium cascade, is the major mechanism through which selective neuronal damage occurs [Choi, 1992, and references therein]. This hypothesis has come about through observations of the relationship between neuronal damage occuring under the above conditions and the regional distribution of voltage-sensitive calcium channels. Populations of neurons containing high concentrations of these channels, notably those activated by glutamate and related excitatory amino acids (aspartate and *N*-methly-D-aspartate, for instance), are particularly vulnerable to short-duration ischemia. However, there are discrepencies in this theory. The excessive amounts of glutamate released into the extracellular space in both the CA1 and CA3 regions during ischemia is very high, but is only transient and returns to normal levels 10-20 min post-ischemia [Benveniste, 1984; Nakata, 1992]. In addition, the amount of *N*-methyl-D-aspartate receptor and its mRNA is not very different between the CA1 and CA3 regions. Even so, the response of these two neuronal populations to ischemia is markedly different [Moriyoshi, 1991; Kataoka, 1993].

Another hypothesis for delayed neuronal death is a disruption of protein synthesis in the neurons. Protein synthesis (particularly the translational step) is highly sensitive to and inhibited by ischemia and recovers in all regions except in the selectively vulnerable populations [Xie, 1989]. Polyribosomes, where proteins are synthesized in the cell, break up into monosomes long after reperfusion [Bodsch, 1985]. If the cell cannot replace key proteins damaged through ischemic injury, the cell will die. It does not explain, however, why protein synthesis is vulnerable in these neuronal populations, nor why protein synthesis should be inhibited for a long time while calcium overload is transient.

A third theory suggests that an apoptotic mechanism of cell death [Barnes, 1988] is responsible for the phenomenon of delayed neuronal injury. When extensive DNA damage occurs, or when neurons are deprived of neurotrophic factors (*e.g.*, nerve growth factor) a cascade of events results in the death of the cell; in effect the cell commits suicide. Certain genes (*p53*, for instance) monitor DNA damage in order to repair the damage, or eliminate the cell through apoptosis. The *p53* gene encodes a sequence-specific DNA-binding protein called p53. The level of this protein increases following DNA damage, allowing the damage to be repaired [Vogelstein, 1992]. The p53 protein induces production of a protein (p21), which arrests the cell cycle in the G_1 state (the gap between mitosis and DNA replication), preventing DNA

replication [Lane, 1992]. If the damage is too severe for repair, the p53 protein, in a manner not yet understood, triggers cell suicide, though the decision by the cell to proceed to apoptosis may depend upon what other genes the cell is expressing [Lowe, 1993].

In proliferating cells, cells must move through the cell cycle or face elimination through apoptosis [Rubin, 1993]. In terminally differentiated cells, such as neurons in the adult brain, disruptions in the cell cycle can occur as well and apoptotic cell death in neurons may occur as a result of aborted attempts to re-enter the cell cycle [Rubin, 1993]. Nerve growth factor (NGF) serves to maintain the neuron in the differentiated state. Withdrawl of NGF, which has been observed following ischemia [Hashimoto, 1992; Shozuhara, 1992], may cause neurons to attempt to de-differentiate and proceed to mitosis, but fail. The use of anti-proliferative agents is a possible treatment for brain tumors, as they will initiate apoptosis in cycling tumor cells and promote survival in normal neurons [Rubin, 1993].

Pretreatment with protein sythesis inhibitor or nerve growth factor has a protective effect on the sensitive CA1 hippocampal neurons from ischemia [Shigeno, 1990; Buchan, 1990; Shigeno, 1991]. Activation of the *bcl-2* gene, which protects against apoptosis, has also been observed [Kano, 1993]. These data indicate that cell death may occur through this mechanism. However, other characteristics of apoptosis, such as early chromatin condensation and nuclear displacement, are missing [Kirino, 1984; Yamamoto, 1990; Deshpande, 1992] and the importance of this mechanism for delayed neuronal injury is in doubt, since glutamate-induced neuronal death does not occur through an apoptotic mechanism [Dessi, 1993].

A new theory suggests that there is a disturbance in mitochondrial gene expression caused by a dysfunction of the mitochondrial shuttle system, which moves mitochondria along microtublules between the soma and the dendritic and axonal processes. This would cause a progressive decrease in energy production in CA1 neurons because of their extended length compared to other types of neurons [Abe, 1995]. An interesting hypothesis, to be sure, and one which remains to be explored.

3. *Glucose and Ischemia*

Ischemic brain injury in patients with elevated blood glucose levels is generally more severe and greater in size than in patients with normal glycemia, leading to poorer neurological outcome [Berger, 1986; Calle, 1989; Candelise, 1985; Davalos, 1990; Helgason, 1988; Kushner, 1990; Olsson, 1990; Pulsinelli, 1983; Stout, 1989; Woo, 1990]. Furthermore, detrimental effects of hyperglycemia during ischemia, including increased infarct size, poorer neurological outcome and increased mortality relative to normoglycemic counterparts, have been demonstrated in animal models of focal [De Courten-Meyers, 1988, 1989; Nedergaard, 1987a, 1987b; Prado, 1988; Wagner, 1992; Yip, 1991] and global [Meyers, 1977; Pulsinelli, 1982a; Siemkowicz, 1978, 1981a, 1985; Smith, 1987] ischemia. Hypoglycemic animals, on the other hand, have decreased brain damage [Nedergaard, 1987b; Voll, 1991a], reduced neurological deficits [Le May, 1988; Strong, 1990; Voll, 1989] and lower mortality rates [Le May, 1988] than normoglycemic animals following cerebral ischemia, although severe hypoglycemia (blood glucose $\leq$3.5 mM) may be incompatible with recovery from ischemic injury [Le May, 1988].

Administration of insulin to reduce blood glucose concentration following ischemia in hyperglycemic rats results in improved recovery compared to animals in which hyperglycemia is continued during reperfusion [Siemkowicz, 1981, 1982, 1985; Voll, 1988]. Lowering blood glucose levels following a normoglycemic ischemic episode also significantly reduces neuronal injury and mortality [Voll, 1989, 1991b]. Raising blood glucose concentrations during [Venables, 1985; Yip, 1991] or after [Pulsinelli, 1982a; Siemkowicz, 1981a, 1985; Vazquez-Cruz, 1990] normoglycemic ischemia exacerbates neuronal injury.

The level of glycemia affects the length of time ion gradients are maintained during ischemia [Hansen, 1978; Siemkowicz, 1981b], being least in hypoglycemia and greatest in hyperglycemia. Presumably, the increased resistance of ion gradients during hyperglycemic ischemia is due to the larger amount of glucose available for anaerobic ATP production. The level of glycemia also affects the extent of brain injury, which is increased by hyperglycemia in models of focal [Nedergaard, 1987a; 1987b; De Courten-Meyers, 1988; Prado, 1988; De Courten-Meyers, 1989; Yip, 1991; Wagner, 1992] and global [Meyers, 1977; Siemkowicz, 1978; Siemkowicz, 1981; Pulsinelli, 1982a; Siemkowicz, 1985; Smith, 1987]

ischemia and decreased by hypoglycemia [Nedergaard, 1987a; LeMay, 1988; Voll, 1989; Strong, 1990; Voll, 1991]. Thus, ischemic damage is not related to the ability to maintain ion gradients during short-duration ischemia, but may be related to their recovery in the reperfusion period. Post-ischemia recovery of extracellular K^+, Ca^{+2} and H^+ is the same following hyper- or normoglycemic ischemia, but EEG recovery, for which ion gradient recovery is a necessary condition, is slower following hyperglycemic ischemia [Siemkowicz, 1981b]. However, recovery of intracellular ion concentrations in hypo- and hyperglycemic animals during reperfusion following cerebral ischemia has not been studied.

4. *Metabolism Following Ischemia*

Immediately following short duration global ischemia an increase in the cerebral metabolic rate of glucose (CMR_g), a measure of the glucose uptake by brain regions, shows a marked increase for the first 30 min of reperfusion [Choki, 1983; Jorgensen, 1993]. This is particularly the case for selectively vulnerable regions of the brain, where CMR_g may reach 300% of control. By 45 min of recirculation, however, less vulnerable regions (*e.g.*, thalamus) show a marked drop in CMR_g, to as low as 50% of control. CMR_g in the selectively vulnerable regions continues to remain elevated to about 1 hr of recirculation. This transient increase of CMR_g in the selectively vunerable regions is greatly diminished when the action of exitatory amino acid neurotransmitters is inhibited [Jorgensen, 1993].

In the period following this increase, CMR_g decreases in all affected regions for at least 48 hr following ischemia [Pulsinelli, 1982b; Kozuka, 1989; Triolo, 1990; Katsura, 1994]. Selectively vulnerable regions show a greater reduction in CMR_g than those less vulnerable to short duration ischemia [Kozuka, 1989]. Followup studies performed several days following ischemia, when delayed neuronal damage would be manifest, have not been done. While CMR_g is depressed following ischemia, the metabolic capacity of the tissue does not seem to be diminished. Bicuculline-induced seizures six hours following ischemia cause large increases in the cerebral metabolic rate of oxygen consumption with a corresponding increase in cerebral blood flow [Michenfelder, 1991].

Ischemia under hyperglycemic conditions depresses CMR_g even further than under normoglycemic conditions [Kozuka, 1989]. In some regions, such as areas of the neocortex,

hyperglycemia causes a 50% reduction in CMR_g relative to contol level following several hours of reperfusion [Kozuka, 1989]. Hyperglycemic ischemia does not depress all aspects of metabolism with respect to normoglycemia, however. The active fraction of pyruvate dehydrogenase complex decreases to 19-25% compared to the control value of 30% following normoglycemic ischemia, with no significant difference between the activity when ischemia is performed under normoglycemic or hyperglycemic conditions [Lundgren, 1990]. It was concluded that the accentuated depression of CMR_g is not coupled to a corresponding post-ischemia depression of pyruvate dehydrogenase complex activity.

5. *Animal Models of Ischemia*

The use of physiologically regulated, reproduceable animal models is essential to the understanding of the mechanisms of cellular injury in ischemia, and consequentially the developement of treatment strategies. There are two classes of ischemic model, namely the focal and global models of ischemia. In global ischemia, disruption of cerebral blood flow occurs in the whole brain, as during cardiac arrest, while in focal ischemia an artery perfusing a region of brain is blocked, resulting in a region of necrotic tissue (pannecrosis, or infarction) surrounded by tissue which is partially perfused (penumbra) and which may again become viable.

A number of experimental models for simulating focal and global ischemia have been developed. In the study of focal cerebral ischemia, the most commonly used model involves the occlusion of the middle cerebral arteries (MCAO model). Generally, the MCA occlusion is accomplished through electrocoagulation proximal to the origins of the lenticulostriate arteries (to minimize collateral blood flow). The occlusion may also be made temporary through the use of a snare ligature. MCA occlusion is highly representative of ischemic hemispheral infarction in humans and as such is instrumental in investigating therapeutic strategies.

This is not the only focal model of ischemia, however, as several models have been developed in order to mimic thromboembolytic stroke. In a photochemically-induced infarction [Watson, 1985], a photosensitizing dye (usally rose bengal) is administered and light at 560 nm wavelength is used to photochemically generate singlet oxygen. This causes peroxidization of lipid molecules within the

vascular endothelium, resulting in platelet aggregation. There is no thermal injury in this model. This model is unique in that the lesion may be placed in any cortical region by simply applying the light to the desired area. The only surgical procedure required for this model is the retraction of the scalp from the area of irradiation. The infarct forms rapidly out from the core, accompanied by edema, but there is no penumbral region in this model [Dietrich, 1987; Green, 1994]. This model is unpopular, despite its ease, as neuroprotective agents fail to decrease ischemic damage.

In a less controllable manner, embolization can be caused by the injection of 35 μm carbon microspheres into the internal carotid artery [Kogure, 1974]. This model produces multifocal infarctions ipsilateral to the injection site. This model is also relatively non-invasive, requiring only access to the internal carotid artery for injection. In a similar manner, the injection of blood clots (< 100 μm) into the common carotid artery [Hill, 1955] has been used. Ipsilateral infarcts are produced in the cerebral cortex, hippocampus and deep gray structures [Kudo, 1982]. In this manner the ability of human recombinant tissue plasminogen activator to improve blood flow was tested on human blood clots in rats [Papadopoulos, 1987].

For the study of global ischemia, two types of model are generally used: the two- and the four-vessel occlusion models. In the latter model, preparation of the animal proceeds in two steps [Pulsinelli, 1979]. First, arterial clasps which can be operated from outside the animal are placed around each of the two common carotid arteries (CCA) through a midline neck incision. A second incision is made dorsally and the two vertebral arteries are located. A small monopolar electrocautery needle is inserted to electrocoagulate these arteries. The occlusion of the vertebral arteries is essential to the elimination of collateral blood flow. One day following this procedure ischemia is produced by occluding each CCA in the awake animal. After a preset time interval, blood flow may be re-established through the removal of the occlusion of each CCA. This model significantly reduces CBF in the striatum and neocortex (<3% of control), and in the hippocampus (3-7% of control) [Pulsinelli, 1982b; Ginsberg, 1981]. CBF in the cerebellar and diencephalic regions (10-15% of control) and in the brain stem (25-30% of control) is less affected [Pulsinelli, 1982b; Ginsberg, 1981]. Post-ischemia hypoperfusion persists for 1 hr in the hippocampus and striatum and for up to 6 hr in the parietal neocorex [Pulsinelli, 1982b].

Using this model, following 30 min of ischemia seizures occur in 20% of rats after 24 hr and 40% after 72 hr, but do not occur after only 10 min of ischemia [Pulsinelli, 1979]. This method is successful in only 75% of animals undergoing the procedure. The remainder fail to become unresponsive with CCA occlusion (2/3 failures) or die from respiratory failure [Pulsinelli, 1979]. Histopathology shows that following 10 and 20 min of ischemia vulnerable hippocampal zones show damage in approximately 40% and 85% respectively of the hemispheres following 3 days of recovery. Damage to the striatum requires longer periods of ischemia, between 20 and 30 min, and the damage is maximally expressed in 24 hrs [Pulsinelli, 1979; Pulsinelli, 1982c].

The second model, two-vessel occlusion, involves the occlusion of both CCAs with concurrent hypotension to a mean blood pressure of 50 mm Hg by controlled arterial hemorrhage [Eklöf, 1972]. CBF measured after 5-15 min of occlusion is reduced to <5% of control in the cerebral cortex, <15% in the caudoputamen, hippocampus, and cingulate cortex, and is affected to a lesser degree in the thalamus, globus pallidus and midbrain [Kägström, 1983]. This model gives rise to ischemic damage in selectively vulnerable regions and the histopathology is similar to that in the 4VO model [Ginsberg, 1989]. However, unlike the 4VO model, ischemic damage to the CA1 and CA4 pyramidal cells in the hippocampus and to the subiculum can occur in as little time as 2 min [Smith, 1984]. Over several days following a 10 min exposure to ischemia, damage to the striatum appears in ^{1}H magnetic resonance images at 24 hr, while hippocampus damage appears after 48 hr [Sutherland, 1991].

Several schemes for the production of ischemic insults involve the elevation of cerebrospinal fluid pressure. The bihemispheral forebrain compression-ischemia model is performed by the infusion of artificial cerebrospinal fluid (CSF) into the cisterna magna to elevate the CSF pressure above the arterial blood pressure (ABP) by 20-70 mm Hg [Ljunggren, 1974]. The effects of complete and incomplete stoppage of blood flow on ischemic damage can be studied using this model through halothane-induced hypotension (50-60 mm Hg). For complete ischemia, the CSF pressure is elevated to 90-130 mm Hg, while for incomplete ischemia it is elevated to only 10-15 mm Hg [Yoshida, 1985].

Temporary unilateral CCA occlusion can be combined with elevation of CSF pressure (40-45 mm Hg) with maintenance of mean ABP between 100-110 mm Hg to produce the graded unihemispheral

ischemia model [Busto, 1985]. Regional CBF is reduced by 85-90% in the dorsolateral and lateral neocortex, the hippocampus and the lateral caudoputamen ipsilateral to the occlusion [Busto, 1985]. A graded pattern of metabolite depletion results, which is severe in the lateral cortex, hippocampus, lateral striatum and thalamus, moderate in the dorsolateral cortex, medial striatum and medial thalamus and lactate concentration is elevated in all neocortical areas [Busto, 1985].

C. NMR Methods for the Study of Cerebral Ischemia

1. *^{31}P NMR Spectroscopic Methods*

1a. *Steady-State High-Energy Phosphate Studies*

^{31}P NMR spectroscopy is a relatively non-invasive method for the study of high-energy phosphate metabolism under a variety of physiological conditions, measuring steady-state levels of PCr , ATP and P_i, and tissue pH. Tissue pH can be found using the equation [Petroff, 1985]:

$$pH = 6.77 + \log\left(\frac{\Delta - 3.29}{5.68 - \Delta}\right), \qquad (1)$$

where Δ is the difference in chemical shift (ppm) between the P_i and the PCr resonances.

The relative steady-state estimates of P_i, PCr and ATP are simply taken from the ^{31}P NMR spectrum, either as peak areas measured using integration or curve fitting, or peak heights. For measurement of ATP the β-ATP resonance is used, since no other compound has resonance frequency in the vicinity. Since the spin-lattice relaxation times T_1 for P_i, ATP and PCr do not change significantly during and following ischemia [Corbett, 1993a], fast repetition rates can be used in order to maximize signal-to-noise ratio when determining per cent changes in their levels. In order to determine accurate ratios or absolute concentrations of these metabolites the effects of saturation on the resonance intensity must be accounted for.

As ischemia begins, the concentrations of high-energy phosphates decrease and that of P_i increases when aerobic metabolism is interupted. Partial ischemia reduces PCr and increases P_i, but does not necessarily cause changes in ATP levels observed by ^{31}P NMR spectroscopy [Macri, 1992]. A glucose-dependent tissue pH decrease occurs concurrently as cells attempt to maintain ATP homeostasis through anaerobic metabolism. These changes are clearly demonstrated in time series ^{31}P NMR spectroscopy (see for example [Sutherland, 1992; Widmer, 1992; Laptook, 1994]). Indeed, in extended periods of ischemia (2.5 hr) the level of ATP and phosphorylation potential correlates well with ischemic damage [Williams, 1994].

Serial ^{31}P NMR spectroscopy can be used to demonstrate the effects of neuroactive drugs on cerebral metabolism during ischemia and its recovery following reperfusion. In 7-day old rat pups pre-

administration with 500 μg/kg of 2-deoxycoformycin caused a small but significant decrease in the rate of high-energy phosphate loss during a 3 hr hypoxia-ischemia insult [Williams, 1992]. Pre-administration of kyurenate, an endogenous excitatory amino acid antagonist, significantly reduced the rate of depletion of PCr and the increase of P_i during 30 min of reversible forebrain ischemia [Roucher, 1991a]. In a similar manner, the metabolic effects of R-phenylisopropyladenosine (R-PIA), an agonist of adenosine A1 receptors, were studied by in vivo ^{31}P NMR spectroscopy during 30 min of reversible forebrain ischemia [Roucher, 1991b]. In the R-PIA group, the extents of high-energy phosphate loss , P_i increase and tissue pH decrease were lower than in untreated animals. Recovery of high-energy phosphates, P_i and tissue pH was faster in the treated group as well, indicating that adenosine has a protective effect on metabolism in the setting of ischemia. These are only a few of the many examples of the application of serial ^{31}P NMR spectroscopy to the problem of cerebrovascular disease.

b. *Determination of Intracellular Mg^{+2}*

Magnesium is an important ion physiologically, being required in many cell processes using ATP [Murphy, 1991; Vink, 1991]. This is reflected by the fact that reported values of $[Mg^{+2}]_i$ are in the range of 1mM, near the K_m of many enzymes [Lawson, 1979; Garfinkel, 1984]. Mg^{+2} also acts as an endogenous inhibitor of calcium entry into neurons, and administration of magnesium chloride or magnesium sulfate, either prior to ischemia or following reperfusion reduces infarct volume in models of global ischemia [McKintosh, 1989; Izumi, 1991; Okawa, 1992]. Consequently, a great deal of interest has been generated about the role of Mg^{+2} in the modulation of specific metabolic processes. Due to the difficulty in the measurement of this ion by the ion selective electrode method [Hansen, 1985], information on the effect of magnesium on cellular processes has been scant until recently. Several techniques have been developed for the measurement of intracellular magnesium, including null-point titrations with metallochromic dyes [Scarpa, 1982], magnesium-sensitive microelectrodes [Rink, 1982] and NMR spectroscopy [Gupta, 1978; Burt, 1990; London, 1991]. One NMR spectroscopic method involves the interaction of Mg^{+2} with an introduced NMR-visible intracellular ligand (generally fluorinated and observed using ^{19}F NMR spectroscopy). The bound and unbound Mg^{+2} moieties are in slow equilibrium, and so, with a knowledge

of the dissociation constant, the relative areas of the bound and free ^{19}F NMR resonances give a measure of the concentration of free Mg^{+2} [Raju, 1989]. A similar method has been used to study intracellular free Ca^{+2}.

A second method involves observing the changes in the chemical shifts of the ^{31}P NMR resonances of ATP due to the reversible formation of Mg-ATP complexes. The method is completely non-invasive, as it involves a ligand which is native to cells. Assuming fast exchange conditions prevail, the intracellular free magnesium concentration $[Mg^{+2}]_f$ may be calculated by [Williams, 1994]:

$$[Mg^{+2}]_f = K_D^{MgATP} \frac{\delta_{\alpha\beta}^{ATP} - \delta_{\alpha\beta}^{obs}}{\delta_{\alpha\beta}^{obs} - \delta_{\alpha\beta}^{MgATP}}, \qquad (2)$$

where the K_D^{MgATP} is the dissociation constant for the Mg-ATP complex and is given by:

$$K_D^{MgATP} = \frac{[Mg^{+2}]_f [ATP]_f}{[MgATP]}, \qquad (3)$$

where $[ATP]_f$ is the sum of all ATP species not complexed to Mg^{+2}, [MgATP] is the concentration of complexed species (generally $MgATP^{-2}$ at physiological pH), $\delta_{\alpha\beta}^{ATP}$ is the ^{31}P chemical shift difference between the α– and β–ATP resonances of uncomplexed ATP, $\delta_{\alpha\beta}^{MgATP}$ is the chemical shift difference between the α- and β-ATP resonances of ATP complexed to Mg^{+2} and $\delta_{\alpha\beta}^{obs}$ is the observed chemical shift difference between the α- and β-ATP resonances. Similarly, the chemical shift difference between the γ- and β-ATP resonances may be used, though this chemical shift difference induced by complexation to Mg^{+2} is much smaller.

The value of K_D^{MgATP} is strongly pH-dependent [Williams, 1994], so that the value used in the above equations must be calculated using the intracellular pH determined by the chemical shift difference between P_i and PCr, as outlined above, or by some other means. The value of K_D^{MgATP} varies from 50 μM at pH 7.0 to 458 μM at pH 5.5. This large change in the dissociation constant results from a negligible affinity of the protonated species of ATP, $HATP^{3-}$, for Mg^{+2}. Since for many ATP-requiring processes the MgATP complex is necessary, the low pH levels attained during ischemia (especially with hyperglycemia) may limit the usefulness of ATP even though a significant level is maintained.

To further complicate matters, protonation of ATP also affects the values of the chemical shift limits $\delta_{\alpha\beta}^{ATP}$, $\delta_{\alpha\beta}^{MgATP}$, $\delta_{\gamma\beta}^{ATP}$ and $\delta_{\gamma\beta}^{MgATP}$, so that they must also be corrected for the effects of changing H^+ concentration [Williams, 1994].

By rearranging equation 3 and substituting for $[Mg^{+2}]$ in equation 2, an expression for the concentration of complexed ATP may be found:

$$[MgATP] = [ATP]_T \frac{\delta_{\alpha\beta}^{ATP} - \delta_{\alpha\beta}^{obs}}{\delta_{\alpha\beta}^{obs} - \delta_{\alpha\beta}^{MgATP}}. \quad (4)$$

If this function is denoted by *c*, then the free species of Mg^{+2} and ATP may be given by:

$$[Mg^{+2}]_f = [Mg^{+2}]_T - c, \quad (5)$$
$$[ATP]_f = [ATP]_T - c. \quad (6)$$

Substituting these back into equation 3 allows calculation of the total intracellular Mg^{+2} if the total ATP is known:

$$[Mg^{+2}]_T = \frac{K_D^{MgATP} c}{[ATP]_T - c} + c. \quad (7)$$

By dividing both sides by $[ATP]_T$ an expression describing the ratio of $[Mg^{+2}]_T$ to $[ATP]_T$ as a function of $\delta_{\alpha\beta}^{obs}$ is obtained:

$$K_D^{MgATP} = \frac{(R[ATP]_T - c)([ATP]_T - c)}{c}, \quad (8)$$

where, $R = [Mg^{+2}]_T / [ATP]_T$.

The level of intracellular free Mg^{+2} in normal rats measured by this method is 0.34 mM, rising to 0.52 mM during 30 min of ischemia and returning to pre-ischemia level at 1 hr of recovery [Williams, 1995]. The increase in $[Mg^{+2}]_f$ during ischemia is consistent with both the decrease in tissue pH and lower availability of ATP for complexing.

Alcohol is well known as a depleter of tissue Mg^{+2} [Altura, 1994]. In fact, very high levels of ethanol (6.6 g/kg) causes hemorrhagic stroke, preventable with pre-administration of $MgCl_2$ [Altura, 1995]. Deficits in $[Mg^{+2}]_f$ occur within 3-5 min following injection of ethanol, as measured using ^{31}P NMR spectroscopy. The decrease in $[Mg^{+2}]_f$ precedes decreases in high-energy phosphates and tissue pH.

1c. *Reacton Rates From Saturation-Transfer ^{31}P NMR Spectroscopy*

The saturation transfer method [Forsen, 1963] is one of the many dynamic NMR methods developed for the study of reaction kinetics is commonly used to study the kinetics of high-energy phosphate metabolism. The reaction catalyzed by creatine kinase:

$$PCr^{-3} + MgADP^{-} + H^{+} \longleftrightarrow Cr^{-} + MgATP^{-2}, \qquad (9)$$

has an equilibrium constant of ca. 140. Thus, as ATP is used up, creating ADP, the reaction is driven towards the right so that the supply of ATP is not diminished.

The net velocity of the reaction may be written as:

$$V_{MgATP^{-2}} = k_{for}[PCr^{-3}][MgADP^{-}][H^{+}] - k_{rev}[Cr^{-}][MgATP^{-2}]. \qquad (10)$$

The saturation transfer method involves the application of a frequency-selective saturation pulse on the resonance corresponding to one of the sites (in this case the γ-ATP phosphorous resonance). Thus, any of the phosphate saturated by the saturation pulse transferred from γ-ATP to Cr by the reverse reaction will not contribute to the intensity of the signal corresponding to the second site (PCr). As the forward reaction carries phosphate from PCr to ATP, the signal of the PCr resonance will decrease. The amount of this intensity decrease is dependent on the rate of reaction in the direction of PCr to γ-ATP, the length of time the γ-ATP resonance has been saturated and the longitudinal relaxation time of the PCr resonance. As the saturation time (τ) is increased, the PCr resonance intensity decreases exponentially so long as the rate parameter k_{for} is larger than the longitudinal relaxation rate ($1/T_{1,PCr}$). For the forward reaction, the saturation transfer experiment measures not the pure unidirectional rate consant k_{for} but the pseudofirst order rate constant k'_{for},

$$k'_{for} = k_{for}[MgADP^{-}][H^{+}]. \qquad (11)$$

Thus, the pseudo-first order rate constant assumes that there are no changes in free cytosolic concentrations of both $MgADP^{-2}$ and H^{+}.

The time dependence of the transverse magnetization of the PCr resonance ($M_{PCr}(\tau)$) is governed by the rate equation:

$$\frac{dM_{PCr}(\tau)}{dt} = \frac{M_{0,PCr}}{T_{1,PCr}} - \frac{M_{PCr}}{\tau_{1,PCr}}, \tag{12}$$

where, $M_{0,PCr}$ is the transverse magnetization due to PCr with no γ-ATP saturation, M_{PCr} is the transverse magnetization due to PCr and

$$\frac{1}{\tau_{1,PCr}} = \frac{1}{T_{1,PCr}} + k_{for}. \tag{13}$$

The solution for the above equation is:

$$M_{PCr}(\tau) = \frac{M_{0,PCr}}{1 + k_{for} T_{1,PCr}} \left(1 + k_{for} T_{1,PCr} e^{\frac{-(1+k_{for} T_{1,PCr})\tau}{T_{1,PCr}}} \right). \tag{14}$$

Saturation transfer offers a non-invasive method to determine the unidirectional rate parameters for the forward and reverse reactions (k_{for} and k_{rev}, respectively) as well as the flux in each direction when combined with the relative concentrations of PCr and ATP as given by the relative peak areas in the one-pulse spectrum. Thus, by irradiating the γ-ATP resonance and observing the intensity of the PCr resonance as a function of saturation time τ the rate parameter for the forward creatine kinase reaction k_{for} may be determined. When the γ-ATP phosphorous resonance is irradiated, a second reaction can be studied: the formation of ATP with P_i. The rate constants for this reaction may be determined in the same way as for the creatine kinase reaction. However, measurement of P_i in the ^{31}P NMR spectrum suffers from contamination by other resonances, notably those due to the phosphomonoesters. To determine the reverse creatine kinase reaction parameters, PCr is selectively irradiated and the γ-ATP signal intensity is observed as a function of saturation time.

Two major errors in the estimation of $T_{1,PCr}$ and k_{for} using saturation-transfer methods, spillover and incomplete saturation, can occur [Spencer, 1993]. Spillover refers to any time-dependent decrease in the resonance of interest (PCr, here) which does not occur through the effects of chemical exchange. As a consequence of the inhomogeneity of the $\mathbf{B}_1$ field generated by surface coils it is possible that the irradiated resonance is not completely saturated. Both of these can cause severe errors. Spillover is easily accounted for by applying the saturation pulse at a frequency equidistant from , but on the high field side of, PCr from γ-ATP. To use the above relation in determining $T_{1,PCr}$ and k_{for} when the amount of spillover is known,

$M'_{0,PCr}$ is substituted for $M_{0,PCr}$, where $M'_{0,PCr}$ is the magnetization of PCr with the saturation pulse applied opposite that of γ-ATP. With incomplete saturation, however, the above equation must be modified to include time-dependent contributions to the PCr signal intensity by transfer of magnetization through the reverse reaction:

$$\frac{d\left(\frac{M_{PCr}(\tau)}{M_{0\,PCr}}\right)}{d\tau} = \frac{1-\frac{M_{PCr}(\tau)}{M_{0,PCr}}}{T_{1,PCr}} - k_{for}\left(\frac{M_{PCr}(\tau)}{M_{0,PCr}}\right) + k_{rev}\left(\frac{M_{0,\gamma\text{-ATP}}}{M_{0,PCr}}\right), \qquad (15)$$

where k_{rev} is the pseudo-first order rate constant for the creatine kinase reaction in the reverse direction.

No information on changes in k_{for} following ischemia are available.

2. *^{23}Na NMR Spectroscopic Methods*

2a. *Single-quantum ^{23}Na NMR Spectroscopy*

The ^{23}Na nucleus is a quadrupolar nucleus of spin $I = 3/2$ in high natural abundance (approaching 100%) and relatively high frequency (26.5 MHz compared to ^{1}H = 100 MHz). Its importance and high concentration in biological tissue make this nucleus of great interest. However, a number of problems make interpretation of ^{23}Na NMR spectra difficult.

First, there is no differentiation in signals coming from intracellular Na^+ (Na^+_i) and extracellular Na^+ (Na^+_e) pools, since the difference in chemical shift between these pools is very small [Civan, 1978]. In an effort to resolve Na^+ in these two pools in the frequency domain, chemical shift reagents were developed [Gupta, 1982; Pike, 1982; Pike, 1983; Chu, 1984; Sherry, 1988]. These reagents are complexes of paramagnetic cations, such as dysprosium complexed to tripolyphosphate or triethylenetetraminehexacetate, and are cell membrane impermeant. Thus, the extracellular Na^+ resonance becomes shifted relative to the unshifted intracellular resonance, the shift being proportional to the concentration of the reagent.

This works well for cell suspensions, tissue slices or perfused organs, but difficulties *in vivo* arise. The effective concentration of the reagent is large (*ca.* 5 mM) and large amounts must be used. These compounds are somewhat toxic at these levels. For brain, these compounds cannot freely cross the blood-

brain barrier, being limited to the vasculature. One successful attempt has been made in introducing a shift reagent into brain *in vivo* by disrupting the blood-brain barrier with a large bolus of a hypertonic solution of mannitol (25%) [Eleff, 1993]. This method is very invasive, and greatly increases damage due to ischemia. Also, because of the complex structure of the microenvironments in tissue, bulk magnetic susceptibility shifts greatly broaden the resonances due to intracellular, extracellular/extravascular and vascular Na^+ [Chu, 1990].

A second concern is whether 100% of sodium in tissue is NMR visible. Interactions with polyelectrolytes (such as proteins) causes changes in the frequency of the 'outer' transitions (the $|-1/2> \rightarrow |-3/2>$ and the $|3/2> \rightarrow |1/2>$ transitions, containing 30% of the total intensity each) dependent on the orientation of the nucleus relative the electric field gradients generated by the polyelectrolytes. Thus, these resonances become broadened and disappear into the baseline. The central resonance ($|1/2> \rightarrow |-1/2>$, containing the remaining 40% of the total intensity) is unaffected by these interactions. Thus, it has been theorized that only 40% of sodium in tissue is 'NMR visible' relative to the same concentration in an isotropic medium [Pike, 1985; Springer, 1987; Malloy, 1990], and may be reduced further through transverse relaxation effects [Forsén, 1981]. However, other workers have reported higher than 40% visibility of sodium in tissues, even approaching 100% [Fossel, 1986; Jelicks, 1989a].

Since the interactions leading to reduced NMR visibility of sodium should be more prevalent in the intracellular compartment, as sodium shifts from the extracellular to the intracellular space a decrease in the overall signal should occur. Single-quantum ^{23}Na NMR spectroscopy has been used in this fashion to follow sodium influx into the extracellular space during bicucculine-induced seizures [Schnall, 1988] and during global ischemia [Eleff, 1991]. In the latter work, it was demonstrated that following ischemia the intracellular Na^+ concentration recovers before either tissue pH or ATP, though there are no differences in the rates of change in intracellular Na^+, pH or ATP during the ischemic event. However, the changes observed in the ^{23}Na NMR signal are small (on the order of 5-10%) and more sensitive methods are available, as outlined below.

2b. *Double-quantum ^{23}Na NMR Spectroscopy*

The discrimination of ^{23}Na NMR signals from Na^+ in the intra- and extracellular spaces is not possible on the basis of a chemical shift difference in the two pools. Using chemical shift reagents which are impermeable to cell membranes, and would thus shift the frequency of the extracellular Na^+ pool relative to the intracellular pool, is one answer to this problem. Unfortunately, the blood-brain barrier is impermeable to such compounds. Thus, another method to monitor intracellular Na^+ by NMR spectroscopy must be used.

One such way is to use the differences in the relaxation characteristics between ^{23}Na nuclei in these two pools [Pekar, 1986a; Pekar, 1986b]. As mentioned in the previous section, interaction between the ^{23}Na nuclei and polyelectrolytes causes biexponential relaxation. Both intra- and extracellular Na^+ encounter such proteins. However, the concentration of proteins in the cytosol is much greater than in the extracellular space, so it is more likely that the intracellular ^{23}Na nuclei show a greater difference between the fast and slow relaxation rates. This leads to production of more intense double-quantum signals, since the intensity increases as R_2^f/R_2^s increases from unity (R_2^f and R_2^s respectively are the fast and slow transverse relaxation rates). This is because the multiple-quantum NMR spectrum consists of the difference of two lines of equal area, but having different widths (due to the differences in relaxation rates of the transitions). The NMR pulse sequence which makes use of biexponential relaxation is known as the multiple-quantum filter.

The double-quantum filter measures only 'free' intracellular sodium and not sodium bound to proteins [Stevens, 1992]. Extracellular Na^+ will still contribute to the overall signal, due to interactions with cell membranes, etc., but its contribution will be somewhat less than expected from the concentrations of Na^+ in and the relative volumes of the intra- and extracellular spaces [Hutchison, 1993]. For instance, plasma shows a measureable double-quantum NMR signal, but it is one-quarter the signal of a sample containing packed red blood cells (hematocrit 80%). Urine and 1.5 M NaCl solution showed only very small double-quantum signals [Hutchison, 1993].

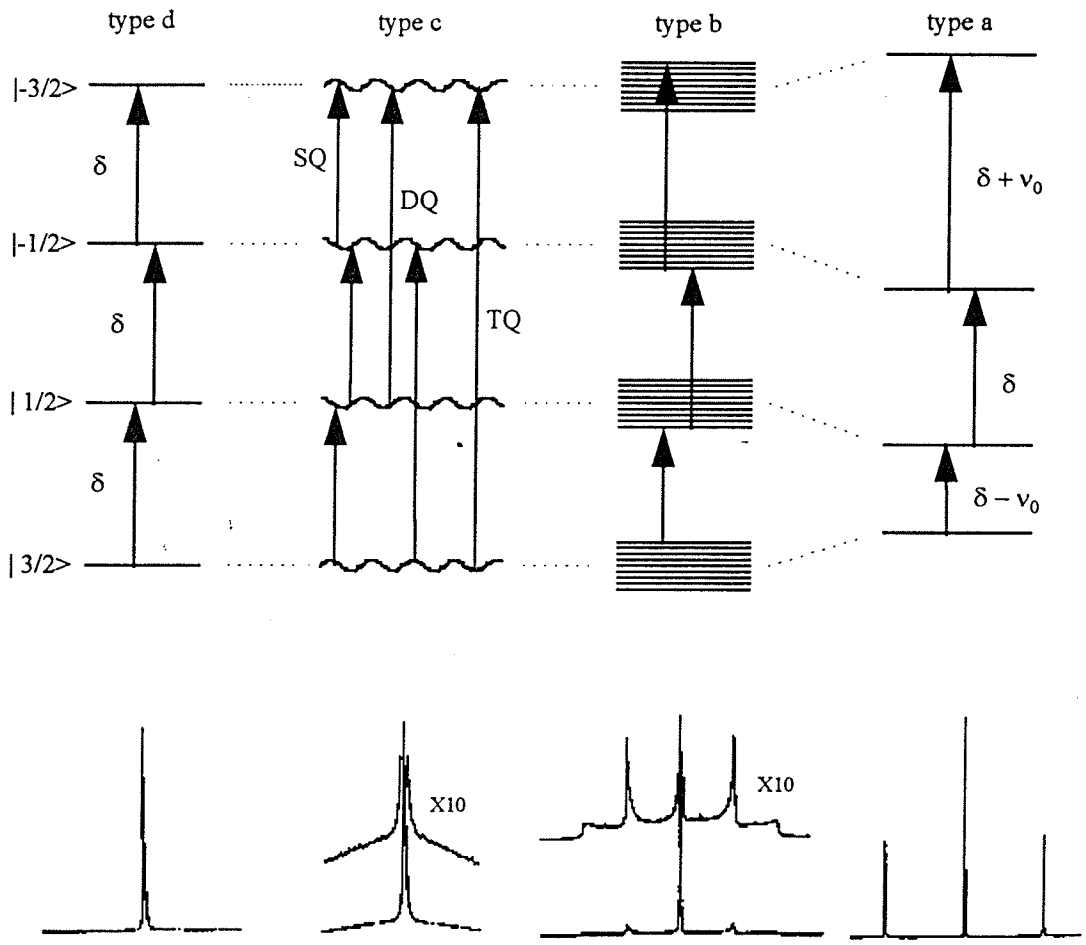

Figure 5. Energy level diagrams for isolated $I = 3/2$ systems (top) and resulting spectra (bottom). The type d spectrumwas produced using a sample of NaCl in water, type c from a sample of aqueous Na^+ in a solution of micelle-solubilized gramicidin channels, types b and a from samples of aqueous Na^+ in unoriented and oriented dodecylsulfate micelles, respectively. From [Rooney, 1991a].

The following is a mathematical exploration of the generation of the double-quantum NMR signal [Rooney, 1991a]. For nuclei having non-zero quadrupole moments ($I \geq 1$), several different classes of NMR spectra can result, depending on the environment that the quadrupolar nucleus is situated (refer to figure 5) [Rooney, 1991a]. A type *d* spectrum results from a homogeneous sample, as for ^{23}Na in

normal saline, giving a single Lorentzian line. The quadrupolar interaction frequency ω_Q is given by the equation

$$\omega_Q = (4h)^{-1} e^2 Q(1+\gamma_\infty) q(3\cos^2 - 1 + \eta \sin^2 \theta \cos 2\phi), \qquad (16)$$

where h is Planck's constant over 2π, eQ is the electric quadrupole moment of the nucleus, γ_∞ is the Sternheimer antishielding factor, eq is the major element of the diagonalized molecular electric field gradient tensor, θ is the (zenithal) angle between the element's direction and that of the magnetic field B_o, η is the tensor's symmetry parameter and ϕ is the azimuthal angle. Since the instantaneous values of the tensor parameters q, θ, η, and ϕ follow a complex time-dependence due to molecular motions, it is simplest to consider the time-averaged value of ω_Q, $\overline{\omega}_Q$:

$$\overline{\omega_Q} = (4h)^{-1} e^2 Q(1+\gamma_\infty) < (3\cos^2 \theta - 1 + \eta \sin^2 \theta \cos 2\phi) >_t . \qquad (17)$$

If an axially symmetric electric field gradient tensor is assumed and γ_∞ is ignored, this reduces to

$$\overline{\omega_Q} = (4h)^{-1} e^2 Q < q(3\cos^2 \theta - 1) >_t . \qquad (18)$$

In this environment, ω_Q fluctuates at such a rapid rate that the correlation times are small with respect to the Larmor period (ω_L^{-1}). These fluctuations are mainly due to H_2O exchange in the hydration shell and are so rapid that the time-averaged value of ω_Q is zero. The three single-quantum coherences give rise to three isochronous resonances of equal (narrow) linewidths.

In tissue, quadrupolar nuclei encounter a number of charged macromolecules, introducing a slower modulation of ω_Q superimposed on the fluctuations due to exchange in the hydration shell. This slower modulation causes $\overline{\omega}_Q$ to become non-zero. If the time of the effective half-period of this slower modulation of ω_Q is similar to ω_L^{-1}, but still less than the value of $\overline{\omega}_Q^{-1}$, a type *c* spectrum is produced. The result is a set of three isochronous lines of different linewidths. The narrower central resonance ($|1/2> \rightarrow |-1/2>$) is superimposed on the higher ($|-1/2> \rightarrow |-3/2>$) and lower ($|3/2> \rightarrow |1/2>$) transitions (equally broad). Thus, relaxation is said to be bioexponential in tissue.

If the average time of the half-period or the value of $\overline{\omega}_Q$ for the slower fluctation of the electric field gradient (or both) becomes larger (so that the half-period time becomes greater than $\overline{\omega}_Q^{-1}$), a type *b* spectrum results. The spectrum shows the central resonance and two different inhomogeneous powder patterns of the two outside resonances. Although transient inner sphere binding of Na^+ to a specific site will generate a type *b* spectrum, this mechanism is not unique in producing the powder-like spectrum. Any mechanism involving Na^+ remaining in regions in which $\overline{\omega}_Q$ is non zero for times long compared to $\overline{\omega}_Q^{-1}$ will produce a type *b* spectrum.

When the value of $\overline{\omega}_Q$ can never be time-averaged to zero, as in single crystals (except for coincidental orientations for which $\overline{\omega}_Q$ happens to be zero) or oriented liquid crystals, a type *a* spectrum results. Generally, the single-quantum NMR spectrum for $I = 3/2$ shows a triplet with a peak separation of $2\,\overline{\omega}_Q$ the first-order quadrupolar interaction.

From Redfield relaxation theory, we may write the relaxation rates for various transitions as Hubbard-type equations (*i.e.*, in terms of the spectral densities J_x):

$$R_{1s}^{2Q} = 12C^2[J_2(2\omega_L)] \tag{19}$$

$$R_{1f}^{1Q} = 12C^2[J_1(\omega_L)] \tag{20}$$

$$R_{2s}^{1Q} = 6C^2[J_1(\omega_L) + J_2(2\omega_L)] \tag{21}$$

$$R_{2f}^{1Q} = 6C^2[J_0(0) + J_1(\omega_L)] \tag{22}$$

$$R_2^{2Q} = 6C^2[J_0(0) + J_2(2\omega_L)] \tag{23}$$

$$R_2^{3Q} = 6C^2[J_1(\omega_L) + J_2(2\omega_L)] \tag{24}$$

where

$$C = \frac{eQ(1+\gamma_\infty)}{6\eta} \qquad \text{or} \qquad C = \frac{eQ}{6\eta},$$

J_0 is the spectral density function at zero frequency, J_1 and J_2 are the spectral densities at the Larmor frequency ω_L and its second harmonic ($2\omega_L$), given by

$$J_n(n\omega_L) = \frac{\tau_c}{1 + n^2\omega_L{}^2\tau_c{}^2}. \tag{25}$$

It should be noted that $R_2^{3Q} = R_{2s}^{1Q}$ and that $R_{2s}^{1Q} = (R_{1s}^{2Q} + R_{1f}^{1Q})/2$. Equations 19-24 would be different for type *b* or type *a* systems.

For the present discussion on the effect of rf pulses on quadrupolar nuclear spins, a single population of isolated spins in fast exchange such that a type *c* one-pulse spectrum is produced is assumed and second-order dynamic frequency shifts are ignored. Placing the spins in a static magnetic field ($\mathbf{B_o}$) produces dipolar order, represented by a tensor of rank 1 T_{10}:

$$T_{00} \xrightarrow{B_o} T_{10}\,. \tag{26}$$

When a single rf pulse of field strength $\mathbf{B_1}$ is applied,

$$\text{Pulse} - d - t_{acq}$$

where d is the pre-acquisition delay and t_{acq} is the acquisition time, nutation by an angle $ß_1$ is produced and single quantum coherence, T_{1-1}, implicit in T_{11}, can be detected:

$$T_{10} \xrightarrow{B_{1y'}} \cos\beta_1 T_{10} - \sin\beta_1 T_{11}, \tag{27}$$

where $ß_1$ (in rad) is given by $-\tau\mathbf{B_1}t_p$ (where τ is the magnetogyric ratio of the nucleus of interest and t_p is the duration of the rf pulse) and the antisymmetric tensor T_{11} is defined by:

$$T_{11} = \frac{1}{\sqrt{2}}(T_{11} - T_{1-1})\,. \tag{28}$$

This describes the one-pulse experiment. If a 90° rf pulse is applied, then only T_{11} exists immediately following the end of the pulse. Under the quadrupolar Hamiltonian, this evolves during $d + t_{acq}$. The transverse relaxation transfer coefficients are given in equations 29-34:

$$r_{T_{11}}(t) = e^{-i\delta}(0.6e^{-R_{2f}^{1Q}t} + 0.4e^{-R_{2s}^{1Q}t}) \tag{29}$$

$$r_{T_{12}}(t) = r_{T_{21}}(t) = 0 \tag{30}$$

$$r_{T_{13}}(t) = \frac{\sqrt{6}}{5}e^{-i\delta}(e^{-R_{2f}^{1Q}t} + e^{-R_{2s}^{1Q}t}) \tag{31}$$

$$r_{T_{33}}(t) = e^{-i2\delta}e^{-R_2^{2Q}t} \tag{32}$$

$$r_{L_{11}}(t) = 0.2e^{-R_{1f}^{1Q}t} + 0.8e^{-R_{1s}^{2Q}t} \tag{33}$$

$$r_{L_{13}}(t) = r_{L_{31}}(t) = 0.4(e^{-R_{1f}^{1Q}t} + e^{-R_{1s}^{2Q}t}), \tag{34}$$

where the notation $r_{T_{ll'}}$ or $r_{L_{ll'}}$ represents the transfer of transverse or longitudinal magnetization from rank l to rank l', respectively. The data acquired during t_{acq} by the receiver is the function $r_{T_{11}}(d + t_{acq})$. The unavoidable loss of magnetization during the pre-acquisition delay d in part results in the NMR visibility problem for quadrupolar nuclei. If $(R_{2f}^{1Q})^{-1}$ is smaller than d, the left-hand term in equation 29 will be diminished or essentially eliminated and the broad component of the resonance will be totally or partially missing from the Fourier-transformed frequency spectrum. Also, if the pulse length (t_p) is of the same order of magnitude as $(R_{2f}^{1Q})^{-1}$, relaxation of the broad components will occur during the pulses themselves, causing a further reduction in observable magnetization. Measuring R_{2f}^{1Q} and R_{2s}^{1Q} is difficult with a simple one-pulse experiment. If $(R_{2f}^{1Q})^{-1}$ is of the same order of magnitude as (R_{2s}^{1Q}), the two terms in equation 29 are hard to separate, since they both have the same sign. Also, the function r_{T11} is sensitive to $\mathbf{B_0}$ inhomogeneities.

One sequence which makes use of the differences in the fast and slow relaxation rates is the double-quantum NMR experiment:

$$\text{Pulse 1} - \text{delay 1} - \text{Pulse 2} - \text{delay 2} - \text{Pulse 3} - \text{delay 3} - \text{Pulse 4} - d + t_{acq} \ .$$

This sequence consists of a preparation period containing pulse 1, delay 1, pulse 2, delay 2 and pulse 3, an evolution period containing delay 3, a mixing pulse, pulse 4, and the acquisition period, $d+t_{acq}$. Pulse 1 converts the magnetization to single-quantum coherence. The single-quantum coherences are allowed to evolve and relax during delays 1 and 2. Pulse 2, a π pulse, simply refocuses the magnetization and makes the experiment chemical-shift insensitive. Pulse 3 generates coherences of all possible orders (from -3 to +3 for $I = 3/2$), but phase cycling of the pulses selects either triple or double quantum coherences:

$$\begin{aligned} T_{10} \xrightarrow{\text{Pulse 1}} & r_{T_{11}}(t_1 + t_2)T_{11} + r_{T_{31}}(t_1 + t_2)T_{31} \xrightarrow{\text{Pulse 3}} \\ & r_{T_{33}} t_3 T_{32} \xrightarrow{\text{Pulse 4}} r_{T_{11}}(d + t_{acq})T_{31} + r_{T_{13}}(d + t_{acq})T_{11}. \end{aligned} \qquad (35)$$

The pulse transfer function for this transfer is given by (with pulse angle β_3):

$$p^3_{2\pm1}(\beta_3) = -\sqrt{\frac{10}{4}}(3\sin 3\beta_3 - \sin\beta_3). \qquad (36)$$

The double-quantum coherence evolves during delay 3 (t_3) and is transferred back to single-quantum coherence with pulse 4. The octopolar transverse coherence, T_{31}, existing during the preparation period, has the time-dependence given by equation 31. R_{2s}^{1Q} and R_{2f}^{1Q} are of opposite sign and of equal weighting. By incrementing the preparation time, $r_{T13}(t_1+t_2,d+t_{acq})$ is obtained by plotting the area of the time-domain signal, or the height of the peak in its FT, as a function of t_1+t_2. The relative size of $(R_{2f}^{1q})^{-1}$ and d is unimportant. Since the observed magnetization is given by $r_{T13}(d+t_{acq})$, it is possible to measure relaxation parameters by fitting the acquired data with equation 31.

Homogeneous B_1 pulses are important in multiple-quantum NMR spectroscopy, if perfect separation of orders during the mixing period (delay 3) is to be achieved. [Jaccard, 1986]. Also, variations in pulse angle from 90° can result in leakage of single-quantum coherences through the filter [Hutchison, 1990].

Once the relaxation parameters are determined, it may be possible to interpret the results through understanding the mechanisms of relaxation. The simplest situation is obtained when the temporal correlation function for the fluctuation of ω_Q decays exponentially with a single correlation time τ_c. The spectral density function is then given by:

$$J_x(x\omega_L) = \frac{24}{5}\left(\frac{h\omega_Q^{RMS}}{2\pi eQ}\right)^2\left(\frac{\tau_c}{1+\left(x\omega_L\tau_c^{\,2}\right)}\right). \qquad (37)$$

When $\tau_c \ll \omega_L^{-1}$ (type *d* spectrum), all of the Js are equal and and all of the Rs are equal. The relaxation rates are given by:

$$R_1 = R_2 = R = \frac{8}{5}(\omega_Q^{RMS})^2\tau_c. \qquad (38)$$

However, the temporal correlation function for ω_Q does not decay as a single exponential function for the ^{23}Na ion. A 0.1 ps process is likely due to H_2O translational motion, while a second 1 ps process is probably due to H_2O rotation. However, because the correlation times are so short, the overall effect is an effective single-exponential decay (and hence a single relaxation time as given in equation 38 is meaningful).

As the correlation time increases and approaches ω_L, so that a type *c* spectrum is generated, it is possible to calculate the τ_c-dependences of the various R values. Using equations 19-24 combined with equation 37 shows that at a resonance frequency of $\omega_L/2\pi$ = 79.4 MHz (300 MHz for ^{1}H), assuming ν_Q^{RMS} = 100 kHz, the spectrum type changes from a type *d* to a type *c* when τ_c becomes greater than 2×10^{-10} s. Above this threshold value, only R_{2f}^{1Q} and R_2^{2Q} continue to increase with τ_c. At longer values of τ_c for a given ω_Q, R_{2s}^{1Q} becomes small again, so that no matter what the environment at least some of the signal from all Na^+ in tissue will be observed in the single-quantum NMR spectrum.

For the transverse double-quantum NMR experiment, the relaxation transfer function describing the development of the respective octopolar tensor operators has the form:

$$r_{T_{31}}(\tau) = k(e^{-R_{2s}^{iQ}\tau} - e^{-R_{2f}^{iQ}\tau}), \tag{39}$$

where k is a constant, i = 1 or 2 and τ is the preparation time. The maximum value of this function occurs when (in terms of the various relaxation parameters):

$$\tau_{2,m} = \frac{\ln(R_{2f}^{iQ}/R_{2s}^{iQ})}{R_{2s}^{iQ} - R_{2s}^{iQ}}, \tag{40}$$

which, when using the ratios of the fast and slow longitudinal (α_1) and 1Q transverse (α_2) relaxation parameters, yields:

$$\tau_{2,m} = \frac{\ln \alpha_j}{R_{js}^{iQ}}(\alpha_j - 1)^{-1}, \tag{41}$$

Substitution back into equation 31 yields:

$$r_{j31}(\tau_{j,m}) = r_{j31,m} = k_j(e^{-\ln\alpha_j/(\alpha_j-1)} - e^{-\alpha_j \ln\alpha_j/(\alpha_j-1)}), \tag{42}$$

or

$$r_{T_{31},m} = k_j(\alpha_j^{-1/(\alpha_j-1)} - \alpha_j^{-\alpha_j/(\alpha_j-1)}). \tag{43}$$

When the Debye model is used to calculate the values of α_1 and α_2, the following limits of each are obtained:

$$\lim_{\tau_c \to \infty} = 4 \tag{44}$$

$$\lim_{\tau_c \to \infty} \alpha_2 = \infty. \tag{45}$$

These give the limiting values for transfer functions for T_{31}:

$$r_{T_{31},m} = 0.49(\infty^{-1/\infty} - \infty^{-1}) \cong 0.49. \tag{46}$$

The calculated ratios of the intensities of double- to single-quantum coherence NMR signals arising from a single population in a type *c* environment can approach 0.15 for transverse double-quantum NMR experiments.

The reality in tissue is that there are at least two correlation times, that for the very short correlation time of the hydration shell and that associated with the fluctuations in the macromolecular environment. However, if there is only a single long correlation time, the above treatment still applies so long as the excess R values are considered (R_{obs}-R_{free}, where R_{obs} and R_{free} are the rate constants measured in the presence and absence of the macromolecular environment, respectively). The excess *R* is that catalyzed by the environment.

For non-Debye relaxation, assuming a distribution of correlation times, $p(\tau_c)$, the inverse Laplace transform of the temporal correlation function is taken to determine the relaxation rates. The normalization condition of this distribution is:

$$\int_0^\infty p(\tau_c) d\tau_c = 1. \tag{47}$$

Thus, a given relaxation parameter R_{jk}^{iQ} may be expressed as:

$$R_{jk}^{iQ} = \int_0^\infty p(\tau_c) R_{jk}^{iQ}(\tau_c) d\tau_c, \tag{48}$$

where $R_{jk}^{iQ}(\tau_c)$ is evaluated by combining equation 37 with the appropriate expression for *R* from equations 19-24. With the assumption that relaxation is primarily due to thermally-activated lattice motions, the temperature dependence of τ_c, in terms of Arrhenius parameters, is given by:

$$\tau_c^{-1} = (\tau_c^0)^{-1}(e^{-E_a/RT}), \tag{49}$$

where τ_c^0 is the pre-exponential factor and E_a is an activation energy. In terms of Eyring parameters, τ_c is given by:

$$\tau_c^{-1} = \frac{k_B T}{h} e^{\Delta S^*/R}\left(e^{-\Delta H^*/RT}\right), \tag{50}$$

where ΔS^* and ΔH^* are, respectively, are activation entropy and activation enthalpy parameters, R is the gas constant and k_B is the Boltzmann constant.

The simple discrete exchange model uses a delta function for equation 48, and modelling data obtained for a single temperature requires adjusting two parameters (ω_Q^{RMS} and τ_c) and for data obtained over several temperatures requires three parameters to be adjusted (ω_Q^{RMS}, τ_c and E_a, in terms of equation 48). A fast-exchange two-site discrete exchange model involves the use of a double delta function for equation 48 and if excess *R* values are used the same three parameters are encountered, but ω_Q^{RMS} becomes a product of the ω_Q^{RMS} of the site and the fractional occupancy. Thus, extending this type of model to multiple binding sites adds several adjustable parameters for each added site. Na^+ does not bind discretely to anything intracellularly [Kushmerick, 1969], either to negatively charged lipid membranes [Eisenberg, 1979; Kurland, 1979; Roux, 1990], nor to nucleic acids [Reuben, 1975; Bleam, 1983; Padmanabhan, 1988; Anderson, 1990]. When Na^+ does bind, it is in an outer-sphere process [Gustavsson, 1978; Kurland, 1982; Lindman, 1987; Pettegrew, 1987].

The use of a continuous distribution of correlation times is the limit of the multi-site discrete exchange model as the number of sites approaches infinity. One example of the use of such a distribution is the log Gauss distribtion:

$$p(\tau_c) = Ne^{-a^2 \ln(\tau_c/\tau_{cm})}; \tau_c \le \tau_{cm} \tag{51}$$

$$p(\tau_c) = Ne^{-b^2 \ln(\tau_c/\tau_{cm})}; \tau_c > \tau_{cm}, \tag{52}$$

where N is a normalizing factor given by

$$N = 2ab(\sqrt{\pi}(a+b))^{-1}, \tag{53}$$

a and b are related to the two different half-widths of the distribution and τ_{cm} is the modal value of the distribution (the correlation time with the highest probability). Thus, there are five fitting parameters with such a model: ω_Q^{RMS}, τ_{cm}^0 (the pre-exponential factor of the modal correlation time), E_a, a, and b.

To date, no one has measured the relative contributions of intra- and extracellular Na^+ to the observed ^{23}Na NMR signal in brain *in vivo*, so that it is not known how significant is the contamination due to extracellular Na^+. Significant double-quantum ^{23}Na NMR signals have been observed in perfused organ studies [Dowd, 1992; Dowd, 1993], which can be quenched using paramagnetic relaxation agents [Jelicks, 1989b], but in these cases the extracellular compartment is much larger than the intracellular volume. In normal rat brain, the intracellular volume is much larger than the extracellular compartment, being 80% of the total brain volume. This volume increases further during the course of ischemia and may reach as high as 90%, due to the co-transport of H_2O with the migration of Na^+ into the intracellular space following energy failure. Even blood will contribute to the overall double-quantum NMR signal, but changes in $[Na^+]_i$, and hence the double-quantum signal, in this source are expected to be negligeable since blood comprises only about 3% of the total brain volume.

In an *ex vivo* preparation of rat brain slices, it was found by comparing DQ ^{23}Na NMR spectra from samples in the presence and absence of the relaxation agent dimeglumine gadopentate that 40% of the observed double-quantum signal is extracellular [Brooks, 1993]. Since this preparation necessarily results in high extracellular/intracellular ratios and surface areas, the contribution of extracellular sodium *in vivo* to the total observed double-quantum signal is expected to be lower. The double-quantum NMR signal increases with the addition of veratridine, a sodium channel opener. However, the double-quantum NMR signal remains constant with the addition of veratridine in the presence of tetrodotoxin, a sodium channel blocker. These results are consistent with the influx of Na^+ from the extracellular to the intracellular compartment when Na^+ channels are opened with veratridine, while no such channel opening occurs in the presence of tetrodotoxin [Brooks, 1993].

Measurement of the double-quantum sodium NMR signal is complicated by a number of factors, including the competition between Na^+ and H^+ ions for protein binding sites, so that the observed signal becomes pH-dependent [Hutchison, 1990].

Changes in relaxation parameters during the course of the experiment may occur, and indeed this is probably the case [Lyon, 1991]. The double-quantum evolution time yielding maximum double-quantum NMR signal in brain differs between live (*ca.* 11 ms) and dead (*ca.* 4 ms) animals, indicating that changes in R_2^f and R_2^s occur [Lyon, 1991]. Thus, if the evolution time is maintained at a constant value during the experiment, any increase in the double-quantum signal may be underestimated. The same experiment also showed that the use of various evolution times passes pools having different double-quantum relaxation rates through the filter, demonstrating heterogeneity in tissue [Lyon, 1991]. However, only two evolution times were shown, so that the relationship between evolution time and sodium pools is not well defined. To better delineate this function would be an interesting and potentially useful experiment, since it may be possible that the two evolution times are selecting intra- and extracellular pools of sodium even further. No such dependence occurs in phantoms containing sodium in agarose gel.

In fact, at short preparation times (~1ms) the DQ NMR signal is predominantly due to intracellular Na^+ [Lyon, 1994]. However, there are two problems with shortening the preparation time this much. First, the preparation time corresponding to the maximum DQ NMR signal intensity is much longer than 1 ms (*ca.* 8 ms), so that signal-to-noise is greatly decreased. Second, order on a molecular level introduces a second-rank tensor in the transverse double- (but not the longitudinal double- or the triple-) quantum filter experiment [Eliav, 1992], resulting in distorted lineshapes [Lyon, 1991].

3. *^{1}H NMR Spectroscopic Methods*

A number of metabolites that are of interest in the study of ischemia and other physiological disorders are observable with the use of ^{1}H NMR spectroscopy. Large changes in relative concentrations of compounds can be observed in ischemia (*e.g.*, [Bruhn, 1989]) and in brain tumors (*e.g.*, [Segebarth, 1990]) *in vivo*. Of special interest is a compound localized almost exclusively to neurons, *N*-

acetylaspartate (NAA). In adult brain, this compound is localized exclusively to neurons (except in oligodendrocyte-type 2 astrocytes [Urenjak, 1993]). Its function is not clear, but it may serve as a regulator of neuronal protein synthesis, myelin production, and as a source of aspartate [Birken, 1989; Miller, 1991]. Other compounds observeable in the ^{1}H NMR spectrum include creatine/phosphocreatine, choline/phosphocholine, glutamate, taurine, and inositol. Most of the resonances of these compounds are observed in the region of 2.0-4.0 ppm with respect to tetramethylsilane (see results, section D). Lactate, of particular interest where conditions resulting in the uncoupling of oxidative phosphorylation occurs, lies in the region of a broad lipid resonance at 1.35 ppm. Concentrations of metabolites determined using *in vivo* ^{1}H NMR spectroscopy are generally higher than those determined *in vitro*. For instance, NAA concentration determined by ^{1}H NMR spectroscopy is 12 mM, but *in vitro* is found to be only 6 mM [Frahm, 1989]. It is possible that the differences are due to post mortem metabolism of tissue and losses of compound due to the destructive nature of analytical techniques in the *in vitro* measurements.

Brain tissue is composed of approximately 78% water (*ca.* 40 M), while metabolites are present in brain are on the mM concentration level. Thus, the primary problem in studying changes in metabolites using ^{1}H NMR spectroscopy is reducing the water resonance in order to observe resonances due to the metabolites of interest, making this a solvent suppression problem well known in magnetic resonance. A great deal of work has been invested to this end. Early on, pre-saturation of the water resonance was used and greatly decreased the water resonance intensity relative to the metabolites. Another method is to use binomial pulses [Hore, 1983] which have an excitation null which is placed at the frequency of the water resonance. Since this yields a non-uniform excitation profile, the intensities of the ^{1}H resonances must be corrected for the frequency dependence of the excitation profile of the binomial pulse. Akin to presaturation, the application of one or more 90° chemical-shift selective (CHESS) pulses on the water resonance with spoiler gradients following each pulse to dephase the resulting water magnetization provides excellent water suppression [Moonen, 1990]. The sequence is placed prior to the acquisition sequence and works well with the STEAM technique (see below).

The second problem is that of localizing the signals to the area of interest. Early work involved the use of surface coils placed directly over the skull [*e.g.*, Behar, 1983] and adjusting the pulse length so

that the region of the 90° flip angle in the $\mathbf{B}_1$ profile corresponded to the region of interest. However, signals are obtained from regions outside of the region of interest and contamination from surrounding tissue inevitably results.

Another approach is to obtain spectra from a number of slices in three dimensions in a cubic array so that a set of volumes is defined by intersecting slices (the ISIS technique, for example [Ordridge, 1986]). Through algebraic manipulation, cancelation of outside signals is obtained. Drawbacks of such techniques include the time required for each experiment, the sensitivity to subtraction errors, and the sensitivity to animal motion.

With the advent of one-shot volume selective techniques such as STEAM [Frahm, 1990; Gyngell, 1991], time-course volume-selected spectra with reasonable time resolution became feasable. The STEAM technique employs three 90° rf pulses to generate a stimulated echo. During each of these rf pulses a magnetic field gradient is applied, each in a direction orthogonal to the others. Since stimulated echoes are produced only by those spins receiving all three 90° rf pulses, signal from only the volume defined by the intersection of these three slices is observed. Combined with a series of CHESS pulses for water suppression, this method offers an excellent means for studying changes in lactate following cardiac arrest to determine the agonal glycolytic rate constant. Care must be taken to make the echo time shorter than 50 ms, as quantitation of metabolites becomes difficult due to spin coupling effects [Ernst, 1991]. Indeed, an unfortunate choice of echo and mixing times can lead to complete elimination of the lactate resonance due to these coupling effects [Wilman, 1992].

Quantification of metabolites *in vivo* by ^{1}H NMR spectroscopy is a major problem. Calculating peak areas of a metabolite of interest relative to a standard metabolite, such as total choline or NAA, assumes that not only is the concentration of the standard known, but also that no changes in the concentration of the standard occur [Longo, 1995]. For instance, following 5 min of global ischemia in gerbils the choline/creatine ratio decreases over five days and remains low, while no change in NAA occurs [Kuhmonen, 1994]. ^{1}H NMR spectroscopy of tissue extracts verified that it was indeed total choline which decreases (by 31%). Using the endogenous water signal as a concentration standard

[Christriansen, 1993] seems to offer the best method for quantification [Longo, 1995]. Using this method, the concentrations of various compounds in human occipital lobe have been calculated: [NAA] = 11.6 ± 1.3 mM, [Cr/PCr] = 7.6 ± 1.4 mM and [Cho/PCho] = 1.7 ± 0.5 mM [Christiansen, 1993]. However, resonances due to compounds bound to macromolecules (*eg.*, myelin lipids), including H_2O, may be broadened and disappear into the baseline [Fischer, 1989, 1990]. It has been estimated that 10-15% of water is bound and does not contribute to the overall signal. Also, water content differs with brain matter type (81% in grey matter, 71% in white [Norton, 1966]), further causing errors in concentration determinations.

During ischemia, the observed lactate signal increases in a blood glucose dependent manner, increasing with increasing blood glucose concentration [Rudin, 1989; Widmer, 1992; Hoffman, 1994]. Following ischemia, the lactate signal, which increases during ischemia, does not follow the return of tissue pH to the pre-ischemia level, which is facilitated by the Na^+/H^+ exchanger, but slowly recovers through passive washout of lactate [Allen, 1988, 1990]. There is evidence, however, that lactate clearance may be facilitated by a transporter not involved in the regulation of pH [Assaf, 1990]. However, lactate levels recover within 1 hr of reperfusion following as much as 30 min of global ischemia [Hope, 1987; Chang, 1990].

II. MATERIALS AND METHODS

A. Study of the Effect of Glucose Level on Cerebral High-Energy Phosphate Metabolism During and Following Forebrain Ischemia

1. *Animal Preparation*

Male Sprague-Dawley rats weighting 250-320 g were fasted for 24 hr prior to use. Each rat was treated with atropine (0.5 mg/kg) to reduce oropharyngeal secretions and anaesthetized with sodium pentobarbital (60 mg/kg), intubated, and mechanically ventilated throughout the experiment. Rats were kept normothermic during preparation using a heated water blanket, the temperature being monitored throughout the experiment using a tympanic thermocouple probe (Physitemp Inst. Inc. MT-29/1).

The tail artery was exposed and catheterized to allow samples of blood to be taken for blood gas, hematocrit, and blood glucose measurement and for blood pressure recording throughout the experiment. To allow administration of glucose and insulin during the studies, the femoral vein was catheterized and the catheter was attached to the vein with n-butyl-2-cyanoacrylate. The carotid arteries were exposed through a midline neck incision. The temporalis muscles, which might contribute to the observed ^{31}P NMR signal, were removed and a two-turn 1.5 cm × 2 cm elliptical surface coil was positioned over the coronal sutures and sewn under the scalp of each animal.

Each rat was placed into an animal holder, the femoral catheter was connected to an infusion pump (Sage syringed pump, model 355) and blood glucose was altered to the desired level (see below). Brain temperature was maintained at 37.5 ± 0.2°C using a heating/cooling water bath designed to control the temperature of both the body and head. The animal holder was placed into the magnet and pre-ischemia ^{31}P NMR spectra were obtained (see below).

2. *Induction of Reversible Forebrain Ischemia*

The animal was removed from the magnet and both carotid arteries were occluded with temporary aneurism clips. The animal was rapidly repositioned in the magnet in identical position as before and the systemic blood pressure was reduced to a mean of 45 mm Hg by the aspiration of blood from the tail catheter into a heparinized syringe. The acquisition of ^{31}P NMR spectra was commenced when the mean blood

pressure reached 45 mm Hg. After the collection of 9 spectra (9 min of forebrain ischemia), the animal was removed from the magnet and the infusion lines were changed (if alteration of blood glucose level was desired). After 10 min of ischemia, the aneurysm clips were removed, the aspirated blood was reinfused, blood samples were obtained for hematocrit and blood glucose measurements, and the animal was repositioned in the magnet. Acquisition of post-ischemia ^{31}P NMR spectra commenced at 1 minute post-ischemia.

At 15 min intervals, the animal was removed from the magnet for 1 min to obtain a sample for blood glucose and hematocrit determination, and then replaced. After the acquisition of 60 spectra, the animal was removed and final blood gas, hematocrit and blood glucose measurements were obtained before termination of the experiment.

3. *Control of Blood Glucose*

Blood glucose was monitored using a blood glucose meter (One Touch, Lifescan Canada Ltd., Burnaby, Canada), with the measurements based on the glucose oxidase method for whole blood [Marks, 1965]. Prior to ischemia, blood glucose was adjusted to one of three groups: hypo group, blood glucose *ca.* 1.5 mM, N=20; normo group, blood glucose *ca.* 5 mM, N=20; hyper group, blood glucose *ca.* 20 mM, N=13. Each of these groups was divided into subgroups, based on the post-ischemia blood glucose: subgroup hypo of each group was made hypoglycemic, subgroup normo was made normoglycemic and subgroup hyper was made hyperglycemic post-ischemia. The notation used throughout this thesis to define post-ischemia subgroups belonging to individual pre-ischemia groups is *a/b*, where *a* is the pre-ischemia group and *b* is the post-ischemia subgroup under *a*. The administration of insulin to hyperglycemic animals following ischemia failed to produce hypoglycemia within the 1 hr period over which the post-ischemia NMR spectra were obtained, so that only eight of the nine permutations could be studied. Blood glucose levels were altered by administration of boli and infusions (titrated against glucose measurements taken every 10-15 min) as described below. Animals were stabilized at their pre-ischemia blood glucose levels within their respective groups for 30 min prior to ischemia.

In the hypo group, hypoglycemia was induced with a bolus of 0.35 ml/100 g of 7 I.U. insulin/ml saline followed by an infusion of the same solution (variable rate, titrated to a blood glucose concentration of 1.5 mM). Post-ischemia subgroups were created in the following manner:

hypo/hypo: insulin infusion was continued post-ischemia (n=9)
hypo/normo: 0.12 ml/100 g bolus and infusion of 65% glucose/saline solution (n=5)
hypo/hyper: 0.40 ml/100 g bolus and infusion of 65% glucose/saline solution (n=6).

Rats in the normo group were given a 0.15 ml/100 g bolus of 5% glucose/saline solution, followed by infusion of the same solution (variable rate, titrated to a blood glucose concentration of 5 mM). Following ischemia, each subgroup was created by:

normo/hypo: 0.35 ml/100 g bolus of 7 I.U. insulin/ml saline solution followed by infusion (n=6)
normo/normo: continuation of the 5% glucose/saline solution infusion (n=7)
normo/hyper: 0.20 ml/100 g bolus of 65% glucose/saline solution followed by infusion (n=7).

Hyperglycemia in the hyper group was produced by giving each animal a 0.20 ml/100 g bolus of 65% glucose/saline solution followed by infusion of the same solution (variable rate, titrated to a blood glucose concentration of 20 mM). Post-ischemia, the two subgroups were created using:

hyper/normo: 0.40 ml/100 g bolus of 7 I.U. insulin/ml saline solution followed by infusion (n=6)
hyper/hyper: infusion of 65% glucose/saline (n=7).

4. *^{31}P NMR Spectroscopy*

The ^{31}P NMR spectra were obtained at 121.1 MHz using a Bruker Biospec 7.1 T/15 cm spectrometer. Shimming was performed using the ^{1}H NMR signal from brain, resulting in PCr linewidths (full width at half height) of 100.5 ± 13 Hz. Each of the 1 min ^{31}P NMR spectra consisted of 56 transients for signal averaging. The pulse length was set to 70 μs, yielding the maximum PCr signal intensity. Five NMR spectra were obtained pre-ischemia, nine during ischemia and sixty spectra were obtained post-ischemia for each rat. Numerous experiments with control animals verified that removal from the magnet and accurate repositioning of the animals in the magnet did not affect the spectral linewidths, and that reproducible spectra could be obtained. Comparison between pre-ischemia and 1 hr post-ischemia ^{31}P NMR spectra PCr linewidths showed that systematic changes in the spectral linewidths over the course of the experiment did not occur.

Each free-induction decay was multiplied with a 12-point trapezoidal function to decrease the contribution of the broad signal from bone phosphorus and by a 30 Hz line-broadening function to increase the signal-to-noise ratio before Fourier transformation. Each spectrum was phased and a baseline correction was applied.

Since measurement of peak height is minimally affected by errors due to phase and baseline correction and peak overlap [Bain, 1991], peak heights were used to follow changes in P_i, PCr and ATP (using the ß-ATP resonance). For each animal, the peak heights throughout the experiment were determined relative to the mean pre-ischemia PCr peak height, rather than to the pre-ischemia level of each metabolite individually, to facilitate inter-group comparisons during the reperfusion interval when blood glucose levels were changed. Tissue pH was determined using equation 1.

5. *Statistical Analysis*

Physiological variables (blood gases, hematocrit, blood glucose and blood pressure) between groups and between subgroups were compared using analysis of variance with *post hoc* comparisons made using Scheffé's method of intergroup comparison. Comparison between pre- and post-ischemia blood gases (pH, pCO_2, pO_2, and HCO_3^-) within each subgroup were made using analysis of variance.

Repeated-measures least-squares analysis was applied to the ischemic and post-ischemia data separately for P_i, PCr, ATP, and tissue pH using a standard statistics package (CSS:Statistica, StatSoft, Tulsa, OK). The first 20 data points following reperfusion were used to show differences between subgroups within the same group. For analyses showing significant interactions between data curves, the p-values of individual points (with Bonferroni correction) were used to show significance. Comparisons between levels of P_i, PCr, and ATP and values of tissue pH pre-ischemia and 1 hr post-ischemia within subgroups were made with the five pre-ischemia spectra and the last five post-ischemia spectra using analysis of variance.

B. Effect of Glucose Level on Sodium Membrane Gradients and Total Brain Sodium During and Following Forebrain Ischemia

1. *Animal Preparation*

Male Sprague-Dawley rats weighing 250-320 g were prepared as in section II A 1. Each rat was placed into the animal holder which contained the transmission coil, the femoral catheter was connected to an infusion pump (Sage syringed pump, model 355), and blood glucose was altered to the desired level (see below). Brain temperature was maintained at 38.2 ± 0.2°C using heated or cooled water circulated about the head. The animal holder was placed into the magnet and pre-ischemia ^{23}Na NMR spectra were obtained (described below).

2. *Induction of Reversible Forebrain Ischemia*

Following the acquisition of the pre-ischemia spectra, blood pressure was lowered to a mean of 45 mm Hg through aspiration of blood from the tail catheter into a heparinized syringe, at which point the carotid arteries were pulled into a small diameter tubing with the ligatures in order to occlude the arteries. This is a more sophisticated method of producing ischemia than in section II A 2, with the animal remaining inside the magnet at all times. In this way, the acquisition of ^{31}P or ^{23}Na NMR spectra can begin at the moment the carotid arterial occlusion commences. After 10 min of ischemia, cerebral perfusion was restored and the aspirated blood was reinfused.

3. *Control of Physiological Parameters*

Blood glucose was monitored using a blood glucose meter (One Touch, Lifescan Canada Ltd., Burnaby, Canada) [Marks, 1965]. Prior to ischemia, blood glucose was adjusted to one of three groups: hypo group, hypoglycemic (blood glucose *ca.* 2 mM, N=7); normo group, normoglycemic (blood glucose *ca.* 6 mM, N=7); hyper group, hyperglycemic (blood glucose *ca.* 20 mM, N=7). Blood glucose levels were altered by administration of boluses and infusions (titrated against glucose measurements taken every 10 min) as described below. The hypo and normo groups were made isoosmolar with the hyper group by including 25% weight/volume (w/v) mannitol in the solutions. A fourth group (blood glucose *ca.* 7 mM, N=7), used as a

control to enable the observation of possible effects due to changes in osmolarity, was made normoglycemic without the addition of mannitol. Animals were stabilized at their pre-ischemia blood glucose levels for 20 min prior to ischemia.

In the hypo group, hypoglycemia was induced with a bolus of 0.20 ml/100 g of 7 I.U./ml insulin-25% w/v mannitol/saline solution followed by an infusion of 0.5% w/v glucose-25% w/v mannitol at a rate of 0.98 ± 0.15 ml/100 g/hr. Rats in the normo group were given a 0.20 ml/100 g bolus of 5% w/v glucose-25% w/v mannitol/saline solution, followed by infusion of the same solution (variable rate (mean 1.10 ± 0.07 ml/100 g/hr), titrated to a blood glucose concentration of 6 mM). Hyperglycemia in the hyper group was produced by giving each animal a 0.20 ml/100 g bolus of 65% w/v glucose/saline solution followed by infusion of the same solution (variable rate (mean 1.00 ± 0.28 ml/100 g/hr), titrated to a blood glucose concentration of 20 mM). The control group was given a 0.20 ml/100 g bolus and infusion (variable rate (mean 1.16 ± 0.18 ml/100 g/hr), titrated to a blood glucose concentration of 6 mM) of 5% w/v glucose/saline solution with no mannitol for adjustment of osmolarity.

4. *In vitro Analysis of Brain Water and Sodium Content*

The brain water and sodium content was determined prior to ischemia, immediately following ischemia and at 20, 40, 60 and 90 min of reperfusion in rats normoglycemic and prior to ischemia and at 70 min following ischemia in rats hypoglycemic during ischemia. Brains were removed from the skull within 30s and the brains placed into pre-weighed vials. The brains were then freeze-dried for 24 hr and the vials again weighed. The difference in mass due to freeze-drying divided by the brain wet weight yielded the water content of the brain.

The dried brains were then dissolved in 20 ml of 8 M nitric acid for a 7 day period. Following this, the solution was diluted to 50.00 ml with de-ionized water. A 5.00 ml aliquot was then taken, and again diluted to 50.00 ml. This procedure diluted the sodium concentration to between 0 and 10 ppm. Sodium content of the solution was determined using flame emission spectroscopy using the sodium D line. For each sample the mean integrated signal (four were taken for each sample and averaged) was compared to a calibration curve created using a series of standards of NaCl dissolved in de-ionized water

and the sample sodium concentration determined. From this the sodium content (mg) per g dry weight was calculated.

5. *In vitro* ^{31}P *and* ^{23}Na *NMR Spectroscopy*

To determine the dependence of the intensity of the ^{23}Na DQ NMR signal on pH, samples of homogenized brain tissue (N=5) were prepared and titrated over the range of pH 7.3 to pH 5.5 at 38°C. At each pH sampled, ^{31}P and SQ and DQ ^{23}Na NMR spectra were obtained.

Pentobarbital-anaesthetized rats were perfused using saline solution, decapitated and the brains were removed. Each of the five samples consisted of one rat brain homogenized in 0.9% NaCl/D_2O solution (1:1 brain/saline ratio) with a small amount (*ca.* 10 mg) of phenylphosphonate added to act as a ^{31}P NMR chemical shift reference. The homogenized samples were then placed in 10 mm NMR sample tubes and frozen till use. During each experiment, the sample was titrated with small amounts of 1 M NaOH/D_2O saline solution to raise pH or 1 M HCl/D_2O saline solution to lower pH. The titration was started at pH 5.5 for three samples and at pH 7.3 for two samples so that any systematic changes in samples over time could be detected.

All *in vitro* 79.39 MHz ^{23}Na NMR experiments were performed at 38.0°C using a Bruker AM300 NMR spectrometer with a commercial multi-nuclear broadband probe. Shimming was performed on the ^{1}H NMR signal from water. Each *in vitro* SQ ^{23}Na NMR spectrum consisted of the sum of 64 transients (1024 data points) with spectral width 5000 Hz, dwell time 50.0 μs, acquisition time 0.050 s and relaxation delay 0.085 s. The spectra were collected using CYCLOPS phase cycling. Both *in vitro* and *in vivo* (see below) DQ filtered ^{23}Na NMR spectra were obtained using the sequence [Bax, 1980]

$$90°_{\phi} - \tau/2 - 180°_{\phi\pm90°} - \tau/2 - 90°_{\phi+90°} - \delta - 90° - \text{Acq},$$

where ϕ is the axis along which the excitation field $\mathbf{B}_1$ is applied in the rotating frame of reference, τ is the echo delay time and δ is the DQ evolution time. In order to select the DQ NMR signal from SQ and triple-quantum signals also generated by this pulse sequence, a 32-step phase cycling procedure was employed [Piantini, 1982]. No significant changes in the area of the ^{23}Na SQ resonance occurred in any sample throughout the experiment, so that the peak height of the ^{23}Na DQ resonance directly reflected the change in intensity of the ^{23}Na DQ signal with pH. Spectral acquisition parameters for the *in vitro* DQ ^{23}Na NMR

spectra were similar to those used for the *in vitro* SQ ^{23}Na NMR spectra, with τ selected to be 8 ms (the optimized value of τ used in the *in vivo* studies (below)).

Sample pH was determined from the difference in chemical shift of inorganic phosphate (P_i) and phenylphosphonate from 121.3 MHz ^{31}P NMR spectra and comparing this value to the corresponding pH from a previously prepared calibration curve (data not shown). Spectra were obtained for 8-15 pH values for each sample.

Linear fits to plots of ^{23}Na DQ peak height (relative to the peak height at pH 7.15) against pH for each sample were prepared and the regression lines were scaled between samples by requiring the peak height at pH 7.15 to be 1.0. The slope of each plot yielded the change in the intensity of the ^{23}Na DQ resonance per pH unit. The linear regression parameters were then averaged to give the pH correction factor, f_{pH}.

6. *<u>In vivo</u> ^{31}P NMR Spectroscopy*

In vivo ^{31}P NMR spectroscopy, performed at 121.2 MHz using a Bruker Biospec 7/21 spectrometer, was used to determine the mean tissue pH of hypo- (N=5), normo- (N=4) and hyperglycemic (N=5) rats during and following ischemia. For data acquisition, a 1.5 cm X 2.0 cm two-turn surface coil tuned to 121.2 MHz was placed over the coronal sutures and served both as transmitter and receiver. Each spectrum consisted of a sum of 32 transients (1024 data points) collected using CYCLOPS phase cycling (with spectral width 10000 Hz, relaxation delay 0.883 s, dwell time 50.0 μs, acquisition time 0.0512 s). To reduce the contribution of bone phosphorus to the overall signal, a pre-saturation pulse was applied 3000 Hz downfield from the PCr ^{31}P NMR resonance during the relaxation delay.

Tissue pH was calculated using equation 1. The plots of tissue pH against time during ischemia for each blood glucose group were fitted to the data with an equation of the form

$$pH^i = pH^i_\infty + (pH^i_0 - pH^i_\infty)\, e^{-k^i_{pH} t^i}, \qquad (54)$$

where the superscript `i' represents `ischemia', pH_0 and pH_∞ are the pH values at time (t) 0 min ischemia and at infinity, respectively, and k_{pH}^{i} is the first-order rate constant for the exponential decrease in pH during ischemia. The data obtained post-ischemia were fit to the equation

$$pH^p = pH_0^p + (pH_\infty^p - pH_0^p)\, e^{-k_{pH}^p t^p}, \qquad (55)$$

where the superscript `p' represents `post-ischemia', pH_0 and pH_∞ are the pH values at the beginning of reperfusion and at an infinite time of reperfusion, and k_{pH}^{p} is the first-order rate constant for the exponential recovery of tissue pH.

7. *<u>In vivo</u> ^{23}Na NMR Spectroscopy*

Interleaved serial *in vivo* SQ and DQ ^{23}Na NMR spectra were obtained at 79.455 MHz using a Bruker Biospec 7/21 spectrometer. For transmission, a 5.0 cm diameter saddle coil tunable to both the ^{1}H (300.13 MHz) and ^{23}Na frequencies was used, while reception was accomplished through the use of a 1.8 X 2.3 cm elliptical surface coil tuned to the ^{23}Na frequency and orthogonalized with respect to the saddle coil. The ^{1}H signal of water was used for shimming.

The SQ ^{23}Na NMR spectra were obtained using a one-pulse experiment, each consisting of 24 transients (512 data points) collected using CYCLOPS phase cycling, with pre-acquisition delay 100 μs, relaxation delay 0.085 s, spectral width 2500 Hz, dwell time 200.0 μs and acquisition time 0.1024 s.

Each DQ ^{23}Na NMR spectrum (512 data points) was obtained using 128 scans and acquisition parameters identical to those for the SQ ^{23}Na NMR spectra, and with the evolution time δ set to 25 μs and the echo delay time τ set to 8 ms. The DQ ^{23}Na NMR signal was found to be at a maximum for this value of τ. The double-quantum coherences were separated from the single- and triple-quantum signals using phase cycling [Piantini, 1982]. The 90° pulse was 280 μs, and was determined by finding the null excitation produced by the 180° pulse. To avoid possible off-resonance effects the spectral frequency was adjusted to ensure fulfilment of the on-resonance condition. Acquisition of a SQ and DQ ^{23}Na NMR spectral pair required 30 s; ten pairs of interleaved SQ and DQ ^{23}Na NMR spectra were obtained pre-ischemia, twenty pairs during ischemia, and 120 pairs post-ischemia for each rat.

A 5 Hz linebroadening function was applied to the SQ ^{23}Na NMR free-induction decays and zero-filling to 2048 data points. The free-induction decays were Fourier transformed and the resulting spectra were phased. Baseline distortion in each spectrum was removed using a deconvolution baseline correction procedure. Peak integrals were used as a measure of total brain sodium concentration ($[Na^+]_t$) relative to the mean pre-ischemia level.

Each DQ ^{23}Na NMR free-induction decay was multiplied with a 25 Hz line-broadening function to optimize signal-to-noise and zero-filled to 2048 data points. Following Fourier transformation of each free-induction decay, the resulting spectrum was phased and the peak height relative to the mean pre-ischemia peak height was used in the analysis. Lineshape simulation of the DQ ^{23}Na spectra was not performed since the signal-to noise ratio was insufficient to obtain precise estimates of intensity and linewidth parameters. Since any changes in the relaxation parameters of the DQ resonance would be negligible to the line-broadening function, and since measurement of peak height is affected less than peak areas by errors due to phase and baseline correction [Bain, 1991], the use of peak height to give a measure of intracellular Na^+ is justified. The raw DQ ^{23}Na NMR peak heights were then multiplied by $1/(1-f_{pH}\cdot\delta pH)$, where f_{pH} is the change in the ^{23}Na DQ NMR peak height per pH unit (above) and δpH is the difference in pH relative to the pre-ischemia pH, to obtain the pH-corrected ^{23}Na DQ NMR peak heights.

Rates of sodium ion homeostasis loss during ischemia and recovery following the insult were found using equations similar to those used for the *in vivo* ^{31}P NMR data. Equation 56 was used to fit the data obtained during ischemia:

$$I^i = I^i_\infty + (1 - I^i_\infty)\, e^{-k^i_{DQ} t^i}, \qquad (56)$$

where t^i is the time of ischemia, $I_\infty{}^i$ is the DQ ^{23}Na NMR signal peak height at $t^i = \infty$ and $k_{DQ}{}^i$ is the first-order rate constant for the increase in the peak heights during ischemia. Since a delay of *ca.* 30 s is observed before the increase in the DQ ^{23}Na NMR peak height occurs in the normo and hyper groups, $t^i = 0$ was set at 30 s of ischemia for these groups.

The DQ peak height falls to below the pre-ischemia value early in reperfusion in the hypo and normo groups, with subsequent recovery. Therefore, to fit the data obtained during reperfusion, a third term was added to give an equation of the form:

$$I^P = I_0^P + (I_\infty^P - I_0^P)\, e^{-k_{DQ}^P t^P} + I_{rec}^P (1 - e^{-k_{DQ}^{rec} t^P}), \qquad (57)$$

where t^P is the reperfusion time, I_0^P and I_∞^P are the DQ peak heights relative to the pre-ischemia peak height at $t^P = 0$ and $t^P = \infty$, I_{rec}^P is the recovery of the peak height at $t^P = \infty$, k_{DQ}^P is the rate constant for the initial fall in the DQ peak height and k_{DQ}^{rec} is the rate constant for the subsequent rise in the peak height late in reperfusion.

8. *Statistical Analysis*

Physiological variables (blood gases, osmolarity, hematocrit, blood glucose and blood pressure), brain water and brain sodium content between groups were compared using analysis of variance with *post hoc* comparisons made using Scheffé's method of intergroup comparison (level of significance taken to be $p < 0.02$) using a standard statistics package (CSS:Statistica, StatSoft, Tulsa, OK).

The temporal curves of SQ and DQ ^{23}Na NMR intensity data from the control, hypo, normo and hyper groups were compared using repeated measures least-squares analysis (level of significance $p = 0.05$) using a commercial statistics package (CSS:Statistica, StatSoft, Tulsa OK). For those curves showing significant interaction and $p > 0.02$, data points were compared (with Bonferoni correction) at each time point. Parameter estimates from eqs. 4 and 5 were obtained using a Levenberg-Marquardt non-linear least squares minimization algorithm [Marquardt, 1963]. Standard deviations of these parameters, obtained from the covariance matrix used in the fitting procedure, were used to calculate confidence limits in the parameters at different p-values using the Student's t-test.

C. Study of the Effect of Glucose Level on the Forward Creatine Kinase Rate Constant Following Forebrain Ischemia

1. *Animal Preparation, Control of Physiological Parameters and Induction of Reversible Forebrain Ischemia*

Male Sprague-Dawley rats 300-350 g were anaesthetized using 0.7% halothane in 1:1 O_2/N_2O gas mixture without intubation. For induction of forebrain ischemia, the tail artery was catheterized and the carotid arteries ligated as described above. Blood gas and blood glucose measurements were obtained from blood samples taken from the tail artery. For the group of rats hyperglycemic during ischemia, blood glucose was altered using an intraparitoneal injection of 65% glucose/saline solution (0.5 ml/100 g dosage). Following 10 min forebrain ischemia, the animals were allowed to recover.

Immediately prior to insertion of the animals into the magnet for saturation transfer measurements, the animals were anaesthetized with the above gaseous mixture, intubated and ventilated. A two-turn 1.5 × 2 cm elliptical surface coil was sewn over the coronal sutures. The animal was then placed into the animal holder which effectively immobilized the head during the spectroscopic measurements. Temperature was monitored using a tympanic thermocouple and controlled with heated and cooled air blown over the animal as necessary. Measurements of k_{for} were taken in normal rats prior to ischemia and at 4 hr (n = 6 following normoglycemic ischemia, n = 6 following hyperglycemic ischemia), 1 day (n = 5, n = 5), 2 days (n = 5, n = 6), 3 days (n = 5, n = 5), 5 days (n = 5, n = 5) and 7 days (n = 5, n = 5) following recovery from ischemia.

2. *In vivo Saturation Transfer ^{31}P NMR Spectroscopy*

In vivo ^{31}P saturation transfer NMR spectroscopy, performed at 121.2 MHz using a Bruker Biospec 7/21 spectrometer, was used to determine the forward creatine kinase rate constant, k_{for}, for normo- and hyperglycemic rats prior to and following ischemia. For data acquisition, the two-turn surface coil served as both transmitter and receiver. Shimming was performed on the ^1H NMR water resonance to produce ^{31}P NMR PCr resonance linewidths (full width at half height) of 93.2 ± 11 Hz.

The γ-ATP peak was saturated using a low-power saturation pulse τ (of duration 0, 6, 0.5, 4, 1 and 2 s, collected in this order). Prior to the on-resonance saturation pulse, an off-resonance saturation pulse of duration (6-τ) s was applied at a frequency downfield from the PCr resonance equal to the frequency difference between the PCr and γ-ATP resonances. Each spectrum consisted of a sum of 90 transients (1024 data points) collected using CYCLOPS phase cycling (with spectral width 10000 Hz, relaxation delay 0.883 s, dwell time 50.0 μs, acquisition time 0.0512 s). The excitation pulse length was determined by maximizing the PCr resonance intensity and was set to 160 μs.

Each free-induction decay was zero-filled to 8192 data points and multuplied with a line-broadening factor of 30 Hz prior to Fourier transformation. Each spectrum was phase- and baseline-corrected using an automatic spline curve fit routine using software supplied with the spectrometer. The PCr peak height in the spectrum obtained with $\tau = 0$ s for each experiment was set to 1 and all other PCr peak heights were measured relative to this value.

3. *Statistical Analysis*

Equation 14 was fitted to the data for each individual rat to determine the values of the parameters k_{for} and $T_{1,PCr}$ using a computer program (Curve Expert, Central, SC). It was found that the value of $T_{1,PCr}$ did not change significantly for any time following ischemia, so that an average value of $T_{1,PCr} = 2.62 \pm 0.18$ s was used to determine the value of the forward creatine kinase rate constant k_{for}. Student's t-test was used to determine significant differences between the pre- and post-ischemia values of k_{for} and differences between rats which were normo- and hyperglycemic during ischemia at each time point following ischemia. A standard statistics package was used for the analysis (CSS, StatSoft, Tulsa, OK).

D. Study of the Effect of Glucose Level on the Agonal Glycolytic Rate Constant Following Forebrain Ischemia

1. *Animal Preparation, Control of Physiological Parameters and Induction of Reversible Forebrain Ischemia*

Male Sprague-Dawley rats 300-350 g were prepared, blood glucose was altered, and ischemia was induced as described above in the creatine kinase experiments. At the time of the measurement of the agonal glycolytic rate constant k_{AGR}, the animals were anesthetized, intubated and ventilated. A midline neck incision was made and the right jugular vein was exposed, ligated and catheterized. The animal was placed into the holder and ventilated, as in section C. Measurements of k_{AGR} were taken in normal rats and at 4 hr, 1 day, 2 days, 3 days, 5 days and 7 days of recovery from normoglycemic or hyperglycemic ischemia (n = 5 in all groups).

2. *<u>In vivo</u> STEAM ^1H NMR Spectroscopy*

A single-turn, 2.5 cm circular surface coil was centered on the scalp over the coronal sutures with the animal in the holder. Shimming was performed using the ^1H NMR signal from water in the tissue. A sagital spin-echo pilot image (256 × 256 pixel resolution, 2mm slice thickness, echo time 20 ms, repetition time 1 s) was taken, followed by a transverse image in order to place the volume of localization in the proper region of the brain.

The STEAM, sequence preceeded by a series of three chemical-shift selective pulses to suppress the water signal,

$$[\text{CHESS} - \text{Spoil}]_3 - 90^\circ_x - \frac{\text{TE}}{2} - 90^\circ_y - \text{TM} - 90^\circ_z - \frac{\text{TE}}{2} - \text{Acq},$$

where TE (set to 20 ms) is the echo time and TM (set to 30 ms) is the mixing time for the stimulated echo, was used to obtain volume-selected ^1H NMR spectra in rat brain. The values of TE and TM were set to similar values used by Frahm, 1991. The volume of interest, 8 × 5 × 5 mm^3, was selected to sample ^1H NMR signals from the hippocampus, thalamus, striatum and the lower cortex layers. Using the STEAM localization sequence, the 90° 1 ms sinc-shaped pulse gains were optimized and shimming was performed

on the volume of interest, resulting in water resonance linwidths (full width at half-height) of better than 0.08 ppm. The gains of the 25.6 ms CHESS water suppression pulses were then optimized by minimization of the water signal in the volume of interest. A pre-mortem spectrum was taken consisting of 256 scans, 1024 data points, repetition time 1.5 s, spectral width 3000 Hz. Immediately following, 1 ml of 4M KCl was injected through the jugular catheter. Simultaneously, a series of 50 post-mortem STEAM ^{1}H NMR spectra were obtained with parameters similar to those used to obtain the pre-mortem spectrum, except 20 scans per spectrum was used (30 s acquisition time each).

The pre-mortem free induction decay was subtracted from each of the post-mortem spectra (correcting for the difference in the number of scans). The subtracted free induction decay was multiplied by a 15 Hz line-broadening function, Fourier transformed and baseline corrected with an automatic spline fit routine. The lactate peak height at the end of the experiment, where no further increase in lactate was apparent, was used to normalize the lactate peak height in each experiment.

3. *Statistical Analysis*

A fit to the equation

$$y = C\left(1 - e^{-k_{AGR}t}\right) \tag{58}$$

where C is a scaling factor proportional to the final lactate concentration, k_{AGR} is the agonal glycolytic rate constant describing the first order kinetics of the formation of lactate from glucose, and t is the time following KCl injection, was made in order to determine the mean values of k_{AGR} for each group at each time point studied following ischemia. The fit was performed using a computer program (Curve Expert, Central, SC) which employed a Levenberg-Marquardt non-linear least-squares minimization algorithm.

Student's t-test was used to determine significant differences between the pre- and post-ischemia values of k_{AGR} and differences between rats which were normo- and hyperglycemic during ischemia at each time point following ischemia. For this purpose, a standard statistical package was used (CSS, StatSoft, Tulsa, OK)

III. RESULTS

A. Effect of Glucose Level on High-Energy Phosphate Metabolism During and Following Forebrain Ischemia

1. *Physiological Variables*

Table 1 shows the physiological variables measured during this study. Blood gases were monitored and maintained within normal limits throughout each experiment. A significant post-ischemia systemic acidosis for each subgroup ($p < 0.02$) was observed, as is normal for this model [Sutherland, 1991].

Hyper group rats had a significantly higher pre-ischemia blood pressure than the other groups ($p < 0.02$). No significant early differences in the post-ischemia blood pressure were observed between subgroups. However, in subgroup hypo/hypo, as the reperfusion interval increased a gradually decreasing or erratic blood pressure (at times reaching over 200 mm Hg) was observed. This was accompanied by changes in the ^{31}P NMR spectrum, including a decrease in the ATP and PCr peak heights and an elevation of the P_i peak height, before the completion of 1 hr reperfusion. The experiment was terminated when these changes appeared, and the data obtained from the time these changes became apparent were not included in the statistical comparisons.

Pre-ischemia hematocrits were higher than those taken before infusion of solutions, but were not significantly different between groups. Post-ischemia subgroup hypo/hyper had significantly lower hematocrits than several of the other subgroups (at 45 min post-ischemia, vs. normo/hypo, $p = 0.0074$; normo/normo, $p = 0.016$; hyper/normo, $p = 0.022$: at 60 min post-ischemia, vs. normo/hypo, $p = 0.043$).

In accordance with the experimental design, pre-ischemia blood glucose concentrations were significantly different between the three groups ($p < 0.002$). Post-ischemia blood glucose concentrations between subgroups within each group showed significant differences within 15 min following reperfusion, except between subgroups hypo/hypo and hypo/normo. In these two subgroups, 30 min were required for blood glucose to become significantly different (level of significance was taken to be $p < 0.02$).

Table 5. Physiological variables (blood glucose (mM), hematocrits (%), blood gases, blood pressure (mm Hg); mean ± SD) prior to and following transient cerebral ischemia (pre-ischemia/post-ischemia blood glucose) for the ^{31}P NMR experiments.

	hypo/hypo (n=9)	hypo/normo (n=5)	hypo/hyper (n=6)	normo/hypo (n=6)	normo/normo (n=7)	normo/hyper (n=7)	hyper/normo (n=6)	hyper/hyper (n=7)
Blood glucose								
Pre-ischemia	1.61 ± 0.38	1.52 ± 0.41	1.56± 0.39	4.58 ± 0.19	4.33 ± 0.35	4.38 ± 0.58	21.2 ± 6.3	19.0 ± 2.2
0 min post	1.14 ± 0.29	1.20 ± 0.40	1.55 ± 0.87	5.62 ± 0.66	5.15 ± 0.87	7.37 ± 1.46	20.2 ± 4.5	24.9 ± 2.7
15 min post	1.18 ± 0.33	5.50 ± 2.21	21.8 ± 10.1	3.12 ± 0.75	4.70 ± 0.64	17.8 ± 5.5	11.1 ± 5.0	21.3 ± 5.9
30 min post	0.98 ± 0.41	7.67 ± 5.64	20.5 ± 6.7	2.10 ± 0.85	4.62 ± 0.82	16.6 ± 4.7	7.07 ± 3.40	22.1 ± 7.5
45 min post	0.98 ± 0.50	3.77 ± 1.67	18.0 ± 2.6	1.64 ± 0.50	5.25 ± 1.33	22.0 ± 3.4	5.53 ± 2.61	22.6 ± 5.4
60 min post	0.80 ± 0.31	5.27 ± 3.18	20.6 ± 2.9	1.20 ± 0.17	4.95 ± 1.47	20.4 ± 4.5	4.27 ± 1.42	21.2 ± 6.1
Hematocrits								
Pre-ischemia	52.8 ± 9.7	53.3 ± 5.1	51.0 ± 6.8	58.0 ± 2.1	53.6 ± 5.2	46.3 ± 8.9	50.8 ± 6.6	48.5 ± 6.6
0 min post	44.0 ± 4.2	47.3 ± 3.1	46.2 ± 4.8	42.4 ± 4.3	43.3 ± 4.8	38.7 ± 3.6	41.0 ± 4.6	35.8 ± 4.3
15 min post	47.6 ± 6.4	44.7 ± 1.5	40.8 ± 2.5	47.2 ± 6.3	48.3 ± 3.4	38.7 ± 3.7	45.3 ± 8.1	37.5 ± 6.6
30 min post	45.4 ± 3.0	44.0 ± 5.2	39.0 ± 1.4	49.8 ± 6.3	49.5 ± 3.7	42.0 ± 3.8	46.3 ± 1.5	34.5 ± 11.1
45 min post	46.0 ± 3.9	46.0 ± 1.7	39.0 ± 1.8	49.6 ± 4.9	48.5 ± 4.2	45.3 ± 3.6	46.7 ± 2.1	41.8 ± 9.3
60 min post	43.4 ± 1.5	45.3 ± 3.8	41.2 ± 3.9	50.4 ± 3.1	47.8 ± 5.3	43.2 ± 5.0	46.7 ± 1.5	40.0 ± 5.8
Blood gases								
Pre pH	7.29 ± 0.06	7.30 ± 0.04	7.26 ± 0.04	7.33 ± 0.02	7.26 ± 0.03	7.32 ± 0.02	7.29 ± 0.06	7.31 ± 0.04
Post pH	7.12 ± 0.06	7.12 ± .06	7.13 ± 0.05	7.22 ± 0.05	7.17 ± 0.08	7.26 ± 0.04	7.17 ± 0.07	7.15 ± 0.09
Pre P_{CO_2}	34.2 ± 5.8	33.5 ± 2.3	36.8 ± 7.4	32.6 ± 4.9	35.6 ± 4.5	37.7 ± 5.0	36.0 ± 6.9	34.6 ± 8.4
Post P_{CO_2}	34.2 ±4.5	37.8 ± 3.3	36.6 ± 5.9	36.5 ± 8.3	41.8 ± 8.2	33.3 ± 3.4	36.5 ± 10.6	35.9 ± 5.8
Pre P_{O_2}	194 ± 75	168 ± 13	180 ± 25	237 ± 89	169 ± 25	164 ± 17	194 ± 24	195 ± 42
Post P_{O_2}	173 ± 56	184 ± 21	192 ± 97	197 ± 29	182 ± 33	161 ± 24	164 ± 75	190 ± 53
Pre HCO_3^-	18.4 ± 5.2	16.8 ± 1.8	17.1 ± 2.1	17.2 ± 2.0	16.1 ± 1.4	19.6 ± 3.0	17.5 ± 2.2	17.8 ± 3.2
Post HCO_3^-	11.4 ± 0.8	12.5 ± 2.2	12.5 ± 2.6	15.8 ± 3.6	15.6 ± 2.7	15.0 ± 1.9	13.3 ± 2.9	12.7 ± 3.2
Blood Pressure								
Pre-ischemia	115 ± 10	100 ± 15	105 ± 13	105 ± 16	108 ± 13	108 ± 21	120 ± 12	122 ± 15
2 min post	110 ± 19	99 ± 24	112 ± 21	126 ± 17	125 ± 14	135 ± 20	128 ± 10	117 ± 16

2. *^{31}P NMR Spectroscopy*

A typical ^{31}P NMR spectrum is shown in figure 6, showing the major resonances observed in adult rat brain. Figure 7 shows a set of ^{31}P NMR spectra taken pre-, during and post-ischemia for a typical rat from each group. Differences in the decrease of ATP and PCr peaks and in the increase of the P_i peak during ischemia are clearly evident, as are the differences in their post-reperfusion recovery. Subsequent decreases in PCr and ATP in hypoglycemic animals (spectra of hypo/hypo subgroup), together with the erratic blood pressure post-ischemia described above, are also apparent.

Figures 8-13 show plots of peak heights of the P_i, PCr and ß-ATP resonances and tissue pH as a function of time for the three groups. No significant differences in the peaks of interest or in tissue pH were observed between the three groups of rats prior to ischemia.

2a. *Changes during ischemia for hypo-, normo- and hyperglycemic rats*

During ischemia, hypo group rats showed a rapid decrease in PCr (vs. normo group, $p = 0.0002$; vs. hyper group, $p = 0.0023$; refer to the bottom figures 8, 10, and 12) and in ATP (vs. normo group, $p < 0.0001$; vs. hyper group, $p = 0.0020$; refer to the top of figures 9, 11, and 13). The decrease in PCr during ischemia was not significantly different between the normo and hyper groups using repeated measures least squares analysis. The apparent first-order rate constants for the decrease in PCr during ischemia were: 1.24 ± 0.08 min^{-1} for hypo, 1.05 ± 0.09 min^{-1} for normo and 0.53 ± 0.05 min^{-1} for hyper groups. The decrease in ATP during ischemia was not significantly different between the normo and hyper groups using repeated measures least squares analysis. Those for the decrease in ATP during ischemia are: 1.10 ± 0.10 min^{-1} for hypo, 0.70 ± 0.08 min^{-1} for normo and 0.41 ± 0.07 min^{-1} for hyper groups. The disappearance of both ATP and PCr in this group was nearly complete at the end of 10 min of ischemia. The concomitant rise in P_i associated with energy failure (apparent first-order rate constants: 0.60 ± 0.06 min^{-1} for hypo, 0.34 ± 0.06 min^{-1} for normo and 0.09 ± 0.04 min^{-1} for hyper groups; refer to the top of figures 8, 10, and 12) was greatest in the hypo group (vs. both normo and hyper groups, $p < 0.0001$) and least in the hyper

group (vs. normo group, $p = 0.018$). The observed drop in tissue pH during ischemia was smallest in the hypo and greatest in the hyper group ($p < 0.0001$ between all groups; apparent first-order rate constants: 1.85 ± 0.64 min^{-1} for hypo, 0.65 ± 0.07 min^{-1} for normo and 0.28 ± 0.04 min^{-1} for hyper groups; refer to the bottom of figures 9, 11, and 13). In the hyper group, tissue pH in several rats decreased below the value which can be accurately measured using ^{31}P NMR spectroscopy [Petroff, 1985] (tissue pH < 5.8). Data points in figure 13 below this value may not represent true tissue pH.

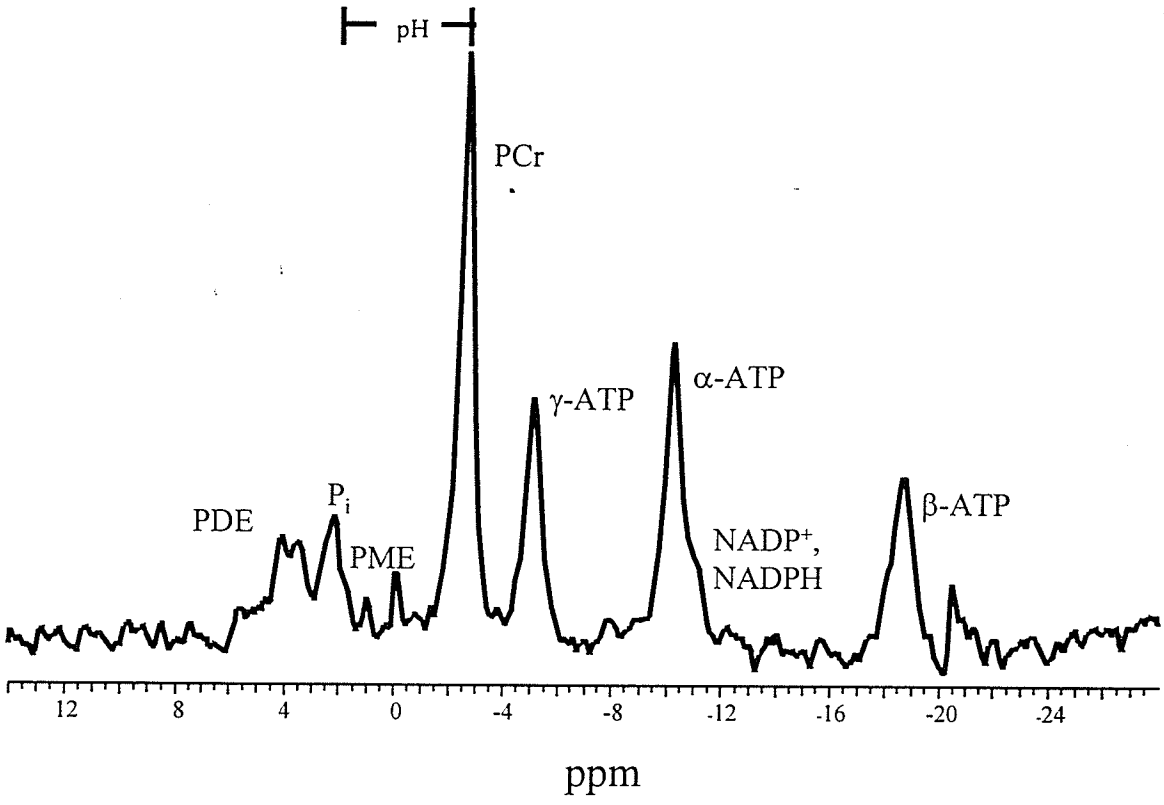

Figure 6. 121 MHz ^{31}P NMR spectrum from a normal rat brain showing the major phosphorus-containing compounds: $NADP^+$, NADPH = nicotinamide adenine dinculeotide phosphate, PDE = phosphodiesters, P_i = inorganic phosphate, PME = phosphomonoesters, PCr = phosphocreatine. The broad bone phosphorus resonance has been removed by presaturation.

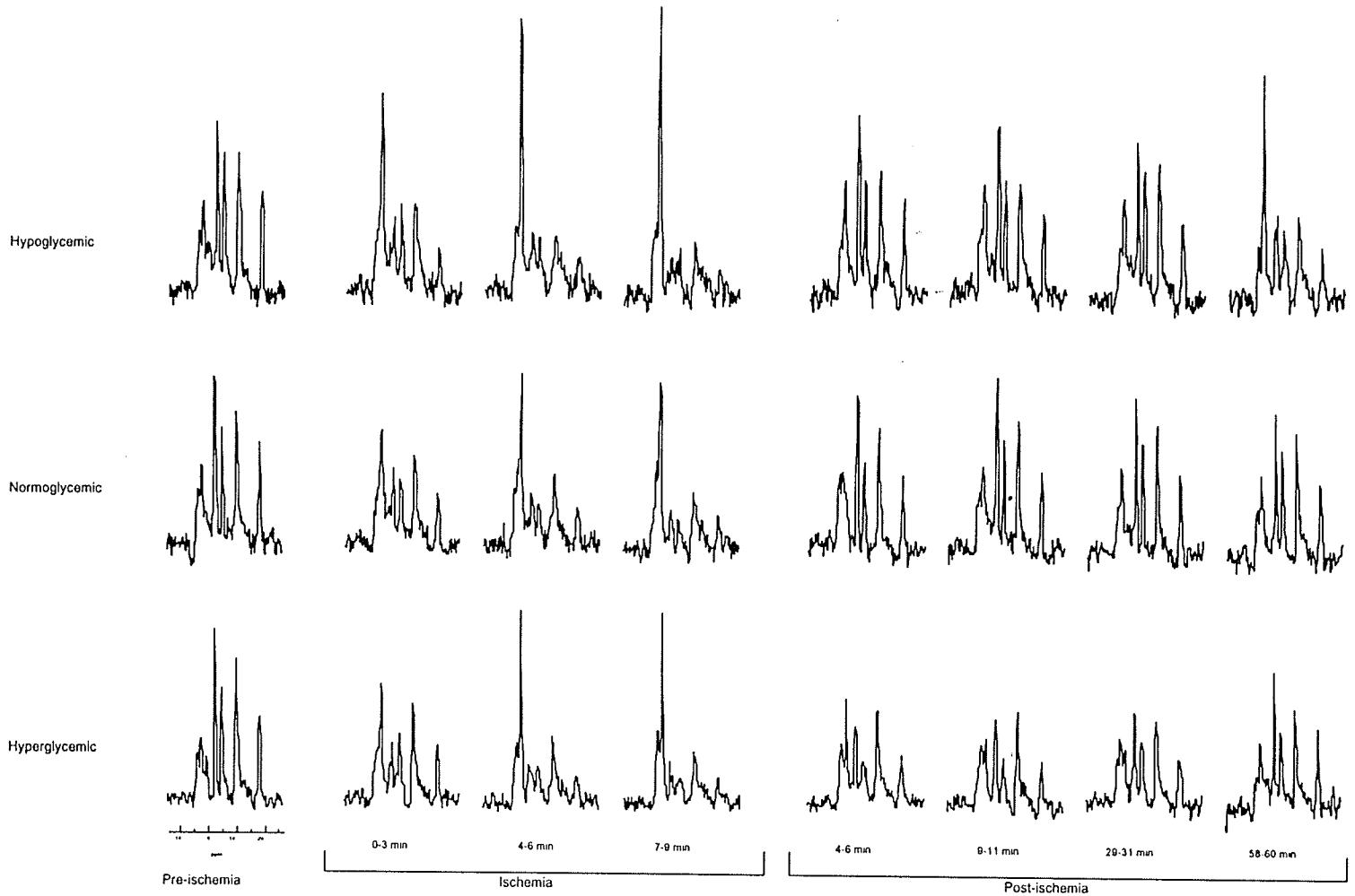

Figure 7. ^{31}P NMR spectra collected prior to, during and following transient cerebral ischemia in hypo-, normo- and hyperglycemic rats. Each spectrum consists of a sum of three one-minute spectra. Note the rise in P_i accompanying the fall in the PCr and the three ATP resonances during ischemia.

2b. *Post-ischemia changes for rats hypoglycemic prior to ischemia*

Post-ischemia in the hypo group, no significant differences in the recovery of PCr and ATP were observed between subgroups. PCr recovered to pre-ischemia levels within 5 min of reperfusion. ATP recovered rapidly, but did not reach pre-ischemia levels, remaining depressed at about 80-85% of pre-ischemia level at the end of the experiment in all subgroups ($p < 0.0001$, compared to pre-ischemia levels). In the hypo/hyper subgroup, P_i remained elevated compared to that in the hypo/normo subgroup ($p < 0.004$ for the first two points post-ischemia) following the addition of glucose, but returned to normal after 5 min. P_i in the hypo/hypo subgroup, but not in hypo/normo or hypo/hyper subgroups, remained elevated throughout the recovery period relative to pre-ischemia levels ($p < 0.0001$ at 60 min post-ischemia). Recovery of tissue pH was impaired for several minutes after the addition of glucose in the hypo/hyper subgroup ($p = 0.0007$ compared to the hypo/normo subgroup), but was not significantly different from pre-ischemia values in any of the subgroups at the end of the experiment.

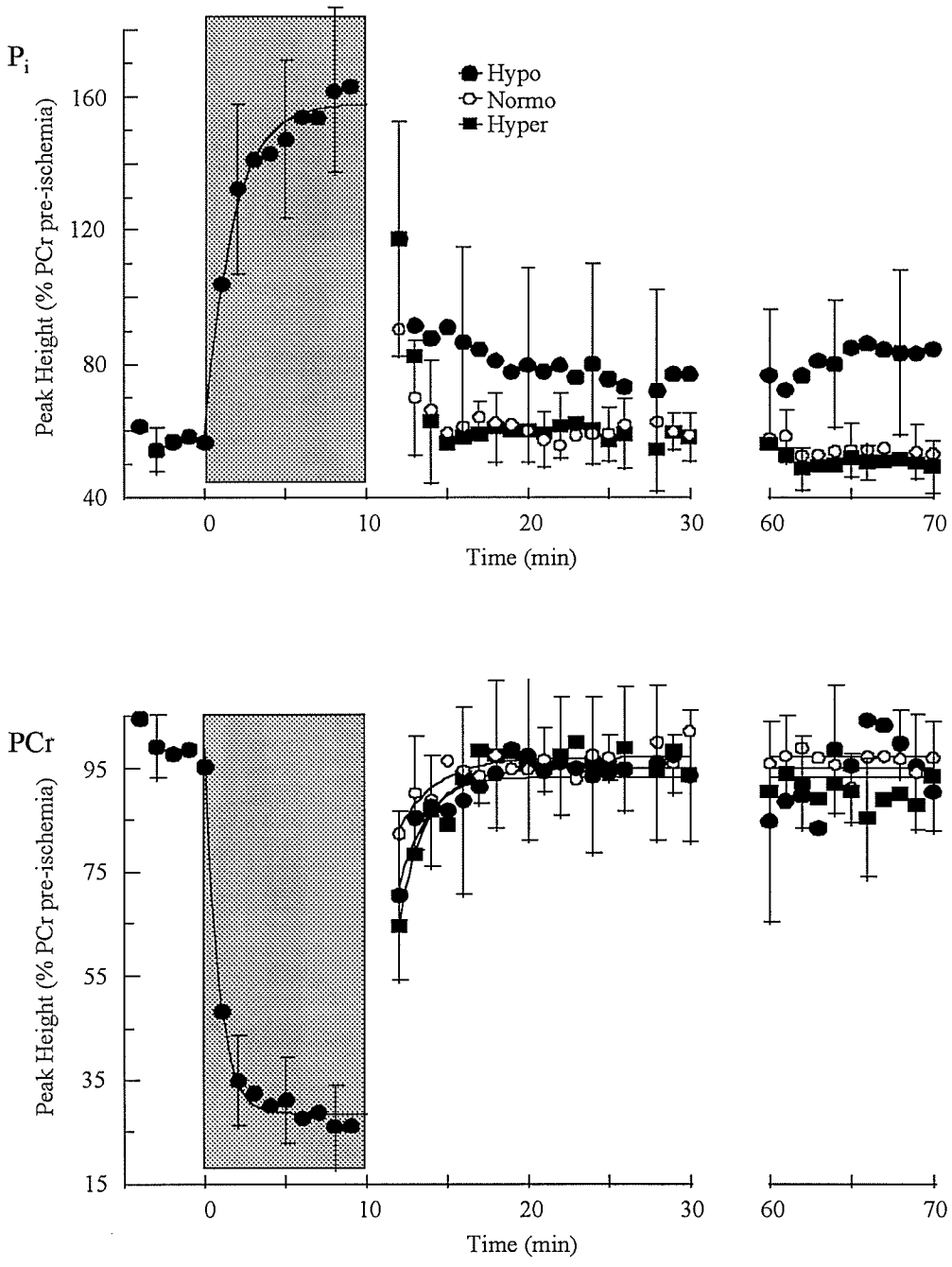

Figure 8. Changes in inorganic phosphate (top) and PCr (bottom) during ischemia (shaded area) and following reperfusion in rats hypoglycemic prior to ischemia. Curves are least-squares fits to equations of the form of equations 54 and 55. Errors are given as standard deviations.

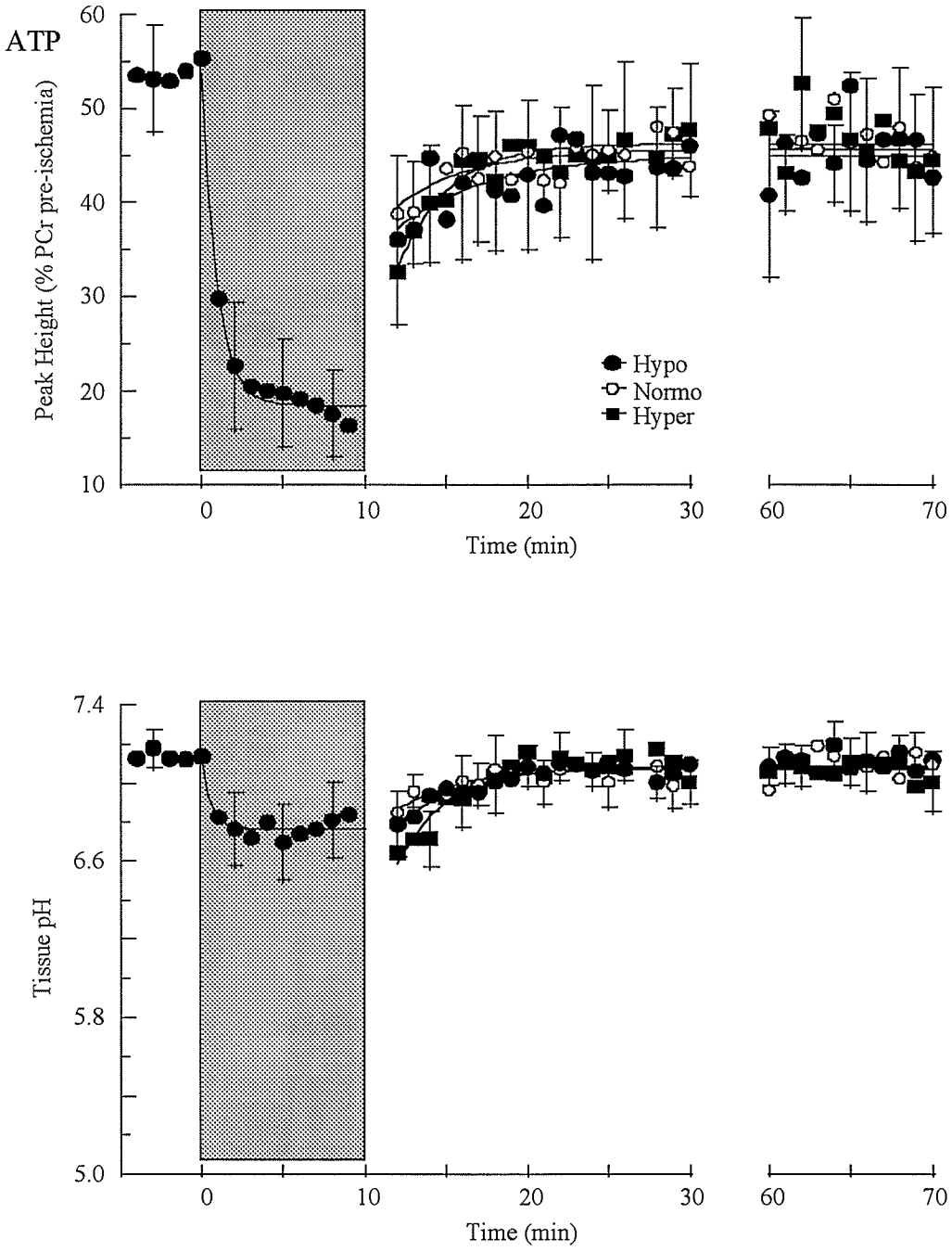

Figure 9. Changes in ATP (top) and tissue pH (bottom) during ischemia (shaded area) and following reperfusion in rats hypoglycemic prior to ischemia. Curves are least-squares fits to equatoins of the form of equations 54 and 55. Errors are given as standard deviations.

2c. *Post-ischemia changes for rats normoglycemic prior to ischemia*

For the normo group, rapid tissue pH recovery (within 4 min) occurred for the normo/hypo and normo/normo subgroups, whereas pH recovery was delayed in the first 7 min post-ischemia ($p < 0.005$) in the normo/hyper subgroup. At the end of the reperfusion period, tissue pH in all subgroups was not significantly different from pre-ischemia values. No significant differences were observed between any of these subgroups in ATP recovery, but by the end of the experimental period ATP had returned to only 85% of that observed pre-ischemia ($p < 0.0002$ for all subgroups). Recovery of PCr in the normo/hyper subgroup was impaired compared to the normo/hypo ($p = 0.051$) and normo/normo ($p = 0.018$) subgroups, reaching only 85% of pre-ischemia levels at the end of 1 hr ($p < 0.0001$ compared to pre-ischemia). The return of P_i to its pre-ischemia level was more rapid for the normo/hyper subgroup (vs normo/hypo, $p = 0.0066$; vs. normo/normo, $p = 0.024$) and indeed decreased below the pre-ischemia level (77% of pre-ischemia, $p < 0.0001$). In the normo/hypo and normo/normo subgroups, P_i at the end of the experiment was not significantly different from that observed pre-ischemia.

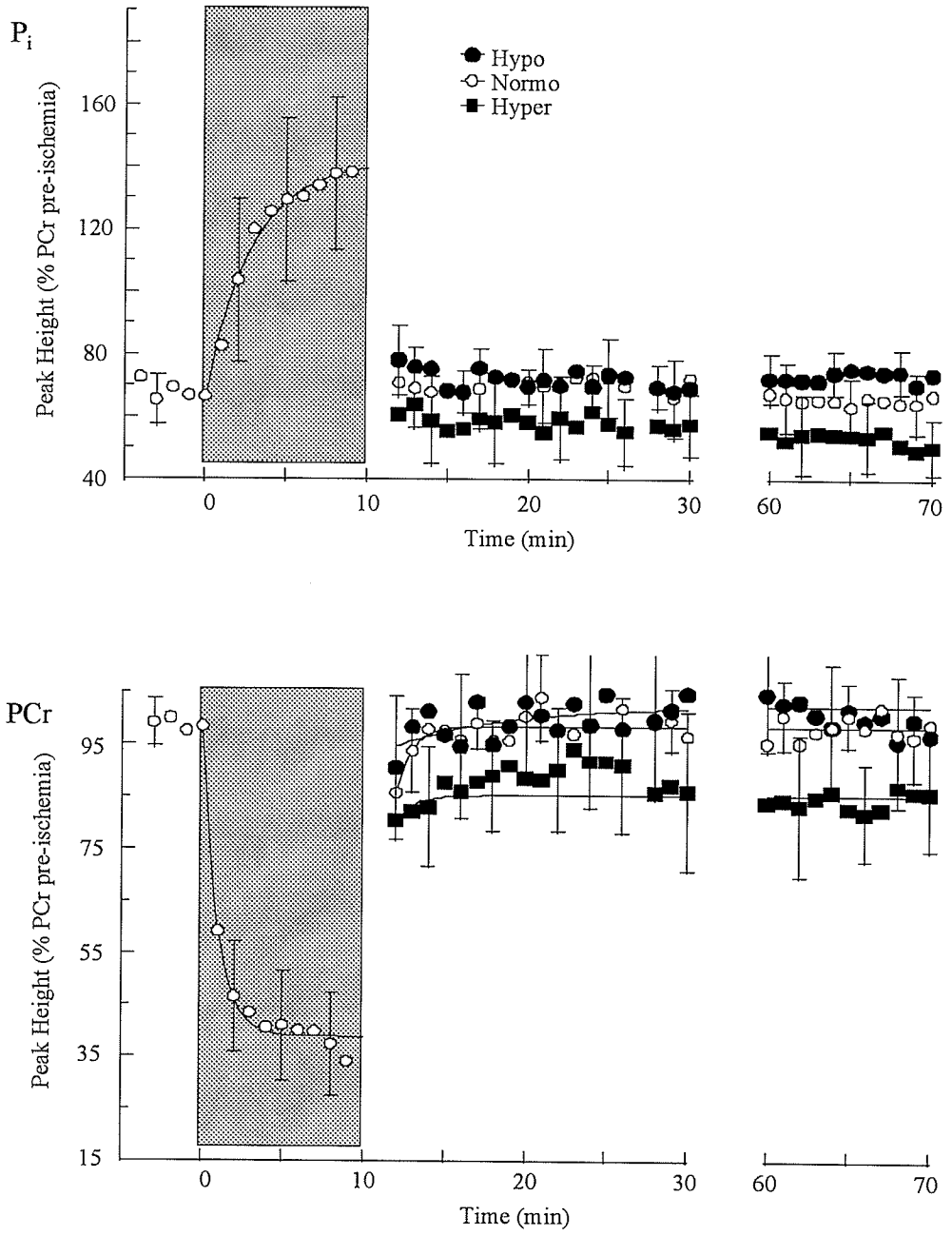

Figure 10. Changes in inorganic phosphate (top) and PCr (bottom) during ischemia (shaded area) and following reperfusion in rats normoglycemic prior to ischemia. Curves are least-squares fits to equations of the form of equations 54 and 55. Errors are given as standard deviations.

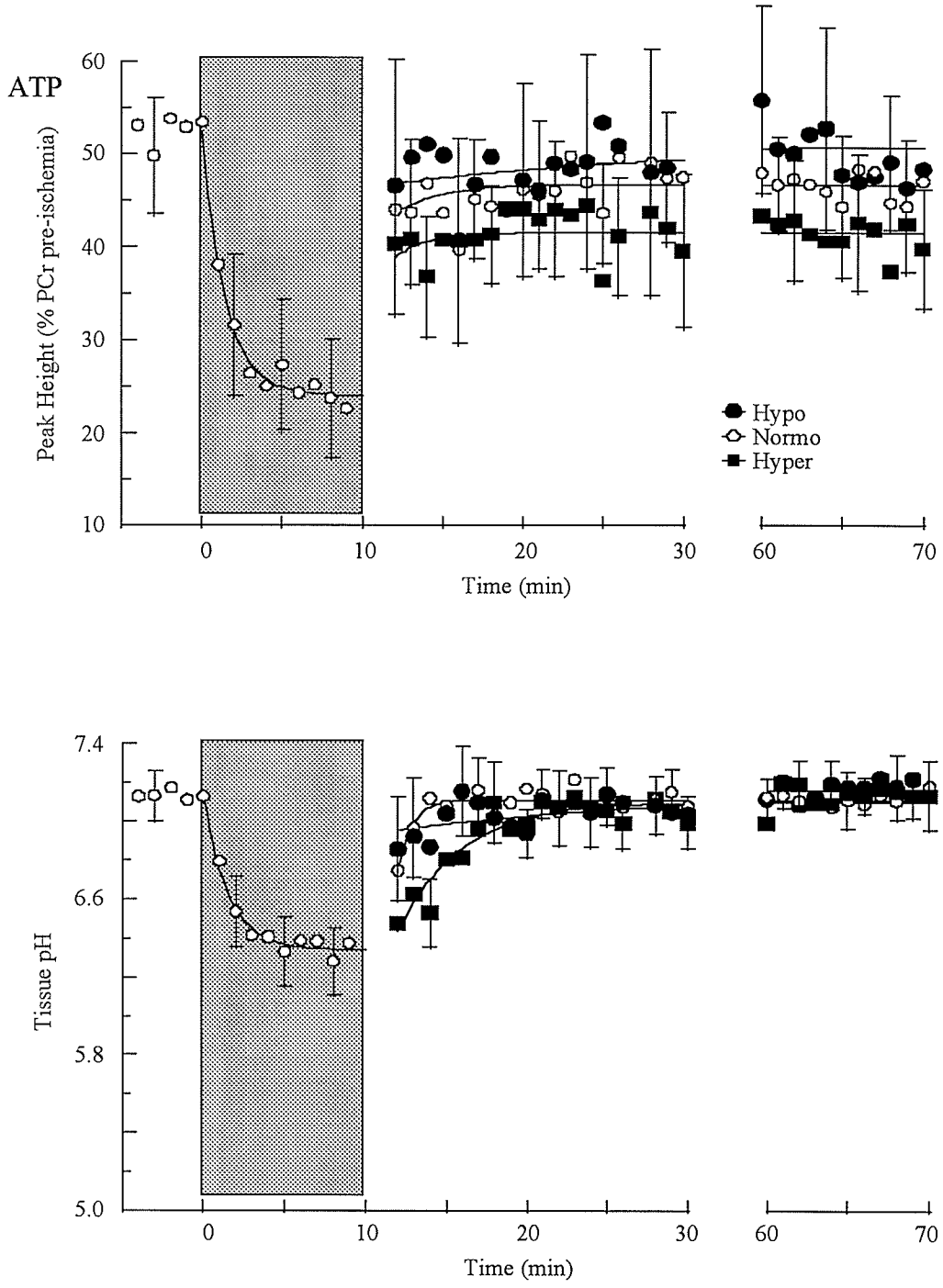

Figure 11. Changes in ATP (top) and tissue pH (bottom) during ischemia (shaded area) and following reperfusion in rats normoglycemic prior to ischemia. Curves are least-squares fits to equatoins of the form of equations 54 and 55. Errors are given as standard deviations.

2c. *Post-ischemia changes for rats hyperglycemic prior to ischemia*

In contrast to all other subgroups, tissue pH in the hyper/hyper subgroup remained at ischemic values for 15 min following reperfusion before beginning to recover, while recovery of tissue pH in the hyper/normo subgroup was significantly faster than in the hyper/hyper subgroup ($p < 0.0001$). At the end of the experiment in both subgroups, tissue pH had returned to pre-ischemic values. P_i returned to pre-ischemic levels after about 10 min of reperfusion. Recovery of PCr and ATP was slow relative to other groups and the final levels were lower than pre-ischemia, with PCr recovering to 92% for both subgroups ($p < 0.0002$) and ATP to 80% ($p < 0.0001$) and to 89% ($p = 0.0003$) of pre-ischemic levels for the hyper/hyper and hyper/normo subgroups by the end of the reperfusion period. Animals in the hyper/normo subgroup showed a more rapid recovery of P_i ($p < 0.0001$), PCr ($p = 0.11$) and ATP ($p = 0.0009$) than those in the hyper/hyper subgroup.

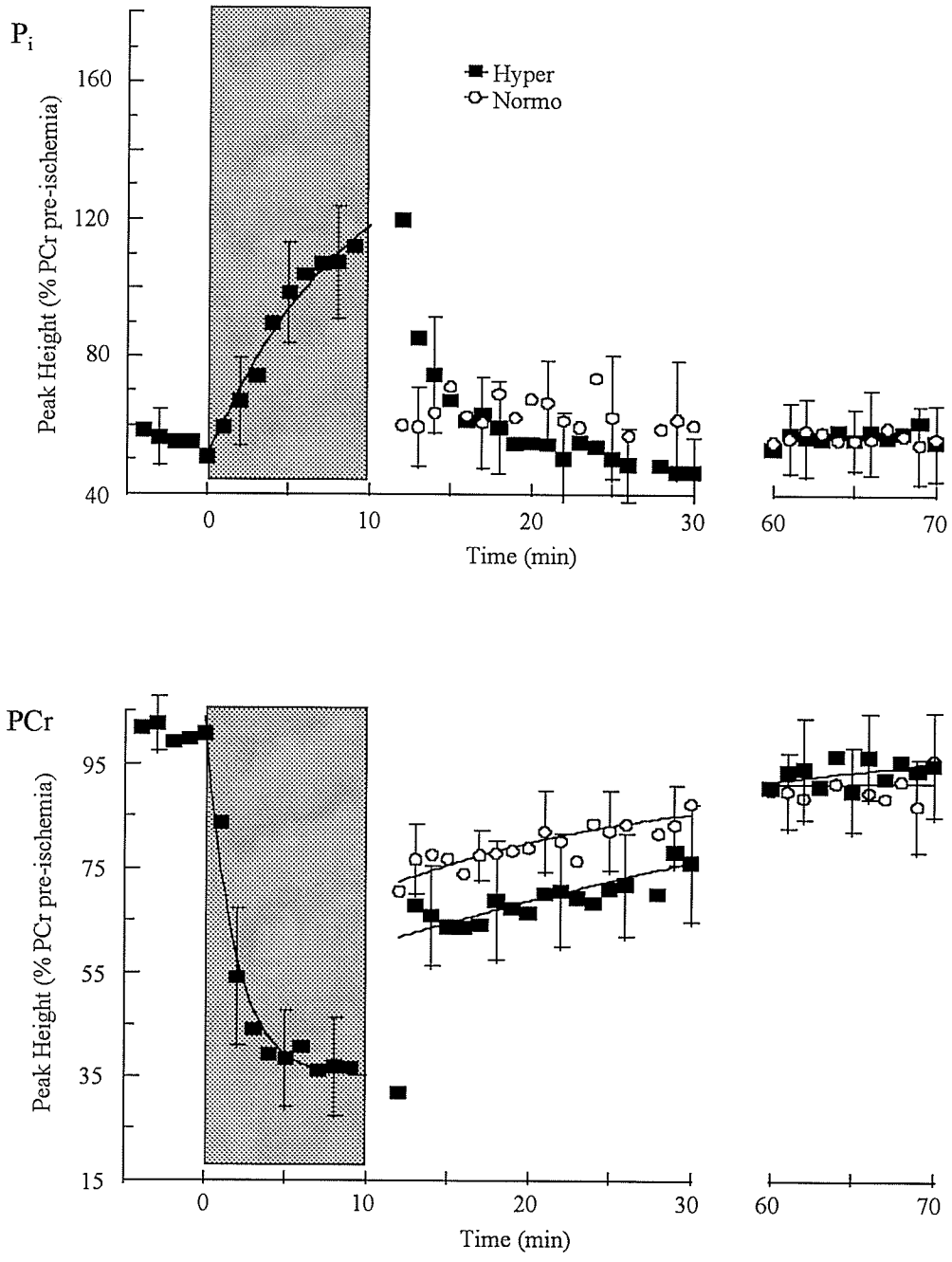

Figure 12. Changes in inorganic phosphate (top) and PCr (bottom) during ischemia (shaded area) and following reperfusion in rats hyperglycemic prior to ischemia. Curves are least-squares fits to equations of the form of equations 54 and 55. Errors are given as standard deviations.

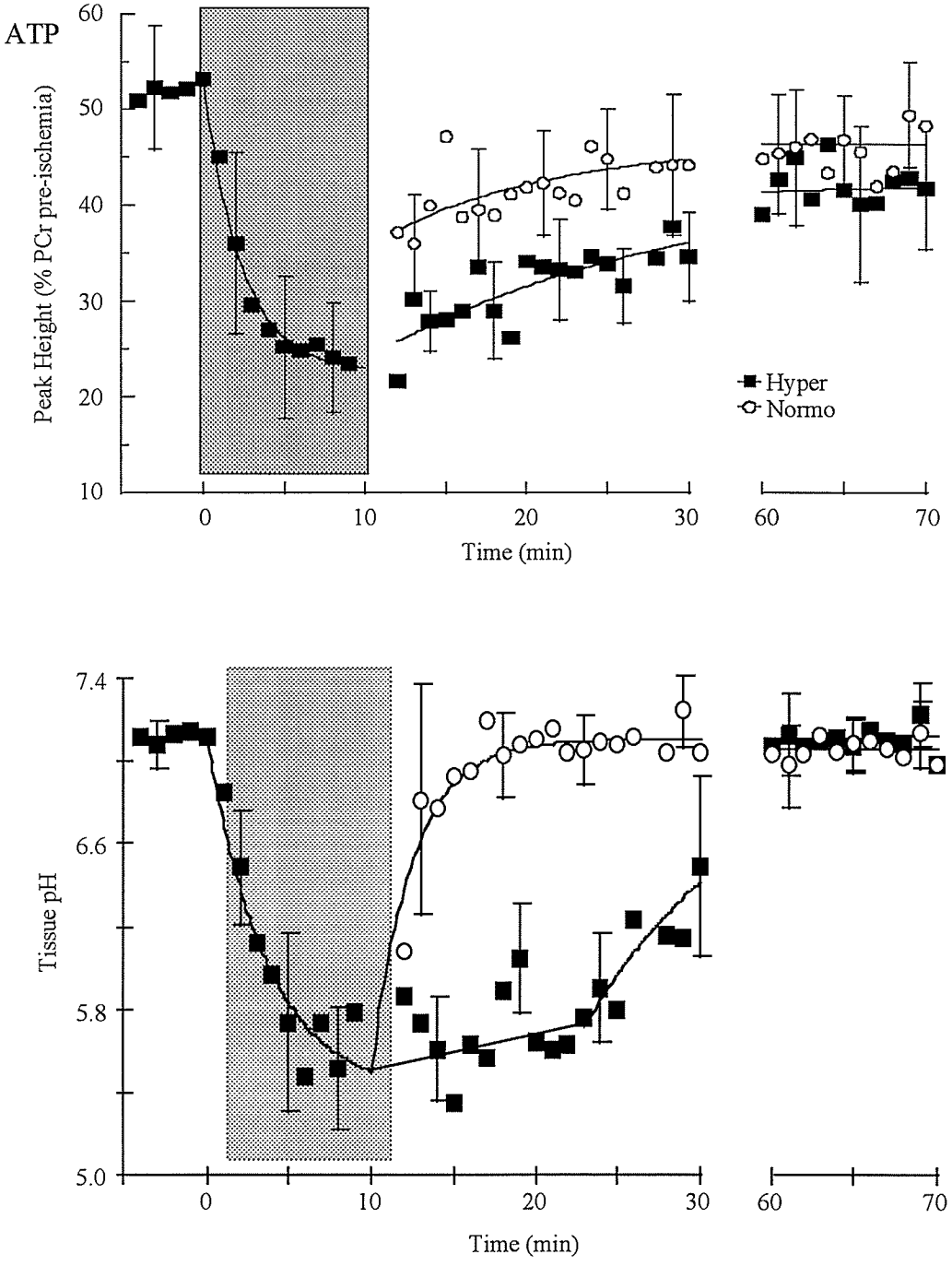

Figure 13. Changes in ATP (top) and tissue pH (bottom) during ischemia (shaded area) and following reperfusion in rats hyperglycemic prior to ischemia. Curves are least-squares fits to equatoins of the form of equations 54 and 55. Errors are given as standard deviations.

B. Effect of Glucose Level on Sodium Membrane Gradients and Total Brain Sodium During and Following Forebrain Ischemia

1. *Physiological Variables*

Table 6 shows the physiological variables measured during this study. The difference in pre-ischemia plasma osmolarity between the control and hyper groups was on the verge of significance ($p = 0.089$), and was significant at 20 ($p = 0.0061$) and 60 min ($p = 0.0056$) of reperfusion. No significant differences in pre- or post-ischemia hematocrits, blood pH, pCO_2, pO_2 or HCO_3^- were observed.

Table 6. Physiological variables (blood glucose (mM), blood osmolarity (mOsm), hematocrit (%), blood gases (mm Hg), and blood pH; mean ± SD) for each blood glucose group prior to and following transient cerebral ischemia for the ^{23}Na NMR spectroscopic experiments.

	Control	Hypo	Normo	Hyper
Blood glucose				
Pre-ischemia	7.3 ± 1.3	2.7 ± 0.8	5.8 ± 0.6	21.6 ± 1.7
Post-ischemia	6.8 ± 1.5	2.0 ± 1.2	5.6 ± 0.9	23.2 ± 4.7
Osmolarity				
Pre-ischemia	293 ± 8	304 ± 7	308 ± 26	313 ± 24
Post-ischemia	297 ± 5	316 ± 10	310 ± 26	339 ± 16
Hematocrit				
Pre-ischemia	49 ± 5	48 ± 7	48 ± 8	44 ± 8
Post-ischemia	38 ± 5	44 ± 8	43 ± 6	41 ± 6
Blood gases				
Pre-ischemia				
pH	7.32 ± 0.18	7.24 ± 0.19	7.30 ± 0.06	7.30 ± 0.09
pCO_2	36.3 ± 2.7	40.8 ± 4.1	40.9 ± 3.1	37.7 ± 2.5
pO_2	134 ± 46	143 ± 48	119 ± 16	118 ± 19
HCO_3^-	14.6 ± 1.0	18.2 ± 6.8	20.6 ± 3.9	18.8 ± 4.5
Post-ischemia				
pH	7.30 ± 0.20	7.17 ± 0.09	7.22 ± 0.11	7.2 ± 0.12
pCO_2	35.0 ± 5.1	37.3 ± 10.6	38.3 ± 9.4	34.2 ± 6.8
pO_2	143 ± 60	146 ± 21	115 ± 20	95 ± 17
HCO_3^-	17.7 ± 5.5	13.4 ± 2.1	15.9 ± 3.8	13.4 ± 1.9

2. *Brain Water and Sodium Content*

Figure 15 shows the changes in brain water content following ischemia in rats normoglycemic and hypoglycemic during ischemia. Figure 16 shows the brain sodium measured using flame emission spectroscopy in the same rats. Brain water content was significantly different from the normoglycemic control group at 90 min following normoglycemic ischemia ($p=0.00026$) and 60 min following hypoglycemic ischemia ($p=0.0011$). At 60 min following hypoglycemic ischemia brain water content was significantly higher than in the hypoglycemic control group ($p=0.022$). No differences between the pre- and post-ischemia brain sodium content were observed.

3. *In vivo* ^{23}*Na NMR Spectroscopy*

3a. *Single-Quantum* ^{23}*Na NMR Spectroscopy*

Figure 17 shows representative SQ ^{23}Na NMR spectra from a hypoglycemic rat. Figure 18 shows the SQ ^{23}Na NMR data for the hypo, normo and hyper groups. No significant differences were observed between the control and normo groups either during ischemia ($p = 0.53$) or reperfusion ($p = 0.73$), so that the control group is not shown. During ischemia, the signal area decreased in all groups within the first 30 s to about 97% relative to pre-ischemia, decreasing the greatest amount in the normo group ($p = 0.17$ for hypo vs. normo; $p = 0.57$ for hypo vs. hyper; $p = 0.38$ for normo vs. hyper groups). Following reperfusion, the area of the SQ ^{23}Na NMR signal in the normo and hyper groups increased to 107% at the end of the 1 hr reperfusion period. The hypo group showed a similar trend, but the increase in area was significantly greater than in the normo and hyper groups (117% relative to pre-ischemia; $p = 0.0060$ compared to the hyper group, $p < 0.05$ from 20 to 60 min of reperfusion compared to the normo group).

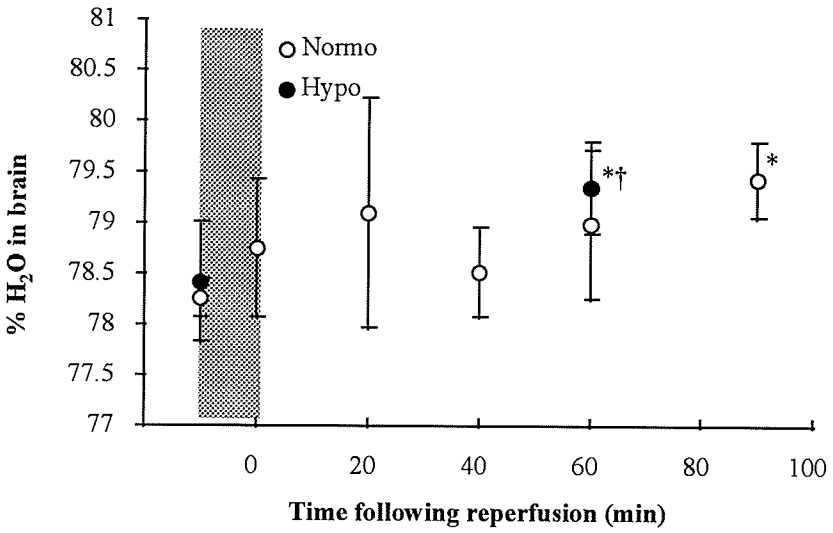

Figure 14. Brain water content (means ± standard deviation) changes following transient ischemia (shaded region). * and † indicate significant difference from normoglycemic and hypoglycemic controls, respectively.

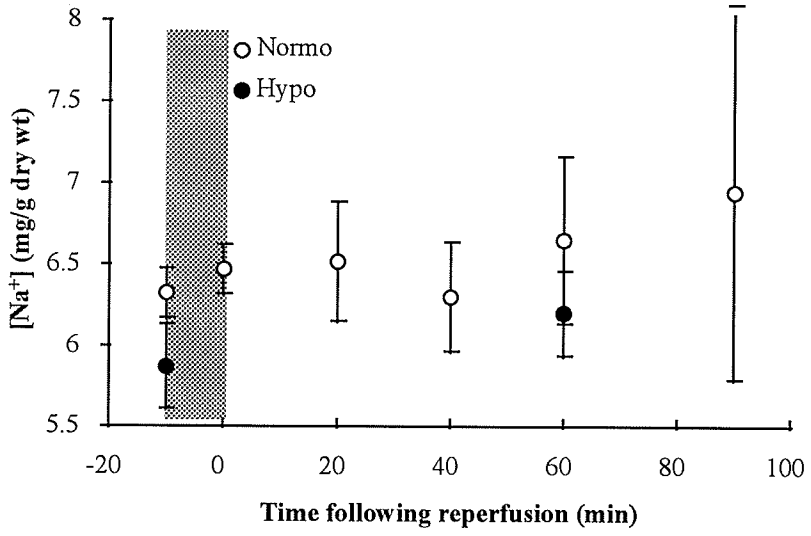

Figure 15. Brain sodiumcontent (means ± standard deviation) changes following transient ischemia (shaded region) measured by flame emission spectroscopy.

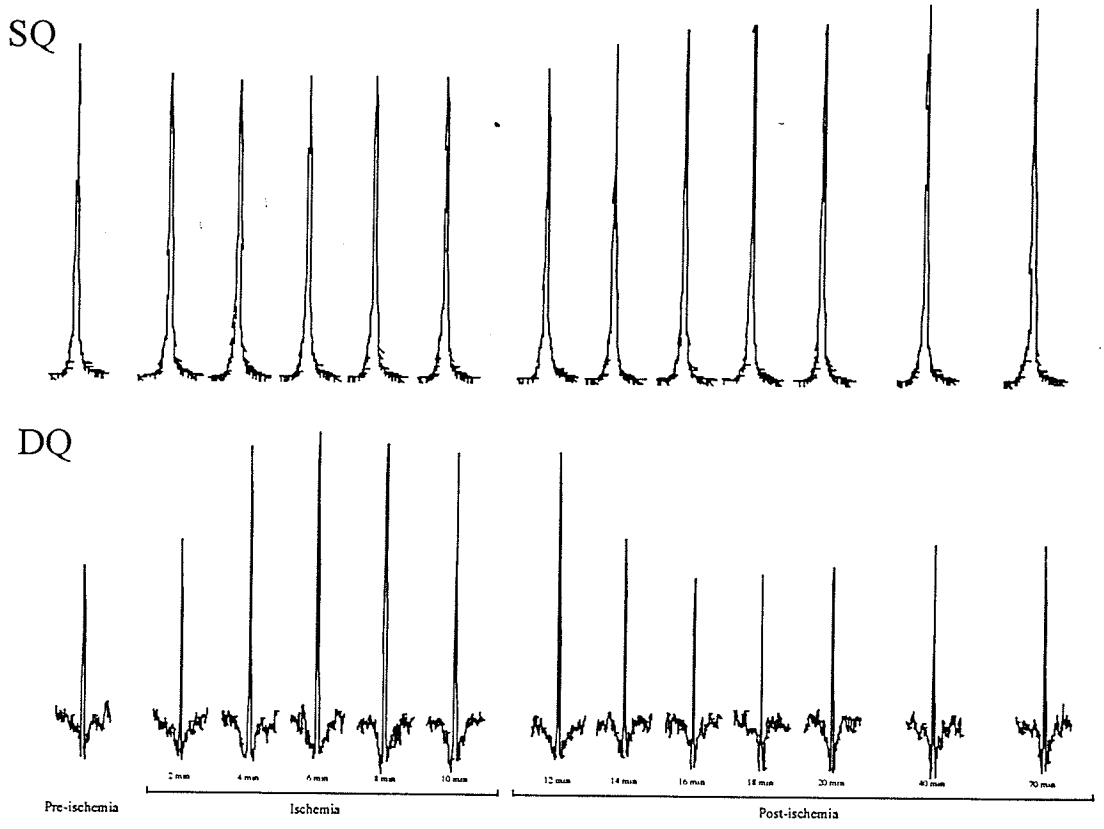

Figure 16. Single- (SQ) and double-quantum (DQ) ^{23}Na NMR spectra prior to, during and following transient forebrain ischemia in a hypoglycemic rat. Each spectrum is the sum of four 30 s acquisitions, spectral width 20 ppm.

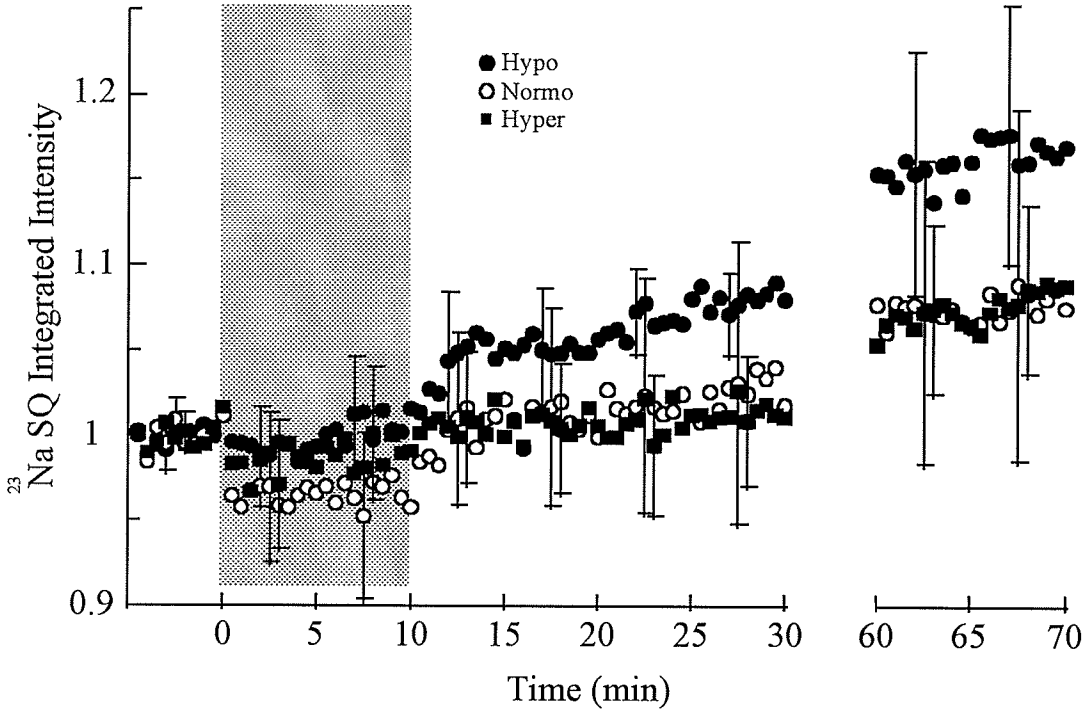

Figure 17. Changes in tissue sodium as measured using single-quantum ^{23}Na NMR peak areas during and following transient cerebral ischemia in hypo-, normo- and hyperglcyemic rats. Error bars indicate standard deviations.

3b. *Double-Quantum ^{23}Na NMR Spectroscopy*

From *in vitro* ^{23}Na DQ NMR experiments using homogenized brain (see figure 18), it was determined that the peak height of the ^{23}Na DQ NMR resonance decreases 22.7 ± 3% per unit decrease in pH. Thus the observed ^{23}Na DQ NMR signal during ischemia can be significantly altered, and altered to different extents in different blood glucose groups, since pH falls below 5.8 in the hyper and to only 6.7 in the hypo groups in this model after 10 min of ischemia.

A series of DQ ^{23}Na NMR spectra for a hypoglycemic rat is shown in figure 16, illustrating the changes in the ^{23}Na DQ NMR resonance during and following ischemia. The time-series raw (pH-uncorrected) data for the hypo, normo and hyper groups is given in figure 19, while the pH-corrected results are shown in figure 20. As in the ^{23}Na SQ NMR results, the normo and control groups show no differences, either during or following ischemia, so the data for the control group is not shown.

The rate constant k_{DQ}^{i}, from equation 56, was significantly different between groups ($p < 0.001$) and graded with respect to the level of glycemia (table 7), being greatest in the hypo group (0.673 min^{-1}) and least in the hyper group (0.285 min^{-1}). In the hypo group, the DQ signal intensity rises within the first 30 s of ischemia, reaching 200% of the pre-ischemic level by 120 s and slowly increases to 225% by the end of 10 min ischemia. In both the normo and hyper groups during ischemia, a delay of about 30 s is observed before the DQ signal intensity increases, reaching 210% of pre-ischemic level at 10 min. The parameter I_{∞}^{i} shows that the DQ ^{23}Na NMR signal for all groups will reach about 220% of pre-ischemia at long ischemia times, representing the signal at complete depolarization.

Following ischemia, the DQ ^{23}Na NMR signal intensity in the hypo and normo groups decreases to 85% of pre-ischemia level in about 7 min and recovers to about 95% of pre-ischemia level by the end of the experiment. The total recovery, given by $I_{\infty}^{P}+I_{rec}^{P}$, in equation 57, for the hypo and normo groups was not significantly different from 1.0, indicating that complete recovery occurs at a time longer than that studied. Recovery of the DQ ^{23}Na NMR signal was rapid during early reperfusion in the hypo and normo groups, the rate of recovery being greatest in the normo group (k_{DQ}^{P} = 0.368 min^{-1} for the hypo group and 0.461 min^{-1} for normo group; $p < 0.001$). In marked contrast to the lower blood glucose groups, recovery

of the DQ signal in the hyper groups is much slower ($k_{DQ}^{p} = 0.058\ min^{-1}$; $p < 0.001$ vs. hypo and normo groups) and the peak height remains elevated (115% relative to pre-ischemia, with $I_{\infty}^{p} = 1.132$, $p < 0.001$ vs hypo and normo groups) at the end of 1 hr of reperfusion, indicating that recovery of the DQ ^{23}Na NMR signal neither occurs during the experimental time nor can it be extrapolated that recovery will occur at longer times. The values of I_{rec}^{p} are not significantly different between the hypo ($I_{rec}^{p} = 0.216$) and normo (0.184) groups, but the rate constants k_{DQ}^{rec} are different ($k_{DQ}^{rec} = 0.022\ min^{-1}$ for the hypo group and 0.018 min^{-1} for the normo group; $p < 0.001$). Thus, the normoglycemic animals show not only a faster initial recovery than hypoglycemic animals, but the recovery from the undershoot is also faster in the normo group. The value of I_{rec}^{p} for the hyper group is not significantly different from zero, so that the final term in equation 57 has no significance in the recovery of the DQ ^{23}Na NMR signal from hyperglycemic rats.

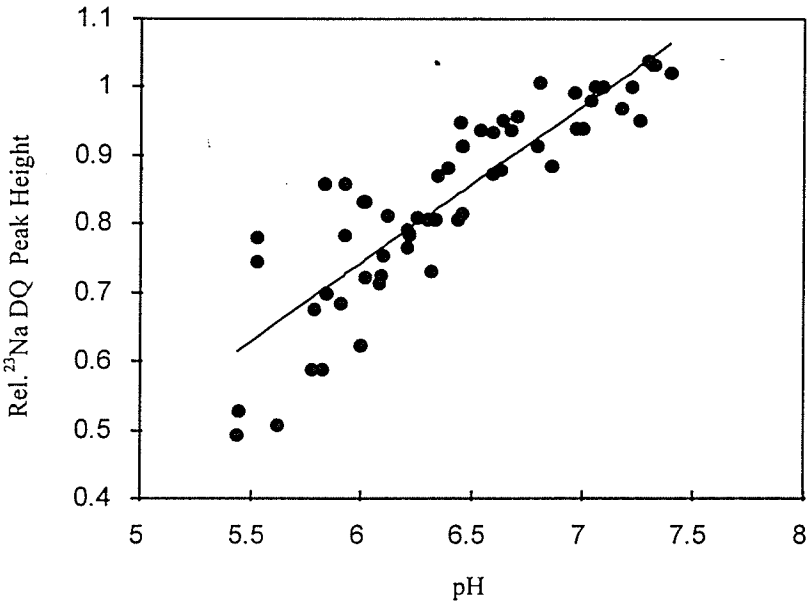

Figure 18. The dependence of the ^{23}Na DQ NMR signal on pH in homogenized brain tissue.

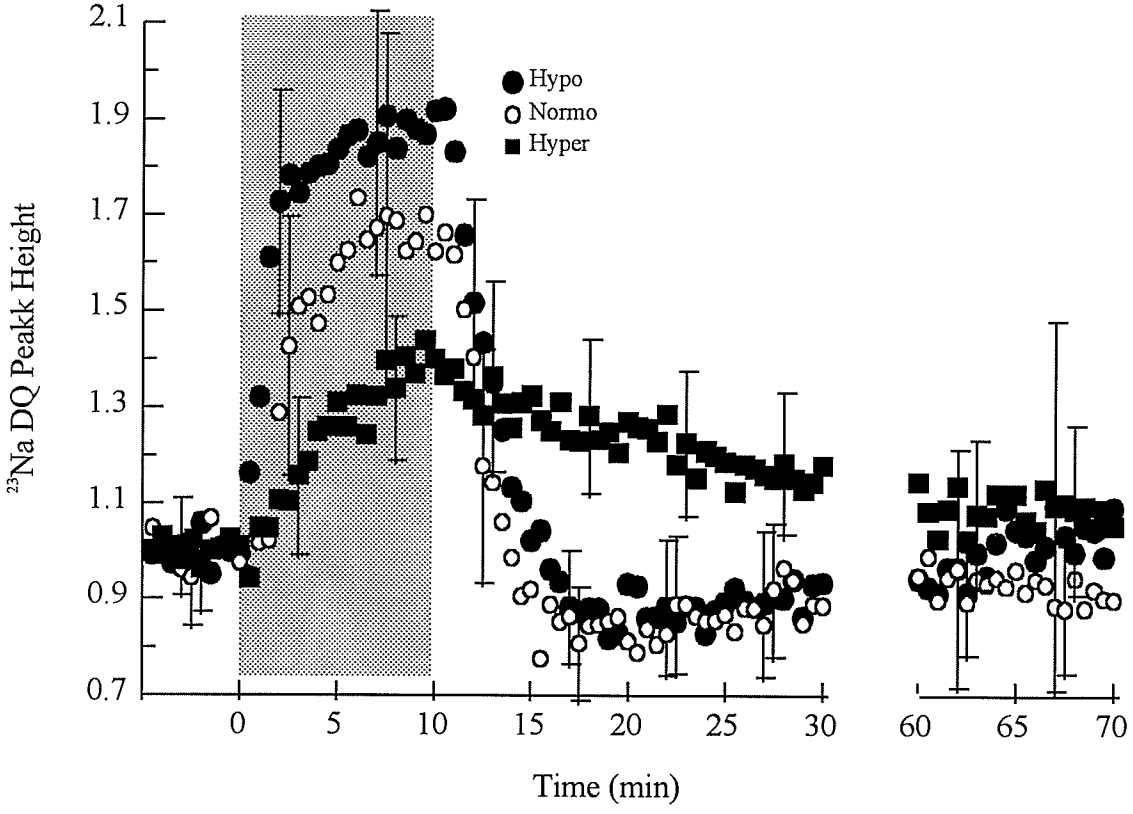

Figure 19. Changes in the double-quantum ^{23}Na NMR peak heights (pH-uncorrected data) during and following transient cerebral ischemia in hypo-, normo- and hyperglcyemic rats. Error bars indicate standard deviations.

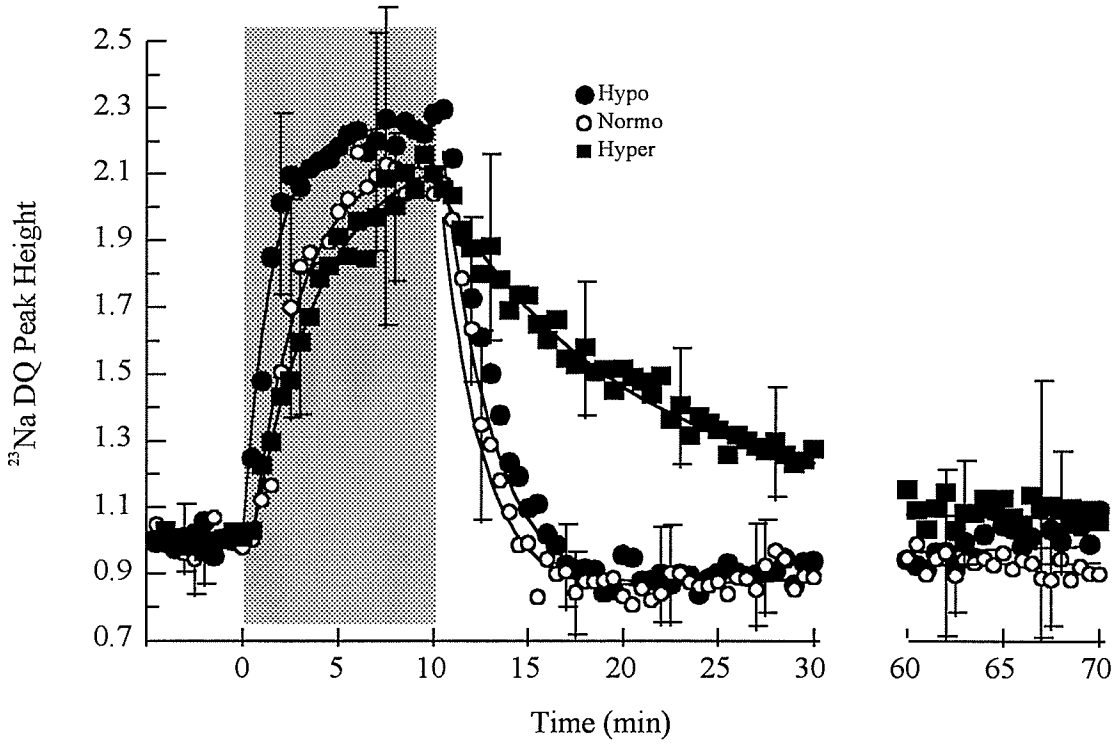

Figure 20. Changes in intracellular sodium as measured using double-quantum ^{23}Na NMR peak heights during and following transient cerebral ischemia in hypo-, normo- and hyperglcyemic rats. Data points are the pH-corrected values of the data contained in figure 20. Error bars indicate standard deviatoin, curves are best fits to the ischemia and post-ischemia data using equations 56 and 57.

Table 7. Results of curve fit to the pH-corrected DQ ^{23}Na NMR peak height data in figure 20 using equations 56 and 57. See text for definition of parameters.

	Hypo	Normo	Hyper
Ischemia			
I_∞^i	2.239 ± 0.026	2.155 ± 0.031	2.184 ± 0.029
k_{DQ}^i (min^{-1})	0.673 ± 0.087	0.404 ± 0.011	0.286 ± 0.024
Reperfusion			
I_0^p	2.174 ± 0.314	2.026 ± 0.413	1.971 ± 0.155
I_∞^p	0.820 ± 0.025	0.824 ± 0.040	1.114 ± 0.146
I_{rec}^p	0.216 ± 0.060	0.184 ± 0.106	-0.075 ± 0.387
k_{DQ}^p (min^{-1})	0.392 ± 0.101	0.518 ± 0.231	0.094 ± 0.039
k_{DQ}^{rec} (min^{-1})	0.022 ± 0.004	0.018 ± 0.006	0.011 ± 0.042

C. Effect of Glucose Level on the Forward Creatine Kinase Rate Constant Following Forebrain Ischemia

1. *Physiological Variables*

Physiological variables for rats studied in the creatine kinase rate constant experiments are given in table 8. No significant differences in the measured physiological parameters were observed between the normo- and the hyperglycemia groups during ischemia or following reperfusion, save blood glucose level. At the time of the spectroscopic measurements the mean blood glucose level for all animals was 6.3 ± 1.5 mM.

2. *^{31}P Saturation Transfer NMR Spectroscopy*

Figure 21 shows a sample set of saturation transfer ^{31}P NMR spectra from a rat showing the decrease in the PCr resonance as the γ-ATP resonance is saturated. Note that the γ-ATP resonance is fully saturated at all saturation times. The data for the control animals and rats hyperglycemic during ischemia following 4 hr of recovery are given in figure 22, along with the curve fits of equation 14. Figure 23 shows that for the normoglycemic animals, k_{for} was found to be significantly different only at 120 hr following ischemia ($p = 0.041$), recovering at 168 hr, and differed only at 4 hr post-ischemia from the hyperglycemic group ($p=0.00067$). The animals made hyperglycemic prior to the onset of ischemia showed a significant drop in k_{for} at 4 hr post-ischemia ($p = 0.00015$), recovering by 24 hr. At 72 hr post-ischemia, k_{for} dropped a second time ($p = 0.074$), with a subsequent recovery at 168 hr (figure 23).

Table 8. Physiological parameters(blood glucose (mM), blood gases) prior to and following induction of transient cerebral ischemia for the creatine kinase rate constant measurements. At the time of the rate constant measurement the mean blood glucose was 6.3 ± 1.5 mM.

	Normoglycemia	Hyperglycemia
Blood glucose		
Pre-ischemia	6.3 ± 1.7	12.9 ± 2.8
Post-ischemia	7.9 ± 2.5	15.4 ± 3.4
Blood gases		
Pre-ischemia pH	7.39 ± 0.09	7.37 ± 0.08
Post-ischemia pH	7.32 ± 0.08	7.25 ± 0.04
Pre-ischemia P_{CO_2}	38.7 ± 8.1	42.7 ± 8.2
Post-ischemia P_{CO_2}	44.5 ± 8.0	49.7 ± 4.5
Pre-ischemia P_{O_2}	123 ± 27	119 ± 29
Post-ischemia P_{O_2}	125 ± 30	124 ± 47

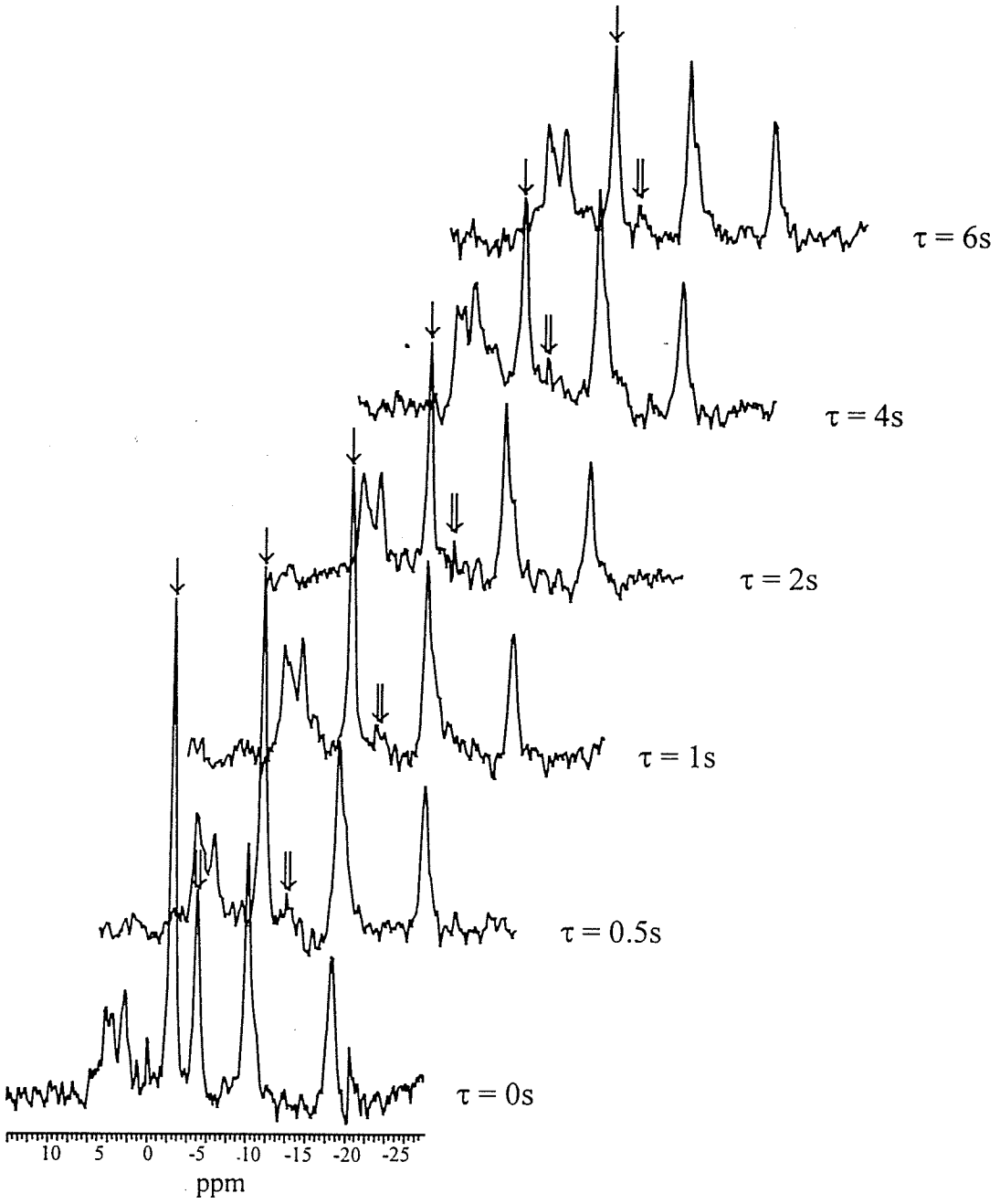

Figure 21. A series of saturation transfer ^{31}P NMR spectra in a normal rat demonstrating the decrease in PCr resonance intensity with γ-ATP saturation time τ. Arrows indicate position of the PCr (single line) and γ-ATP (double line) resonances.

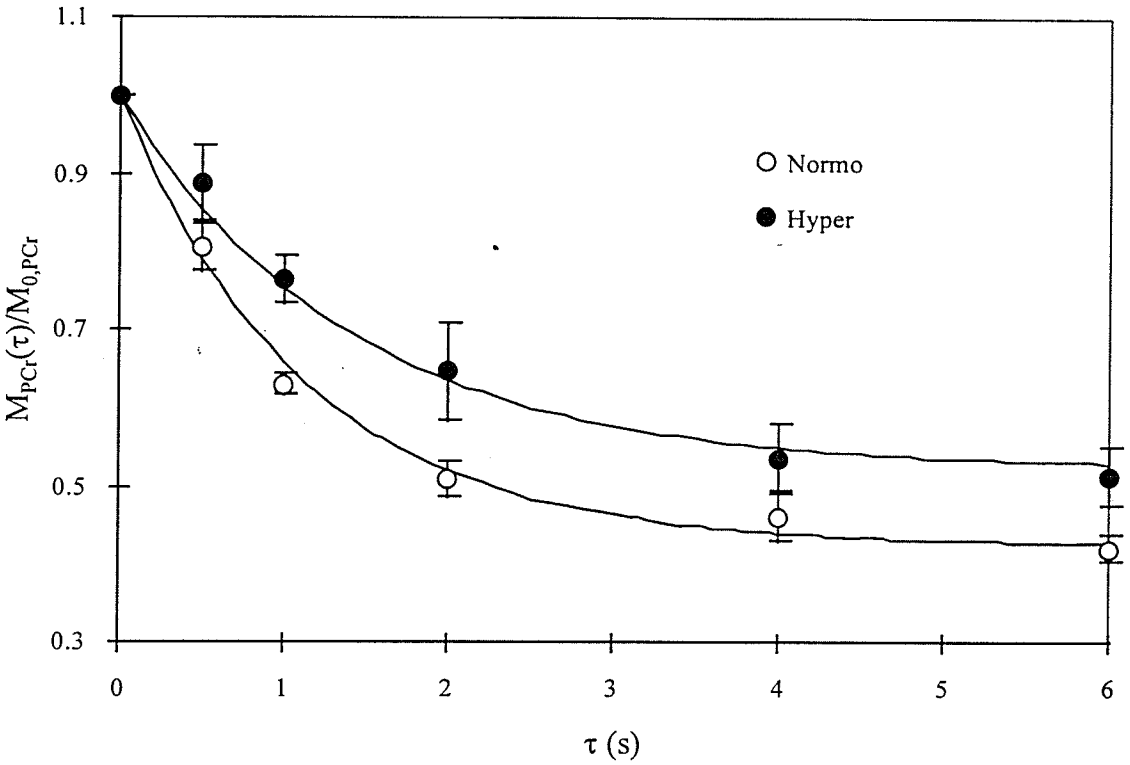

Figure 22. Curve displaying the decrease in PCr signal intensity with γ-ATP saturation time τ for normal rats and following 4 hr of recovery from hyperglycemic ischemia. Curves are best fits of equation 14, error bars indicate standard deviations.

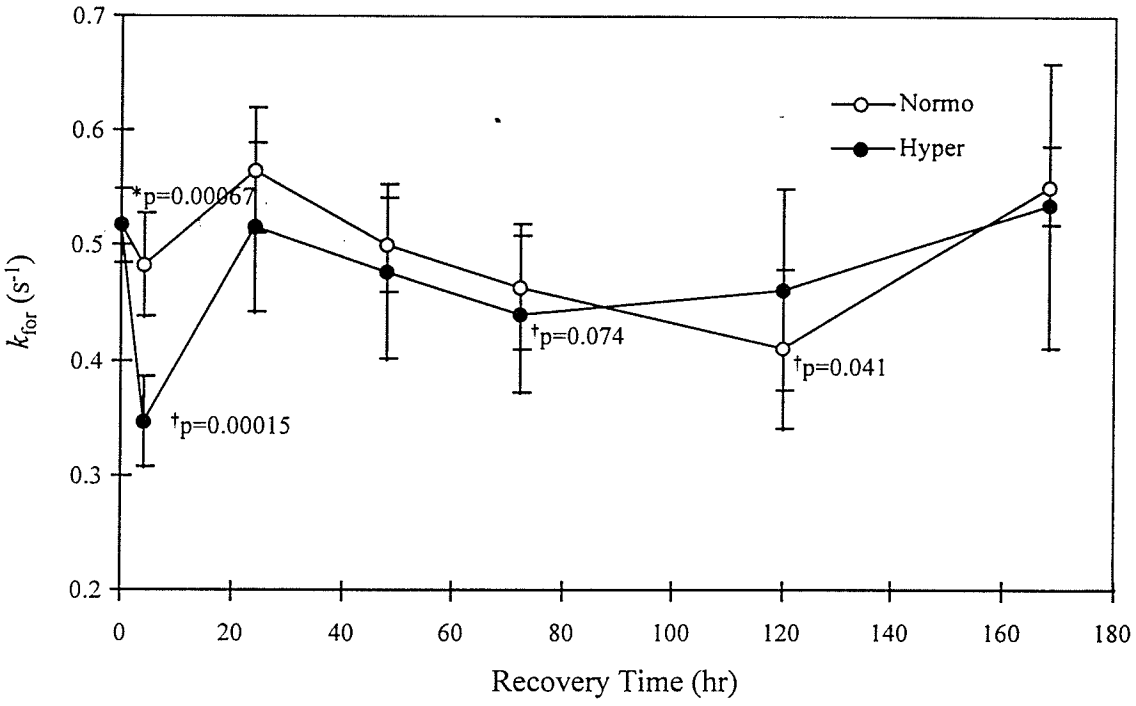

Figure 23. Changes in the forward creatine kinase rate constant k_{for} over time following transient cerebral ischemia in normo- and hyperglycemic rats. Error bars indicate standard deviations. († = with respect to pre-ischemia k_{for}; * = with respect to hyperglycemia k_{for})

D. Effect of Glucose Level on the Agonal Glycolytic Rate Constant Following Forebrain Ischemia

1. *Physiological Variables*

The physiological parameters for rats prior to and following induction of forebrain ischemia are given in table 9. No significant differences in the physiological parameters between groups were observed, except for blood glucose (as per experimental design). Blood glucose at the time of the agonal glycolytic rate constant measurement was 6.1 ± 1.6 mM. In the agonal glycolytic and creatine kinase rate constant measurements mortality following hyperglycemic ischemia (39% (25/65)) was higher than that after normoglycemic ischemia (12% (7/61)).

2. *STEAM ^{1}H NMR Spectroscopy*

Figure 24 shows a STEAM ^{1}H NMR spectrum from a 175 μl voxel of a normal rat brain, with the major resonances assigned to the various metabolites (after [Frahm, 1988]). No significant lactate resonance was observed in any of the pre-mortem ^{1}H NMR spectra for any time point following transient forebrain ischemia. The lactate methyl resonance at 1.33 ppm is situated on the lipid methyl resonance and which may mask its presence. Its absence is not due to J modulation effects, since these are minimal with the short TE (20 ms) used [Wilman, 1993]. Figure 25 shows a series of difference spectra (pre-mortem subtracted from the post-mortem ^{1}H NMR spectrum) over time to demonstrate the increase in lactate following injection of KCl. The results of a series of experiments for pre-ischemia rats and rats hyperglycemic during ischemia after 24 hr of recovery are given in figure 26 along with fits of the first-order rate equation, equation 58. The values of the first-order rate constant k_{AGR} at increasing times following ischemia for normo- and hyperglycemic rats are shown in figure 27. The normoglycemic animals show a decrease in k_{AGR} at 48 hr relative to pre-ischemia ($p = 0.017$) and k_{AGR} remains low throughout the 168 hr period of study ($p = 0.0051$, 0.0081, 0.016 at 72 hr, 120 hr and 168 hr vs. pre-ischemia, respectively). The hyperglycemic animals show an immediate drop in k_{AGR} ($p = 0.035$ at 4 hr post-ischemia) and k_{AGR} remains low throughout the 168 hr study period. A difference between the normo- and hyperglycemia groups occurs only at 24 hr post-ischemia ($p = 0.040$).

Table 9. Physiological parameters (blood glucose (mM), blood gases) prior to and following induction of cerebral ischemia for the measurement of the agonal glycolytic rate constant. The blood glucose at the time of measurement of the rate constant was 6.1 ± 1.6 mM.

	Normoglycemia	Hyperglycemia
Blood glucose		
Pre-ischemia	7.0 ± 1.5	12.1 ± 3.5
Post-ischemia	9.8 ± 2.5	15.6 ± 2.8
Blood gases		
Pre-ischemia pH	7.33 ± 0.10	7.32 ± 0.09
Post-ischemia pH	7.24 ± 0.08	7.21 ± 0.05
Pre-ischemia P_{CO_2}	41.4 ± 8.5	45.7 ± 11.8
Post-ischemia P_{CO_2}	49.9 ± 11.7	51.9 ± 7.7
Pre-ischemia P_{O_2}	154 ± 98	116 ± 46
Post-ischemia P_{O_2}	147 ± 83	118 ± 33

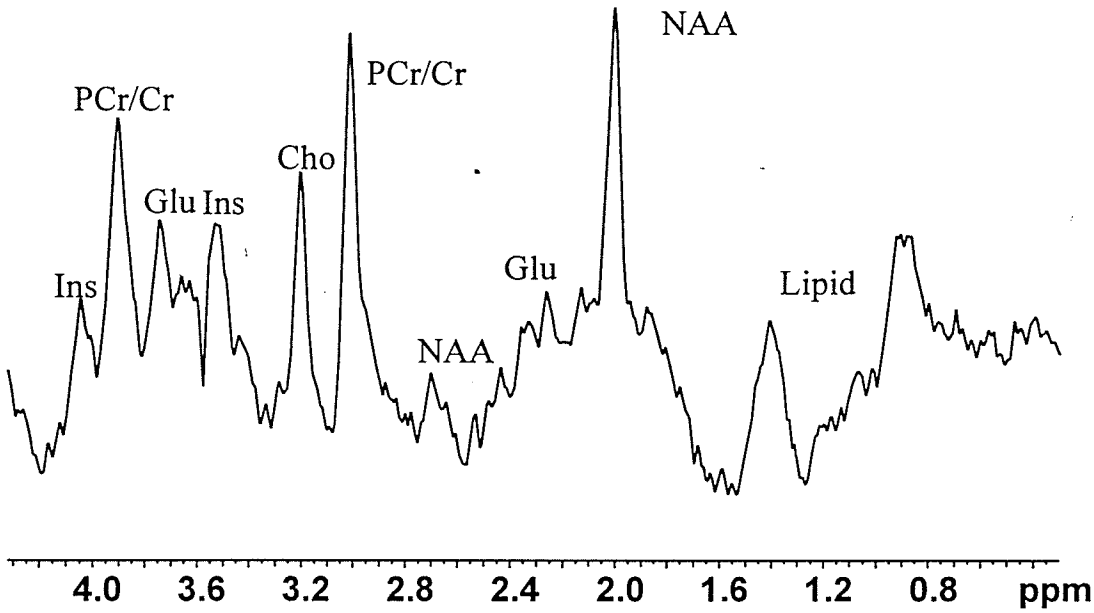

Figure 24. STEAM localized ^{1}H NMR spectrum from a 7 X 5 X 5 mm (175 μl) voxel of brain *in vivo*. NAA = *N*-acetylaspartate; Glu = glutamate/glutamine; Cho = total choline (choline/phosphocholine); Cr = total creatine (creatine/phosphocreatine); Ins = inositol.

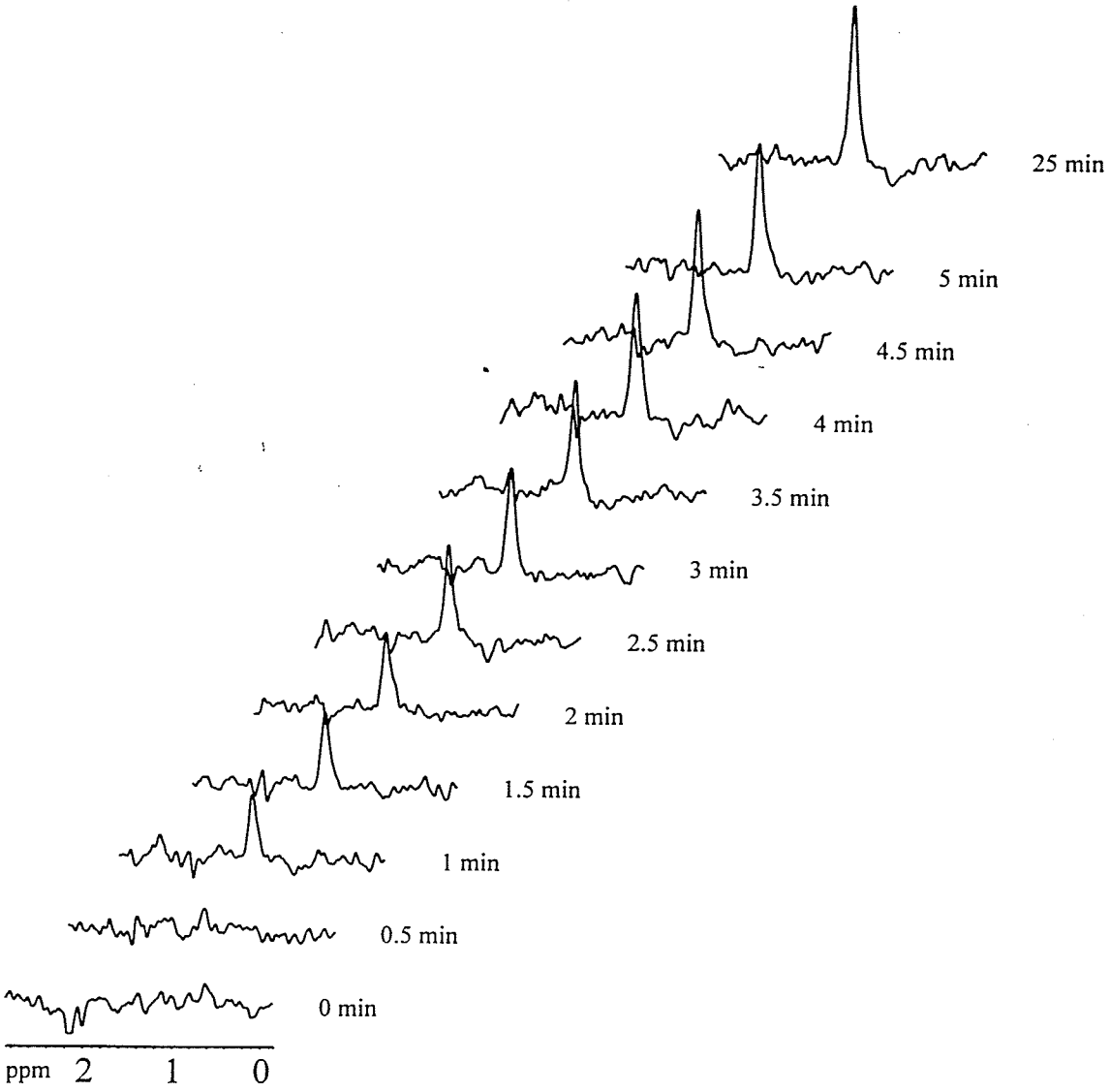

Figure 25. Difference STEAM localized ^{1}H NMR spectra demonstrating the increase in the lactate resonance post-mortem. Each spectrum is a result of the subtraction of a pre-mortem fid from the post-mortemfid.

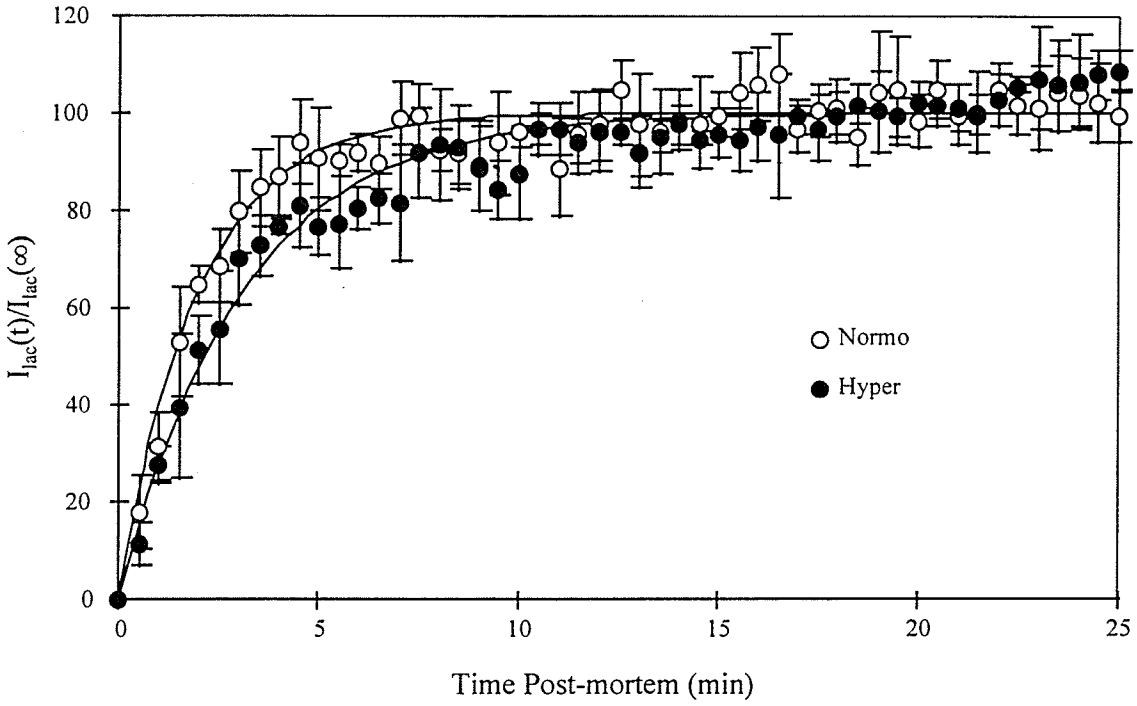

Figure 26. Increase in brain lactate peak height with time following KCl injection in normal rats and following 1 day of recovery from hyperglycemic ischemia. Curves are best fits of equation 58, error bars indicate standard deviation.

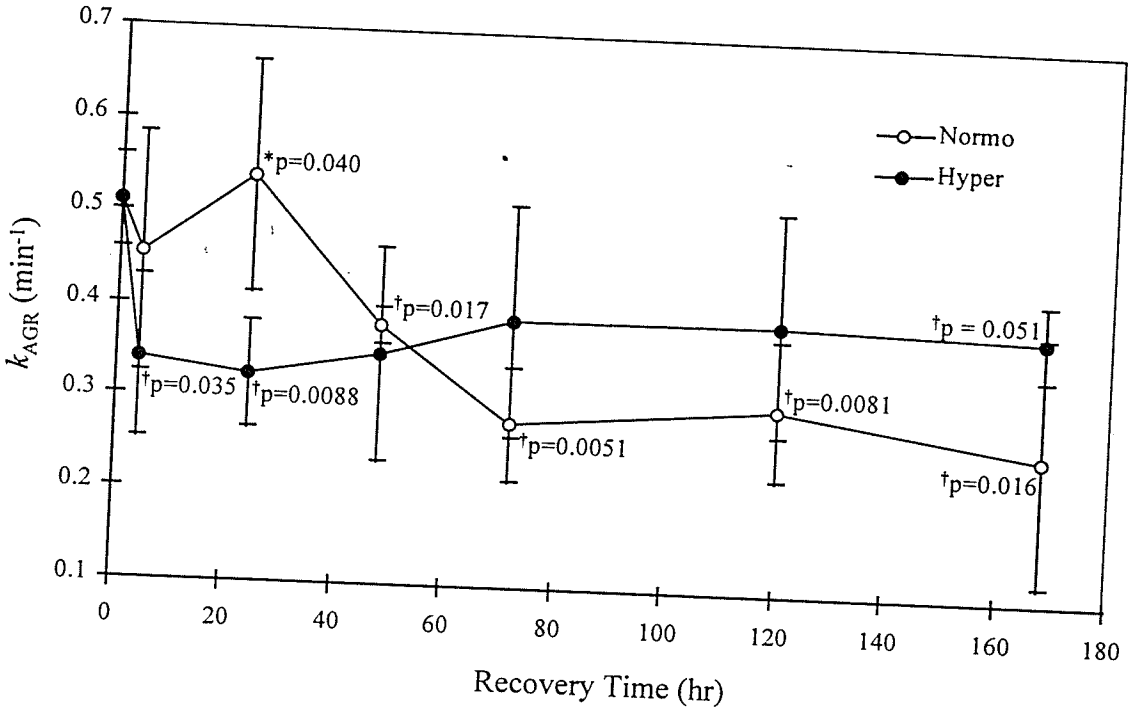

Figure 27. Changes in the agonal glycolytic rate constant k_{AGR} with time following transient ischemia in normo- and hyperglycemic rats. Error bars indicate standard deviations. († = with respect to pre-ischemia k_{AGR}; * = with respect to hyperglycemia k_{AGR})

IV. DISCUSSION

A. Effect of Glucose Level on Cerebral High-Energy Phosphate Metabolism During and Following Forebrain Ischemia

The objective of this study was to determine the influence of the level of glycemia on cerebral energy failure and acidosis in a rat model of forebrain ischemia, and in particular to test the hypothesis that post-ischemic manipulation of blood glucose level can optimize the recovery of cerebral energy metabolism and acidosis. Accordingly, ^{31}P NMR spectroscopy was used to follow changes in the cerebral pH and levels of adenosine triphosphate (ATP), phosphocreatine (PCr) and inorganic phosphate (P_i) during forebrain ischemia and reperfusion in rats in which the blood glucose level was altered post-ischemia.

Using surface coils for both transmission of radiofrequency pulses and the reception of NMR signals has been used to localize the region of brain from which NMR signals are observed. The B_1 inhomogeneity created using the surface coil arrangement causes regions of tissue to experience different tip angles as a function of distance from the coil. When the pulse length corresponding to the maximum signal intensity of the resonance of interest is obtained, the effective depth (from the centre of the coil) of the region observed is approximately equal to the radius of the surface coil (figure 28) [Edelman, 1985]. The depth at which the ^{31}P NMR signals are obtained correspond mainly to the hippocampus, cortex and striatum.

During ischemia, anaerobic glycolysis continues to produce ATP from available glucose and glycogen stores, albeit inefficiently, so that cell function can continue for a time in the absence of oxygen. While preserving some degree of energy supply, such anaerobic glycolysis leads to a decrease in tissue pH, the extent of which is dependent on the amount of substrate available. A graded pH effect is clearly observed in the present study where, during ischemia, pH falls to 6.75, 6.35, and <5.8 in hypoglycemic, normoglycemic, and hyperglycemic animals, respectively. Anaerobic metabolism can preserve low levels of high-energy phosphate metabolites in the normo- and hyperglycemic groups, but is incapable of doing so with the limited supply of glucose in the hypoglycemic group. Catabolic enzymes (lipolytic, proteolytic

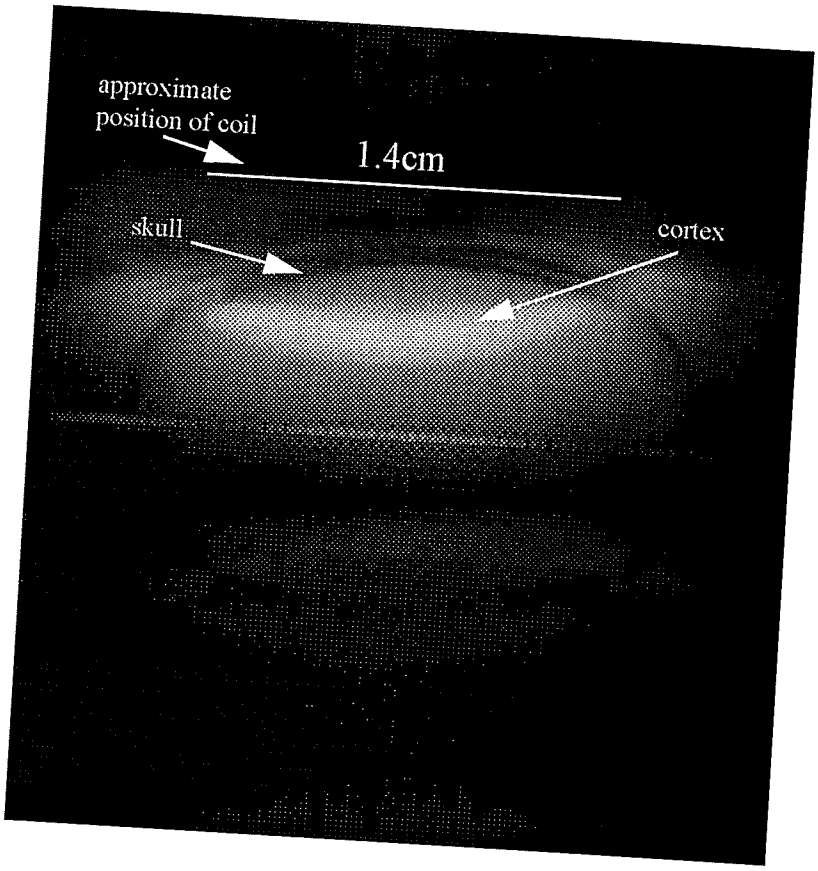

Figure 28. Transverse ^{1}H MR image taken using a surface coil of similar dimensions to the ^{31}P and ^{23}Na surface coils used in experiments A, B and C. Bright region corresponds to the region with pulse angle approximately 90°. Animal did not have scalp removed, so that another *ca.* 2 mm of depth would be achieved. Courtesy Dr. Richard Buist.

and nucleolytic), implicated in ischemic neuronal damage, are activated by intracellular Ca^{+2} [Siesjö, 1984], which can be released from sequestration sites by acidosis [Ames, 1983]. This may account for the observation that ischemia in hypoglycemic animals, which is accompanied by greater energy failure (and hence a lower ability to maintain normal intracellular Ca^{+2} concentration) but less acidosis than occurs following ischemia in animals in the higher blood glucose groups, is associated with decreased neuronal injury; in the presence of only slight acidosis, calcium activation of catabolic enzymes may be depressed

relative to that in normo- and hyperglycemic animals [Siesjö, 1984]. However, it should be noted that insulin, used to create and maintain hypoglycemia, is itself somewhat neuroprotective [Voll, 1991] and may contribute to the improved outcome in hypoglycemia. Insulin has a number of functions in brain, including the regulation of food intake, potentiation of neuronal growth, stimulation of onithine decarboxylase activity and protein synthesis, increases glucose uptake in glial cells [Wozniak, 1993]. However, the mechanism of the neuroprotective effect of insulin is not known. The more severe acidosis occurring when ischemia is induced under normo- or hyperglycemic conditions may result in intracellular Ca^{+2} concentrations in excess of the ability of the cell to buffer the Ca^{+2} load [Siesjö, 1984], resulting in increased damage by activated catabolic enzymes. The low pH reached in the brains of these animals during ischemia may also have adverse effects on other enzyme systems and on cellular structure, contributing to the increasing injury observed following ischemia in animals with higher blood glucose levels.

The rapid recovery of high energy phosphate metabolites and tissue pH during reperfusion in the normo/normo and hypo/hypo subgroups is in keeping with the known resistance of mitochondrial function to short-duration ischemia [Rehncrona, 1979]. In the hyper/hyper subgroup, on the other hand, recovery of high energy phosphate metabolites and tissue pH is delayed, perhaps indicating that the marked ischemic-induced acidosis has already had a significant effect on cellular viability. A similar delay in recovery of cerebral pH was noted following 16 min global ischemia in hyperglycemic cats [Chopp, 1987; 1988]. That this delay represents more extensive cerebral damage is supported by the observation that much more severe ischemia, 1 hr of complete global ischemia in the cat, is followed by a much longer delay (32 min on average) in recovery of tissue pH and high energy phosphates following recirculation [Behar, 1989].

Following global ischemia in hyperglycemic cats, a further decline in cerebral pH was observed during initial reperfusion [Chopp, 1987; 1988]. This was not observed in the present study, possibly indicating differences in the animal (cat vs rat) or in the model of cerebral ischemia (16 min ischemia induced by a pressure cuff around the neck plus hypotension, vs 10 min carotid occlusion plus hypotension).

Eventual outcome can also be affected by changes in the glucose supply post-ischemia. Recovery of high energy phosphates and tissue pH is not improved significantly by normalizing blood glucose levels post-ischemia in the hypo/normo subgroup. However, recovery of tissue pH, but not of high energy phosphate metabolites, is significantly delayed in the normo/hyper and hypo/hyper subgroups. During reperfusion, electrolyte gradients must be re-established before normal oxidative metabolism can resume. Comparison of ATP recovery shown in figures 9, 11 and 13 with intracellular sodium recovery shown in figure 20 demonstrates a strong correlation between these two processes. During this interval, glucose being supplied to the tissue may continue to be metabolized anaerobically, contributing to the ongoing acidosis. Further exacerbation post-ischemia undoubtedly contributes to the more severe tissue injury observed following ischemia in untreated hyperglycemic animals [De Courten-Meyers, 1988; Nedergaard, 1987a; Pulsinelli, 1982a; Vazquez-Cruz, 1990; Yip, 1991]. Similarly, the delayed recovery of pH in post-ischemic hyperglycemia following normoglycemic ischemia may be the origin of the observed detrimental effects of raising blood glucose levels post-ischemia.

On the other hand, there is no difference in pH recovery in the normo/normo and normo/hypo subgroups, so that improved outcome in the latter [Voll, 1989, 1991a] must be due to other factors, possibly the action of insulin [Voll, 1991b]. Hypoglycemia during ischemia is protective, and, in the absence of hypoglycemia severe enough in itself to initiate cerebral energy failure, post-ischemic recovery of pH and high energy phosphates is rapid. No further improvement in recovery is apparent on normalizing blood glucose levels post-ischemia in the hypo/normo subgroup.

In the hypoglycemic animals blood glucose levels were maintained as closely as possible to 1.5 mM. However, the glucose level tended to decrease post-ischemia in the hypo/hypo subgroup, occasionally falling below 1 mM. In this subgroup increases in P_i and decreases in ATP and PCr was always accompanied by an erratic blood pressure (at times over 200 mm Hg). It is not clear whether this severe hypoglycemia induced the cerebral energy failure or whether cardiac function was compromised by severe hypoglycemia, resulting in subsequent cerebral energy failure.

Pre-ischemic hyperglycemia enhances post-ischemic depression of the cerebral metabolic rate [Kozuka, 1989]. This effect manifests itself as a relatively slow recovery of ATP and PCr in hyperglycemic animals. Impairment of ATP recovery remains evident at the end of the 1 hr reperfusion period in all subgroups. This may be due to a net loss of adenosine during ischemia. In addition, however, PCr recovery is complete at the end of the experiment in all cases except for those subgroups hyperglycemic prior to or following ischemia (namely, the hypo/hyper, normo/hyper, hyper/normo and hyper/hyper subgroups). Since P_i recovers in all cases at 30 min reperfusion, the total ^{31}P spectral intensity is decreased at the end of the experiment, suggesting a diminished total phosphate pool following ischemia and reperfusion. This is possibly due to either washout from tissue and/or a movement of phosphate from an observable state to a state not observable by ^{31}P NMR spectroscopy (mitochondrial sequestration, $Ca_3(PO_4)_2$ precipitation, or protein binding for example) during or early following ischemia.

Whether altering blood glucose levels will improve clinical outcome following ischemic brain injury in humans remains to be examined. However, the results of this study clearly demonstrate that recovery of high energy phosphate metabolites and tissue pH can be affected by altering the blood glucose level post-ischemia. In particular, hyperglycemia post-ischemia is detrimental to recovery, whether ischemia occurs in the setting of hypo-, normo-, or hyperglycemia. Lowering of blood glucose via insulin administration improves recovery of high energy phosphates and pH following hyperglycemic ischemia. Finally, the study does not suggest that there is any further benefit to be had by inducing hypoglycemia following ischemia.

B. Effect of Glucose Level on Membrane Sodium Gradients and Total Brain Sodium Content of Brain During and Following Ischemia

Approximately 40% of anaerobic metabolism in resting brain is dedicated to the maintenance of ion homeostasis [Astrup, 1981], which enables the transmission of neuronal impulses and the maintenance of cell volume, substrate transport and other processes. The Na^+ gradient, maintained by Na^+/K^+ ATPase, is of particular importance, since this form of potential energy is used to maintain Ca^{+2} homeostasis through the Na^+/Ca^{+2} exchanger, to maintain optimal intracellular pH through the Na^+/H^+ antiport, and to cotransport glucose and amino acids across the cell membrane. During cerebral ischemia, high-energy phosphates are rapidly depleted, so that ion gradients can no longer be maintained and efflux of K^+ into the extracellular space and influx of Na^+, Ca^{+2}, Cl^- and HCO_3^- into the intracellular space occurs. Since the calcium cascade is thought to be a major mechanism of damage in delayed neuronal injury, calcium removal from the cytosol through the action of the Na^+/Ca^{+2} exchanger would be of paramount importance. Since the level of glycemia affects the rate of recovery of high-energy phosphates following transient forebrain ischemia [Tyson, 1993] it is possible that blood glucose level at the time of ischemia may influence the rate of recovery of the Na^+ membrane gradient.

The measured brain water in this experiment content prior to ischemia agrees well with that found elsewhere (ranging from *ca.* 77% to 83%, depending on brain region [Kadoya, 1995; Yamasaki, 1995]. Post-ischemia increases in brain water due to tissue edema was observed here at 90 min of reperfusion. This is somewhat longer than has been found by others [Mellergard, 1989]. However, the 15 min ischemia period is longer than the duration used by Mellergard, presumable resulting in more severe edema. Ischemia of 5 min of duration, for instance, is insufficient to cause significant edema in the bilateral carotid occlusion model of ischemia [Mellergard, 1989].

The arrangement of the coils used in following changes in the single- and double-quantum ^{23}Na NMR signals is different than that used in the ^{31}P NMR experiments. The saddle coil used in the transmission of radiofrequency pulses yields a homogeneous B_1 field over the volume of interest. Since the surface coil is acting only as a receiver in this case, the signal from the volume of interest decreases in

approximately a cubic fashion with the disance from the surface coil [Edelman, 1985]. Thus, the signals of greatest strength correspond to regions of the sample closest to the surface coil (cortex), with decreasing contributions from structures farther away from the coil (hippocampus, striatum and thalamus).

The increase in brain tissue sodium (Na^+_t) concentration following 10 minutes of forebrain ischemia observed in the present study agrees well with increases found using a four-vessel occlusion model of global ischemia of 15 minute duration [Nakao, 1990] and using a temporary middle cerebral arterial occlusion model of 1 hr duration [Ito, 1979]. Although no such changes were observed using flame emission spectroscopy in the experiments performed herein, there is a large spread in the data, particularly at 60 and 90 min post-ischemia. The increase in Na^+_t observed using ^{23}Na SQ NMR spectroscopy following ischemia may be due to increased leakage across the blood-brain barrier due to stimulation of Na^+/K^+ ATPase in the endothelial cells of microvessels [Mrsulja, 1980], thereby transferring Na^+ (and water) from blood to the extracellular compartment. It has been suggested that free fatty acids and free radicals generated during ischemia may contribute to such a stimulation of Na^+/K^+ ATPase [Asano, 1987]. Glucose, on the other hand, inhibits endothelial Na^+/K^+ ATPase [Knudsen, 1989; Yorek, 1991], so that post-ischemic stimulation may be more pronounced in hypoglycemic rats, leading to a greater increase in Na^+_t in these animals. This may explain the greater increase in the SQ ^{23}Na NMR signal intensity following ischemia observed in hypoglycemic rats in this study.

Changes in the DQ ^{23}Na NMR signal due to ischemia and reperfusion reflect movement of Na^+ between the extracellular and the intracellular compartments. The values in table 7 for the apparent first-order rate constants $k_{DQ}{}^{i}$ and $k_{DQ}{}^{P}$ demonstrate that there is a clear dependence in the rates of movement of Na^+ on the level of glycemia. During ischemia, $k_{DQ}{}^{i}$ is smallest in hyperglycemic and largest in hypoglycemic animals, and in addition the onset of the increase in the DQ ^{23}Na NMR signal is delayed in the higher blood glucose groups. These observations indicate that there is a slower and delayed increase in the intracellular Na^+ concentration during ischemia in the setting of elevated blood glucose levels. The concentrations of the high-energy phosphates PCr and ATP similarly decrease at rates which decrease with increasing blood glucose level [section A results]. These observations are consistent with prolonged

maintenance of Na^+ homeostasis due to ongoing Na^+/K^+-ATPase activity, supported by ATP produced through anaerobic glycolysis of elevated brain glucose stores, during ischemia in rats with higher blood glucose levels. A similar glucose-dependent delay in the increase of extracellular K^+ during ischemia has been observed using ion-selective microelectrodes [Hansen, 1978; Siemkowicz, 1981a].

With re-established blood flow, the DQ ^{23}Na NMR signal rapidly decreases in intensity in the hypo and normo groups, (k_{DQ}^{P} = 0.392 and 0.518 minutes^{-1}, respectively), consistent with rapid movement of Na^+ out of the intracellular space. However, under hyperglycemic conditions, recovery is significantly slower (k_{DQ}^{P} = 0.094 minutes^{-1}). This parallels the much slower recovery of ATP during reperfusion in hyperglycemic animals [Tyson, 1993], so that the slower recovery of Na^+ homeostasis may be due in part to prolonged suppression of Na^+/K^+-ATPase activity following hyperglycemic ischemia. However, in addition there is a large increase in the intracellular H^+ concentration during ischemia in hyperglycemic animals [Wagner, 1992; Sutherland, 1992; Haraldseth, 1992; Tyson, 1993], and slower recovery of normal pH following reperfusion [Tyson, 1993]. The elevated intracellular H^+ levels may contribute to the slow recovery of Na^+_i by stimulation of the Na^+/H^+ antiport [Jakubovicz, 1989], countering the removal of Na^+ from the intracellular space by Na^+/K^+-ATPase.

The $I_\infty^{\ i}$ values for the three blood glucose groups are similar, consistent with intracellular Na^+ reaching a similar concentration during ischemia in all groups. The maximum change in the DQ signal attained during ischemia is similar to that obtained in hypoxic brain slices [Hutchison, 1993], and the 220% increase ($I_\infty^{\ i}$ in table 2) agrees well with a 205% increase in the intracellular concentration of Na^+ measured using microelectrodes in rat cortex during global ischemia [Hansen, 1985].

Following reperfusion, the DQ ^{23}Na NMR signal in the hypo and normo groups falls below the pre-ischemia level before complete recovery, as given by the values of $I_\infty^{\ P}$ in table 7. The significance of the Na^+ undershoot in the hypo and normo groups early in reperfusion is not clear, but similar undershoots involving extracellular K^+ concentrations have been observed following ischemia [Sick, 1982; Roberts, 1987] and neuronal excitation [Heinemann, 1975], and have been attributed to enhanced post-ischemia activity of Na^+/K^+ ATPase [Krnjevic, 1975; Cordingly, 1978] in these cases. Following reperfusion in

hyperglycemic animals, however, the DQ ^{23}Na NMR signal returns much more slowly to the pre-ischemia level with no undershoot, consistent with the argument above that delayed recovery of ATP levels may impede the resumption of Na^+/K^+ ATPase activity in these rats. This slower recovery of intracellular Na^+ following ischemia may be an important factor contributing to the accentuated ischemic brain injury in the presence of elevated blood glucose levels. For instance, Na^+ carries water as it is transferred across cell membranes, so that the slower removal of intracellular Na^+ may contribute to the observed increase in post-ischemic cytosolic edema in hyperglycemic animals [Berger, 1986;, Jakubovicz, 1987; Kraig, 1990]. Furthermore, slower recovery of Na^+ homeostasis may impede the function of the Na^+/Ca^{+2} exchanger [Stys, 1992], a major transporter of Ca^{+2} from the intracellular space, and contribute to the observed slower recovery of Ca^{+2} following ischemia in hyperglycemic animals [Araki, 1992]. Indeed, at high intracellular Na^+ concentrations the exchanger operates in reverse, increasing the intracellular concentration of Ca^{+2} until the intracellular concentration of Na^+ is sufficiently low to allow for normal operation [Zivin, 1991].

Changes in the SQ ^{23}Na NMR signal intensity have been used to follow Na^+ movement between the intracellular and extracellular spaces during generalized seizure in cats [Schnall, 1988] and global cerebral ischemia in dogs [Eleff, 1991]. The present study shows that, while small changes in SQ ^{23}Na NMR signal intensity occur during ischemia, the DQ ^{23}Na NMR signal intensity is a much more sensitive monitor of changes in intracellular Na^+ concentration during and following ischemia.

C. Effect of Glucose on Changes in the Forward Creatine Kinase and Agonal Glycolytic Rate Constants Following Forebrain Ischemia

It has already been established that hyperglycemia is detrimental to metabolic recovery and increases mortality. A threshold blood glucose (10-13 mM) exists, above which is generally fatal in combination with short duration ischemic injury [Siesjö, 1992]. The increased damage with hyperglycemia has been attributed to acidotic damage due to the greater amount of glucose available for anaerobic metabolism . Indeed, the results outlined in section A imply that recovery of aerobic metabolism is slower in hyperglycemic animals than for those with lower levels of blood glucose.

Transient cerebral ischemia is known also to cause a lowering of the cerebral metabolic rate of glucose consumption (CMR_g) in normoglycemic animals for at least 48 hr [Pulsinelli, 1982c]. This decreased metabolism is worsened with hyperglycemia. The reasons for this lowering in CMR are unclear, as are the reasons for the enhanced decrease by hyperglycemia. A number of possible reasons for this decrease exist, including inhibition of glucose transport, reduced neuronal activity or damage to energy-producing pathways [Kozuka, 1989]. The activity of one enzyme, the pyruvate dehydrogenase complex, decreases following transient forebrain ischemia, but no further enhancement in the post-ischemic decrease in activity was observed with hyperglycemia [Lundgren, 1990]. However, no long term recovery data on the activity of this enzyme has been reported. In order to determine what aspect(s) of metabolism cause the depression in the cerebral metabolic rate, the effect of ischemia on the kinetics of glycolysis (as reflected by the agonal glycolytic rate) and ATP turnover (reflected by the forward creatine kinase rate constant) were studied.

While the results in section A (and other similar studies) yield valuable information on the steady-state amounts of high-energy phosphates, they do not give any information on the rate of high-energy phosphate turnover. The various forms of creatine kinase in brain are in sufficient concentration to ensure that the reaction:

$$PCr^{-3} + MgADP^{-} + H^{+} \leftrightarrow Cr^{-} + MgATP^{-2}$$

operates near equilibrium, so that the forward creatine kinase rate is comparable to the rate of ATP consumption [Ogurno, 1977; Ericenska, 1989]. Thus, the saturation transfer technique, by measuring the forward rate constant in the above reaction, offers a non-invasive method for observing the rate of ATP turnover in tissue.

Figure 21 shows the decrease in PCr with γ-ATP saturation time. Note that the β-ATP peak height remains constant throughout and that the γ-ATP resonance is fully saturated, so that the use of equation 14 is justified. Figure 22 demonstrates the fit of equation 14 to the control group. From equation 11 it is seen that k_{for} is not a pure first-order rate constant, as it assumes that both $[H^+]$ and $[MgADP^-]$ are the same for each measurement. Using equation 1, no differences in tissue pH were observed. ADP levels are assumed not to change over time following ischemia. This is supported by the observation that the [ATP]/[PCr] ratio does not change following ischemia. Thus, changes in k_{for} should reflect changes in the ATP turnover rate.

The value of k_{for} obtained for normal rats (the pre-ischemia group) in this study was $0.52 \pm 0.03\ s^{-1}$ (with the spin-lattice relaxation time $T_{1,PCr}$ of 2.62 ± 0.18 s), lying in the upper range of those listed in table 2. One important point to note is the inverse relationship of k_{for} and $T_{1,PCr}$ shown in table 2. When a multiple-parameter fit is performed on any data set the parameters are not, in general, independent. Thus, it is advisable to reduce the number of parameters to be determined as much as possible. Since the value of $T_{1,PCr}$ did not change with progressing time post-ischemia, the fit was reduced to a single variable in order to minimize errors in the measurement of k_{for}. However, error may still exist in the measurement of k_{for}, since the mean value of $T_{1,PCr}$ from the individual fits was used, but this error is systematic and constant over all of the fits of equation 14 to the data. Relative changes in k_{for} should then be clearer with the single parameter fit. Figure 22 demonstrates that the sufficiently good fits are obtained using the mean $T_{1,PCr}$ value.

No change in k_{for} (figure 23), and hence no change in ATP turnover, following ischemia under normoglycemic conditions is seen for 48 hr (in contrast to the case of pyruvate dehydrogenase activity), followed by a slow decrease becoming significant 5 days post-ischemia and subsequently recovers by 7

days of reperfusion. The slow decrease between 2 and 5 days may be a manifestation of delayed mitochondrial damage [Sims, 1987] accompanying delayed neuronal injury in the selectively vulnerable regions of the brain. Except for a significant drop in k_{for} at 4 hr, the time course changes in ATP turnover for the hyperglycemic group parallels that for the normoglycemic group closely. Thus, a decrease in k_{for} occurs whether the animal is normo- or hyperglycemic. However, the time following reperfusion at which k_{for} decreases depends on the level of glucose at the time of ischemia. Since a high mortality rate occurs in the hyperglycemic group by 24 hr post-ischemia, it is possible that the rats surviving till later time points were not injured as severely as hyperglycemic animals which died within 1 day post-ischemia. The large decrease in ATP turnover at 4 hr following hyperglycemic ischemia may be partly responsible, in addition to strong activation of the Na^+/H^+ antiport, for the slow recovery of $[Na^+]_i$ in these animals [Tyson, 1996]. Since recovery of ATP at 1 hr post-ischemia is incomplete following hyperglycemic ischemia [Tyson, 1993], the slower ATP turnover at 4 hr of recovery in these animals implies that the rate of ATP formation is also decreased.

The effect of ischemia on glycolysis in normo- and hyperglycemic animals was studied through the post-ischemic changes in the agonal glycolytic rate constant k_{AGR}. The agonal glycolytic rate is a measure of the potential of glycolysis to convert glucose to lactate. This rate constant is not a single rate constant, but an effective rate constant for the whole glycolytic pathway. It is likely that the key rate-determining enzymes in glycolysis, hexokinase and phosphofructokinase, have the greatest effect on the overall rate constant. This method cannot, however, separate changes in the kinetics of the glycolytic pathway or determine if the rate of glycolysis is limited by glucose transport [Corbett, 1991].

The curve fit of equation 58 to the data shown in figure 26 confirms that the post-mortem rise in lactate can be fitted using a single apparent first-order rate constant and that the conversion of glucose to lactate follows apparent first-order kinetics [Nilsson, 1975; Petroff, 1988; Corbett, 1991]. The value of the apparent first-order rate constant in normal rats was found to be 0.51 ± 0.05 min^{-1}, in excellent agreement with that found for adult rabbit brain [Petroff, 1988].

The data contained in figure 27 differ from that obtained for changes in the cerebral metabolic rate of glucose following ischemia in normoglycemic animals. CMR_g is known to decrease following ischemia in normoglycemic animals and remains depressed for at least 48 hr [Pulsinelli, 1982c; Kozuka, 1989; Triolo, 1990; Katsura, 1994]. CMR_g measures the rate of glucose uptake into tissue which is not under metabolic stress (aside from the initial ischemic event), while k_{AGR} is measured in tissue where glycolytic enzymes are maximally stimulated. Thus, k_{AGR} is a measure of the capacity of glycolysis to use glucose. Factors which may inhibit glycolysis in the unstressed tissue and which may decrease CMR_g (*eg.*, high ATP and low ADP levels), are removed under agonal conditions. This is analogous to the recovery of the metabolic capacity of ischemic brain tissue demonstrated by seizure activity induced by bicucculine [Katsura, 1994]. Despite a post-ischemic decrease in the cerebral metabolic rate of oxygen and cerebral blood flow, during seizures induced 6 hr following 15 min ischemia both cerebral metabolic rate of oxygen and cerebral blood flow are similar to that during seizures in non-ischemic animals [Katsura, 1994]. Thus, normoglycemic ischemia does not affect the metabolic capacity of tissue. Since k_{AGR} does not change for at least 24 hr post-ischemia, the post-ischemic decrease in CMR_g observed elsewhere cannot be due to changes in glucose transport or to damage of enzymes in the glycolytic pathway. Following this period there is a decrease in k_{AGR} similar to that seen in k_{for}. Unlike k_{for}, there is no subsequent recovery in k_{AGR} by 7 days post-ischemia.

The glycolytic capacity is significantly decreased at 4 hr post-ischemia in hyperglycemic animals and remains depressed. Metabolism is generally depressed at 4 hr, since k_{for} also decreases, but some aspects of metabolism recover following 24 hr of reperfusion. It is thus possible that the post-ischemic depression in CMR_g is due at least in part to the decreased ability of glycolysis to make use of glucose. Thus, there is a decrease in both k_{for} and k_{AGR}, the time following ischemia at which these decreases occur being dependent on the glucose level at the time of ischemia.

The use of saturation transfer ^{31}P and STEAM-localized ^{1}H NMR spectroscopy has been shown to be useful in elucidating what aspects of metabolism are (or are not) affected by ischemia at various times during recovery. The relatively small number of animals necessary and the non-invasive aspect of NMR

spectroscopy make it a desirable method in such studies.

V. CONCLUSION

It has been clearly demonstrated that hyperglycemia induced prior to transient forebrain ischemia has serious consequences on metabolism in the post-ischemic period, depressing the recovery of high-energy phosphate levels and sodium gradient recovery early during reperfusion, as well as long-term affects on tissue metabolism. In the clinical setting, these results indicate that immediate lowering of blood glucose upon admission would be of benefit to recovery. Since the sodium gradient is the primary energy source for the removal of excess Ca^{+2} from the cytosol, the administration of Na^{+}/H^{+} antiport blocking agents to delay the removal of excess H^{+} ions generated during hyperglycemic ischemia may be helpful in ameliorating both Ca^{2+}-induced and edemic tissue damage. This is a methodology that would be of particular importance for diabetic victims of ischemia.

The use of *in vivo* spectroscopic techniques has been demonstrated to be of great value in determining the effects of ischemia on cerebral metabolism and in elucidating mechanisms of damage. NMR spectroscopy offers relatively non-invasive methods to make repeated measurements of metabolic parameters in single animals, not only reducing the number of animals required but also reducing errors in measurement of parameters.

The knowledge gained of the interplay between glucose and short-duration cerebral ischemia will have a direct bearing on the treatment of ischemia in the clinical setting. Hyperglycemia resulting from a systemic response to ischemia is often observed upon admittance to hospital care. Reduction of blood glucose level to normoglycemia from hyperglycemia early in treatment of ischemia will significantly moderate cerebral metabolic disturbances and decrease neuronal damage. Presumably, this will result in decreases in mortality and in the amount of care necessary for recovery following cerebral ischemia.

VI. REFERENCES

Abe K, Aoki M, Kawagoe J, Yoshida T, Hattori A, Kogure K, Itoyama Y (1995) Ischemic delayed neuronal death. A mitochondrial hypothesis. *Stroke* **26**:1478-1489

Allen K, Busza AL, Crockard HA, Frackowiak RS, Gadian DG, Proctor E, Russell RW, Williams SR (1988) Acute cerebral ischaemia: concurrent changes in cerebral blood flow, energy metabolites, pH, and lactate measured with hydrogen clearance and 31P and 1H nuclear magnetic resonance spectroscopy. III. Changes following ischaemia. *J Cereb Blood Flow Metab* **8**:816-821

Allen KL, Busza AL, Proctor E, Williams SR, Van Bruggen N, Gadian DG, Crockard HA (1990) Restoration of energy metabolism and resolution of oedema following profound ischaemia. *Acta Neurochirurgica Suppl* **51**:171-173

Allis JL, Seymour AL, Radda GK (1991) Absolute quantification of intracellular Na^+ using triple-quantum-filtered sodium-23 NMR. *J Magn Reson* **93**:71-76

Altura BM, Altura BT (1994) Role of magnesium and calcium in alcohol-induced hypertension and strokes as probed by in vivo television microscopy, digital image microscopy, optical spectroscopy, 31P-NMR, spectroscopy and a unique magnesium ion-selective electrode. *Alcoholism, Clinical & Experimental Research* **18**:1057-68

Altura BM, Gebrewold A, Altura BT, Gupta RK (1995) Role of brain [Mg2+]i in alcohol-induced hemorrhagic stroke in a rat model: a 31P-NMR in vivo study. *Alcohol* **12**:131-6

Ames A, Nesbett FB (1983) Pathophysiology of ischemic cell death. I. Time of onset of irreversible damage; importance of the different components of the ischemic insult. *Stroke* **14**:219-226

Anderson CF, Record MT (1990) Ion distributions around DNA and other cylindrical polyions: theoretical descriptions and physical implications. *Ann Rev Biophys Chem* **19**:423-465

Araki N, Greenberg JH, Sladky JT, Uematsu D, Karp A, Reivich M (1992) The effect of hyperglycemia on intracellular calcium in stroke. *J Cereb Blood Flow Metab* **12**:469-476

Asano T, Shigeno T, Johshita H. A novel concept on the pathogenetic mechanism underlying ischaemic brain oedema: relevance of free radicals and eicosanoids. *Acta Neurochir Suppl Wien.* 1987;41:85-96

Assaf HM, Ricci AJ, Whittingham TS, LaManna JC, Ratcheson RA, Lust WD (1990) Lactate compartmentation in hippocampal slices: evidence for a transporter. *Metabolic Brain Disease* **5**:143-154

Astrup J, Symon L, Branston NM, *et al* (1977) Cortical evoked potential and extracellular K^+ and H^+ at critical levels of brain ischemia. *Stroke* **8**:51-57

Astrup J, Moller-Sorensen P, Rahbek-Sorensen H (1981) Oxygen and glucose consumption related to Na^+-K^+ transport in canine brain. *Stroke* **12**:726-730

Bain AD, Fahie BJ, Kozluk T, Leigh WJ (1991) Improvements in the quantitation of NMR spectra by the use of statistical methods. *Can J Chem* **69**:1189-1192

Barnes DM (1988) Cells without growth factors commit suicide. *Science* **242**:1510-1511

Basson CT, Grace AM, Roberts R (1985) Enzyme kinetics of a highly purified mitochondrial creatine kinase in comparison with cytosolic forms. *Mol Cell Biochem* **67**:151-159

Bax A, Freeman R, Kempsell SP (1980) Natural abundance ^{13}C-^{13}C coupling observed via double quantum coherence. *J Amer Chem Soc* **102**:4849-4851

Behar KL, Den Hollander JA, Stromski ME, Ogino T, Shulman RG, Petroff OAC, Prichard JW. (1983) High-resolution ^1H nuclear magnetic resonance study of cerebral hypoxia *in vivo*. *Proc Natl Acad Sci USA* **80**:4945-4948

Behar KL, Rothman DL, Hossmann KA (1989) NMR spectroscopic investigation of the recovery of energy and acid-base homeostasis in the cat brain after prolonged ischemia. *J Cereb Blood Flow Metab* **9**:655-665

Bell GI, KayanoT, Buse JB, Burant CF, Takeda J, Lin D, Fukamoto H, Seino S (1990) Molecular biology of mammalian glucose transporters. *Diabetes Care* **13**:198-208

Benveniste H, Drejer J, Schousboe A, Diemer NH (1984) Elevation of the extracellular concentrations of glutamate and aspartate in rat hippocampus during transient cerebral ischemia monitored by intracerebral microdialysis. *J Neurochem* **43**:1369-1374

Berger L, Hakim AM (1986) The association of hyperglycemia with cerebral edema in stroke. *Stroke* **17**:865-871

Birken DL, Oldendorf WH (1989) N-acetyl-L-aspartic acid: a literature review of a compound prominent in 1H-NMR spectroscopic studies of brain. *Neurosci Biobehav Rev* **13**:23-31

Birnbaum, MJ, Haspel, HC, Rosen, OM (1986) Cloning and characterization of a cDNA encoding the rat brain glucose-transporter protein. *Proc Natl Acad Sci USA* **83**:5784-88

Bittl JA, DeLayre J, Ingwall JS (1987) Rate equation for creatine kinase predicts the in vivo reaction velocity: ^{31}P nmr surface coil studies in brain,heart, and skeletal muscle of the living rat. *Biochemistry* **26**:6083-6090

Bleam ML, Anderson CF, Record MT (1983) Sodium-23 nuclear magnetic resonance studies of cation-deoxyribonucleic acid interactions. *Biochemistry* **22**:5418-5424

Bodsch W, Takahashi K, Barbier B, Ophoff G, Hossmann KA (1985) Cerebral proteins and ischemia. *Prog Brain Res* **63**:197-210

Branston NM, Symon L, Crockard HA, *et al* (1974) Relationship between the cortical evoked potential and local cortical blood flow following acute middle cerebral artery occlusion in the baboon. *Exp Neurol* **45**:195-208

Branston NM, Strong AJ, Symon L (1977) Extracellular potassium activity, evoked potential and tissue blood flow. *J Neurol Sci* **32**:305-321

Brooks KJ, Pirttila T-RM, Kauppinen RA (1993) Delayed increase in intracellular Na^+ in cerebral cortical slices during severe hypoxia as measured by double-quantum filtered ^{23}Na NMR. *Neuroreport* **4**:139-142

Bruhn H, Frahm J, Gyngell ML, Merboldt KD, Hanicke W, Sauter R (1989) *Magn Reson Med* **9**:126

Buchan AM, Williams L, Bruederlin B (1990) Nerve growth factor: pretreatment ameliorates ischemic hippocampal neuronal injury. *Stroke* **21**:s177 (abstract)

Bull TE (1972) Nuclear magnetic relaxation of spin-3/2 nuclei involved in chemical exchange. *J Magn Reson* **8**:344-353

Burés J, Buresova O (1981) Cerebral $[K^+]_e$ increase as an index of the differential susceptibility of brain structures to terminal anoxia and electroconvulsive shock. *J Neurobiol* **12**:211-220

Burt CT, Cheng H-M, Gabel S, London RE (1990) *J Biol Chem* **108**:441-448

Busto R, Ginsberg MD (1985) Graded focal cerebral ischemia in the rat by unilateral carotid artery occlusion and elevated intracranial pressure: hemodynamic and biochemical characterization. *Stroke* **16**:466-476

Calle PA, Buylaert WA, Vanhaute OA (1989) Cerebral Resuscitation Study Group: Glycemia in the post-resuscitation period. *Resuscitation* **17**:S181-S188

Candelise L, Landi G, Orazio EN, Boccardi E (1985) Prognostic significance of hyperglycemia in acute stroke. *Arch Neurol* **42**:661-663

Chang LH, Shirane R, Weinstein PR, James TL (1990) Cerebral metabolite dynamics during temporary complete ischemia in rats monitored by time-shared 1H and 31P NMR spectroscopy. *Magn Reson Med* **13**:6-13

Choi DW (1992) Excitotoxic cell death. *J Neurobiol* **23**:1261-1276

Choki J, Greenberg J, Reivich M (1983) Regional cerebral glucose metabolism dring and after bilateral cerebral ischemia in the gerbil. *Stroke* **14**:568-574

Chopp M, Frinak S, Walton DR, Smith MB, Welch KMA (1987) Intracellular acidosis during and after cerebral ischemia: in vivo nuclear magnetic resonance study of hyperglycemia in cats. *Stroke* **18**:919-923

Chopp M, Welch KMA, Tidwell BS, Helpern JA (1988) Global cerebral ischemia and intracellular pH during hyperglycemia and hypoglycemia in cats. *Stroke* **19**:1383-1387

Christiansen P, Henriksen O, Stubgaard M, Gideon P, Larsson HB (1993) In vivo quantification of brain metabolites by 1H-MRS using water as an internal standard. *Magn Reson Imaging* **11**:107-118

Chu SC, Pike MM, Fossel ET, Smith TW, Balschi JA, Springer CS Jr. (1984) Aqueous shift reagents for high-resolution cationic nuclear magnetic resonance. III. $Dy(TTHA)^{-3}$, $Tm(TTHA)^{-3}$, and $Tm(PPP)_2^{-7}$. *J Magn Reson* **56**:33-47

Chu SCK, Xu Y, Balschi JA, Springer CS, Jr (1990) Bulk magnetic susceptibility shifts in NMR studies of compartmentalized samples: use of paramagnetic reagents. *Magn Reson Med* **13**:239-262

Chung C, Wimperis S (1990) Optimum detection of spin-3/2 biexponential relaxation using multiple-quantum filtration techniques. *J Magn Reson* **88**:440-447

Civan MM, Shporer M (1978) NMR of sodium-23 and potassium-39 in biological systems. In *Biological Magnetic Resonance*, Berliner LJ and Reuben J eds., Plenum, New York. pp. 1-32.

Collins RC, Dobkins BH, Choi DW (1989) Selective vulnerability of the brain: new insights into the pathophysiology of stroke. *Ann Intern Med* **110**:992-1000

Combs DJ, Dempsey RJ, Maley M, Donaldson D, Smith C (1990) Relationship between plasma glucose, brain lactate, and intracellular pH during cerebral ischemia in gerbils. *Stroke* **21**:936-942

Corbett RJT, Laptook AR, Ruley JI, Garcia D (1991) The effect of age on glucose-modulated cerebral agonal glycolytic rates measured *in vivo* by ^{1}H NMR spectroscopy. *Pediatric Res* **30**:579-586

Corbett RJ, Laptook AR, (1993a) ^{31}P NMR relaxation does not affect the quantitation of changes in phosphocreatine, inorganic phosphate, and ATP measured in vivo during complete ischemia in swine brain. *J Neurochem* **61**:144-149.

Corbett RJT, Laptook AR, Sterett R, Tellefsbol G, Garcia D (1993b) The effect of hypercarbia on age-related changes in cerebral glucose transport and glucose-modulated agonal glycolytic rates. *Pediatric Res* **34**:370-378

Corbett RJT, Sterett R, Laptook AR (1995) Evaluation of potential effectors of agonal glycolytic rate in developing brain measured *in vivo* by ^{31}P and ^{1}H nuclear magnetic resonance spectroscopy. *J Neurochem* **64**:322-331

Cordingly GE, Somjen GG (1978) The clearing of excess potassium from the extracellular space in spinal cord and cerebral cortex. *Brain Research* **151**:291-306

Cottrell JE (1995) Pharmacologic brain protection: specific agents. *Ann Fr Anesth Reanim* **14**:134-141

Cox DW, Morris PG, Bachelard HS (1988) Kinetic analysis of the cerebral creatine kinase reaction under hypoxic and hypoglycaemic conditions in vitro. A ^{31}P-n.m.r. study. *Biochem J* **255**:523-527

Davalos A, Cendra E, Teruel J, Martinez M, Genis D, (1990) Deteriorating ischemic stroke: risk factors and prognosis. *Neurology* **40**:1865-1869

Deckwerth TL, Johnson Jr EM (1993) Temporal analysis of events associated with programmed cell death (apoptosis) of sympathetic neurons deprived of nerve growth factor. *J Cell Biol* **356**:314-317

De Courten-Meyers GM, Myers RE, Schoolfield L (1988) Hyperglycemia enlarges infarct size in cerebrovascular occlusion in cats. *Stroke* **19**:623-630

De Courten-Meyers GM, Kleinholz M, Wagner KR, Myers RE (1989) Fatal strokes in hyperglycemic cats. *Stroke* **20**:1707-1715

Desphande J, Bergstedt K, Linden T, Kalimo H, Wieloch T (1992) Ultrastructural changes in the hippocampal CA1 region following transient cerebral ischemia: evidence against programmed cell death. *Exp Brain Res* **88**:91-105

Dessi F, Charriaut-Marlangue C, Khrestchatisky M, Ben-Ari Y (1993) Glutamate-induced neuronal death is not a programmed cell death in cerebellar culture. *J Neurochem* **60**:1953-1955.

Dietrich WD, Busto R, Watson BD, Scheinberg P, Ginsberg MD (1987) *Acta Neuropathol* **72**:326-334

Dowd TL, Gupta RK (1992) Multinuclear NMR studies of intracellular cations in perfusied hypertensive rat kidney. *J Biol Chem* **267**:3637-3643

Dowd TL, Gupta RK (1993) NMR studies of the effect of hyperglycemia on intracellular cations in rat kidney. *J Biol Chem* **268**:991-996

Edelman RR, McFarland E, Stark DD, Ferrucci JT Jr., Simeone JF, Wismer G, White EM, Rosen BR, Brady TJ (1985) Surface coil MR imaging of abdominal viscera. Part I. Theory, technique, and initial results. *Radiology* **157**:425-430

Ehrlich P (1885) Das Sauerstoff-Dedurfniss des Organismus. Eine farganalytische Studie. Berlin.

Eisenberg M, Gresalfi T, Riccio T, McLauglin SGA (1979) Adsorption of monovalent cations to bilayer membranes containing negative lipids. *Biochemistry* **18**:5213-5223

Eklöf B, Siesjö BK (1972) The effect of bilateral carotid artery ligation upon the blood flow and energy state of the rat brain. *Acta Physiol Scand* **86**:155-165

Eleff SM, Maruki Y, Monsein LH, Traystman RJ, Bryan N, Koehler RC (1991) Sodium, ATP, and intracellular pH transients during reversible complete ischemia of dog cerebrum. *Stroke* **22**:233-241

Eleff SM, McLennen IJ, Hart GK, Maruki Y, Traystman RJ, Koehler RC (1993) Shift reagent enhanced concurrent ^{23}Na and ^{1}H magnetic resonance spectroscopic studies of transcellular sodium distribution in the dog brain *in vivo*. *Magn Reson Med* **30**:11-17

Eliav U, Shinar H, Navon G (1991) An observation of ^{23}Na NMR triple-quantum dynamic shift in solution. *J Magn Reson* **94**:439-444

Eliav U, Shinar H, Navon G (1992) The formation of a second-rank tensor in ^{23}Na double-quantum-filtered NMR as an indicator for order in a biological tissue. *J Magn Reson* **98**:223-229

Erecinska M, Silver IA (1989) ATP and brain function. *J Cereg Blood Flow Metab* **9**:2-19

Erecinska M, Silver IA (1992) Relationship between ions and energy metabolism: cerebral calcium movements during ischemia and subsequent recovery. *Can J Physiol Pharmacol* **70**:S190-S193

Ernst T, Hennig J (1991) Coupling effects in volume selective 1H spectroscopy of major brain metabolites. Magn Reson Med **21**:82-96

Fischer HW, van Haverbeke Y, Schmitz-Feuerhake I, Muller RN (1989) The uncommon longitudinal relaxation dispersion of human brain white matter. *Magn Reson Med* **9**:441-446

Fischer HW, Tinck PA, van Haverbeke Y, Muller RN (1990) Nuclear relaxation of human brain grey and white matter: Analysis of field dependence and implications for MRI. *Magn Reson Med* **16**:317-334

Forsén S, Hoffman RA (1963) Study of moderately rapid chemical exchange reaction by means of nuclear magnetic double resonance. *J Chem Physiol* **40**:1189-1196

Forsén S, Lindman B (1981) Ion binding in biological systems as studied by NMR spectroscopy. *Methods Biochem Anal* **27**:289-486

Fossel ET, Höfeler H (1986) Observation of intracellular potassium and sodium in the heart by NMR: a major fraction of potassium is 'invisible'. *Magn Reson Med* **3**:534-540

Frahm J, Bruhn H, Gyngell ML, Merboldt KD, Hanicke W,Sauter R (1989) Localized proton NMR spectroscopy in different regions of the human brain *in vivo*. Relaxation times and concentrations of cerebral metabolites. *Magn Reson Med* **11**:47-63

Frahm J, Michaelis T, Merboldt KD, Bruhn H, Gungell ML, Hanicke W (1990) Improvements in localized NMR spectroscopy of hyman brain. Water suppression, echo times, and 1 ml resolution. *J Magn Reson* **90**:464-473

Fujii K, Sadoshima S, Yao H, Yoshida F, Iwase M, Fujishima M (1989) Cerebral ischemia in spontaneously hypertensive rats with type 2 (noninsulin-dependent) diabetes mellitus, cerebral blood flow and tissue metabolism. *Gerontology* **35**:78-87

Gaitonde MK, Evison E, Evans GM (1983) The rate of utilization of glucose via the hexose-monophosphate shunt in brain. *J Neurochem* **41**:1253-1260

Garfinkel L, Garfinkel D (1984) *Biochemistry* **23**:3547-3552

Ginsberg MD (1981) Local brain blood flow-metabolism interrelationships in an experimental model of diffuse cerebral ischemia. In, Cerebral Vasular Disease 3. Proceedings of the Tenth International Salzburg Conference, Meyer JS, Lechner H, Reivich M, Ott EO, eds. Amsterdam, Excerpta Medica, pp 195-200

Ginsberg MD, Busto R (1989) Rodent models of ischemia. *Stroke* **20**:1627-1642

Goldberg ND, Passonneau JV, Lowry OH (1966) Effects of changes in brain metabolism on the levels of citric acid cycle intermediates. *J Biol Chem* **241**:3997-4003

Green AR, Cross AJ (1994) *Neurosci Lett* **173**:27-30

Griffey RH, Griffey BV, Matwiyoff NA (1990) Triple-quantum-coherence-filtered imaging of sodium ions *in vivo* at 4.7 Tesla. *Magn Reson Med* **13**:305-313

Grinstein S, Cohen S, Rothstein A (1984) Cytoplasmic pH regulation in thymic lymphocytes by an amiloride-sensitive Na^+/H^+ antiport. *J Gen Physiol* **83**:341-369

Gupta RK, Benovic JL, Rose ZB (1978) *J Biol Chem* **253**:6165-6171

Gupta RK, Gupta P (1982) Direct observation of resolved resonances from intra- and extracellular sodium-23 ions in NMR studies of intact cells and tissues using dysprosium (III) tripolyphosphate as paramagnetic shift reagent. *J Magn Reson* **47**:344-350

Gustavsson H, Lindman B (1978) Alkali ion binding to aggregates of amphiphilic compounds studied by nuclear magnetic resonance chemical shifts. *J Am Chem Soc* **100**:4647-4654

Gyngell ML, Ellermann J, Michaelis T, Hanicke W, Merboldt KD, Bruhn H, Frahm J (1991) Non-invasive ^1H NMR spectroscopy of the rat brain *in vivo* using a short echo time STEAM localization sequence. *NMR in Biomed* **4**:150-156

Hansen AJ (1978) The extracellular potassium concentration in brain cortex following ischemia in hypo- and hyperglycemic rats. *Acta Physiol Scand* **102**:324-32

Hansen AJ, Gjedde A, Siemkowicz E (1980) Extracellular potassium and blood flow in the post-ischemic rat brain. *Pflugers Arch* **389**:1-7

Hansen AJ (1985) Effect of anoxia on ion distribution in the brain. *Physiol Rev* **65**:101-148

Haraldseth O, Nygård O, Gronås T, Southon T, Gisvold SE, Unsgård G (1992) Hyperglycemia in global cerebral ischemia and reperfusion: a 31-phosphorus NMR spectroscopy study in rats. *Acta Anaesthesiol Scand* **36**:25-30

Hashimoto Y, Kawatsura H, Shiga Y, Furukawa S, Shigeno T (1992) Significance of nerve growth factor content levels after transient forebrain ischemia in gerbils. *Neurosci Lett* **139**:45-46

Heinemann U, Lux HD (1975) Undershoots following stimulus-induced rises in extracellular potassium concentration in the cerebral cortex of cat. *Brain Research* **120**:231-249

Heiss WD, Hayakawa T, Waltz AG (1976) Cortical neuronal function during ischemia. Effects of occlusion of one middle cerebral artery on single-unit activity in cats. *Arch Neurol* **33**:813-820

Helgason CM (1988) Blood glucose and stroke. *Stroke* **19**:1049-1053

Hemmer W, Wallimann T (1993) Functional aspects of creatine kinase in brain. *Developmental Neurosci* **15**:249-260

Hill ND, Millikan CH, Wakim KC, Sayre GP (1955) Studies in cerebrovascular disease. VII. Experimental production of cerebral infarction by intracarotid injection of homologous blood clot. *Mayo Clin Proc* **30**:625-633

Hillered L, Smith M-L, Seisjö BK (1985) Lactic acidosis and recovery of mitochondrial function following forebrain ischemia in the rat. *J Cereb Blood Flow Metab* **5**:259-266

Hoffman TL, LaManna JC, Pundik S, Selman WR, Whittingham TS, Ratcheson RA, Lust WD (1994) Early reversal of acidosis and metabolic recovery following ischemia. *J Neurosurg* **81**:567-573

Holtzman D, Offutt M, Tsuji M, Neuringer LJ, Jacobs D (1993a) Creatine kinase-catalyzed reaction rate in the cyanide-poisoned mouse brain. *J Cereb Blood Flow Metab* **13**:153-161

Holtzman D, Tsuji M, Wallimann T, Hemmer W (1993b) Functional maturation of creatine kinase in rat brain. *Dev Neurosci* **15**:261-270

Hope PL, Cady EB, Chu A, Delpy DT, Gardiner RM, Reynolds EO (1987) Brain metabolism and intracellular pH during ischaemia and hypoxia: an in vivo 31P and 1H nuclear magnetic resonance study in the lamb. *J Neurochem* **49**:75-82

Hore PJ (1983) A new method for water suppression in the proton NMR spectra of aqueous solutions. *J Magn Reson* **54**:539-542

Hossman KA, Sakaki S, Zimmerman V (1977) Cation activities in reversible ischemia of the cat brain. *Stroke* **8**:77-81

Hu BR, Wieloch T (1993) Casein kinase II activity in the postischemic rat brain increases in brain regions resistant to ischemia and decreases in vulnerable areas. *J Neurochem* **60**:1722-1728

Hutchison RB, Malhotra D, Hendrick E, Chan L, Shapiro JI (1990) Evaluation of the double-quantum filter for the measurement of intracellular sodium concentration. *J Biol Chem* **265**:15506-15510

Hutchison RB, Huntley JJA, Zhou DJ, Ciesla DJ, Shapiro JI (1993) Changes in double quantum filtered sodium intensity during prolonged ischemia in the isolated perfused heart. *Magn Reson Med* **29**:391-395

Ibayashi S, Fujishima M, Sadoshima S, Yoshida F, Shokawa O, Ogata J, Omae T (1986) Cerebral blood flow and tissue metabolism in experimental cerebral ischemia of spontaneously hypertensive rats with hypo-, normo- and hyperglycemia. *Stroke* **17**:261-265

Ito U, Ohno K, Nakamura R, Suganuma F, Inaba Y (1979) Brain edema during ischemia and after restoration of blood flow. *Stroke* **10**:542-547

Izumi Y, Roussel S, Pinard E, Seylaz J (1991) Reduction of infarct volume by magnesium after middle cerebral artery occlusion in rats. *Journal of Cerebral Blood Flow & Metabolism* **11**:1025-30

Jaccard G, Wimperis S, Boddenhausen G (1986) Multiple-quantum NMR spectroscopy of S=3/2 spins in isotropic phase: A new probe for multiexponential relaxation. *J Chem Phys* **85**:6282-6293

Jakubovicz DE, Grinstein S, Klip A (1987) Cell swelling following recovery from acidification in C6 glioma cells: an in vitro model of postischemic brain edema. *Brain Res* **435**:138-146

Jakubovicz DE, Klip A (1989) Lactic acid-induced swelling in C6 glial cells via Na^+/H^+ exchange. *Brain Res* **485**:215-224

Jelicks LA, Gupta RJ (1989a) Double-quantum NMR of sodium ions in cells and tissues. Paramagnetic quenching of extracellular coherence. *J Magn Reson* **81**:586-592

Jelicks LA, Gupta RJ (1989b) Observation of intracellular sodium ions by double-quantum-filtered ^{23}Na NMR with paramagnetic quenching of extracellular coherence by gadolinium tripolyphosphate. *J Magn Reson* **83**:146-151

Jelicks LA, Gupta RK (1989c) Multinuclear NMR studies of the Langendorff perfused rat heart. *J Biol Chem* **264**:15230-15235

Jorgensen MB (1993) The role of signal transduction in the delayed necrosis of the hippocampal CA1 pyramidal cells following transient ischemia. *Acta Neurologica Scandinavica Supplementum* **143**:1-20

Kadoya C, Domino EF, Yang GY, Stern JD, Betz AL (1995) Preischemic but not postischemic zinc protoporphyrin treatment reduces infarct size and edema accumulation after temporary focal ischemia in rats. *Stroke* **26**:1035-1038

Kägström E, Smith M-L, Siesjö BK (1983) Recirculation in the rat brain following incomplete ischemia. *J Cereb Blood Flow Metab* **3**:183-192

Kano M, Sugita K (1993) Expression of bcl-2 in ischemic cerebral injury of rats. *Jpn J Cereb Blood Flow Metab* **5**:74

Kasaniki MA, Cairns MT, Davies A, Gardiner RM, Baldwin SA (1987) Identification and characterization of the glucose transport protein of the bovine blood-brain barrier. *Biochem J* **247**:101-108

Kataoka K, Mitani A, Andou Y, Enomoto R, Ogita K, Yoneda Y (1993) Binding of [^{3}H]MK-801, NMDA-displaceable [^{3}H]glutamate, [^{3}H]glycine, [^{3}H]spermidine, [^{3}H]kainate and [^{3}H]AMPA to regionally discrete brain membranes of the gerbil: a biochemical study. *Neurochem Int* **22**:37-43

Katsura K, Ekholm A, Seisjö BK (1992) Tissue P_{CO2} in brain ischemia related to lactate content in normo- and hypercapnic rats. *J Cereb Blood Flow Metab* **12**:270-280

Katsura K, Folbergrova J, Gido G, Seisjö BK (1994) Functional, metabolic, and circulatory changes associated with seizure activity in the postischemic brain. *J Neurochem* **62**:1511-1515

Kauppinen RA, Williams SR (1994) Nuclear magnetic resonance spectroscopy studies of the brain. *Prog Neurobiology* **44**:87-118

Kirino T (1982) Delayed neuronal death in the gerbil hippocampus following ischemia. *Brain Res* **239**:57-69

Kirino T, Sano K (1984) Fine structural nature of delayed neuronal death following ischemia in the gerbil hippocampus. *Acta Neuropathol (Berlin)* **62**:209-218

Knudsen GM, Jakobsen J (1989) Blood-brain barrier permeability to sodium. Modification by glucose or insulin? *J Neurochem* **52**:174-178

Kogure K, Busto R, Scheinberg P, Reinmuth OM (1974) Energy metabolites and water content in rat brain during the early stage of development of cerebral infarction. *Brain* **97**:103-114

Kohler SJ, Kolodny NH, D'Amico DJ, Balasubramaniam S, Mainardi P, Gracoudas ES (1989) Magnetic resonance imaging determination of ^{23}Na visibility and T_2^* in the vitreous body. *J Magn Reson* **82**:505-517

Kozuka M, Smith M-L, Siesjö BK (1989) Preischemic hyperglycemia enhances postischemic depression of cerebral metabolic rate. *J Cereb Blood Flow Metab* **9**:478-490

Kraig RP, Pulsinelli WA, Plum F (1986) Carbonic acid buffer changes during complete brain ischemia. *Am J Physiol* **250**:R348-R357

Kraig RP, Chesler M (1990) Astrocytic acidosis in hyperglycemic and complete ischemia. *J Cereb Blood Flow Metab* **10**:104-114

Krnjevic K, Morris ME (1975) Factors determining the decay of k^+ potentials and focal potentials in the central nervous system. *Can J Physiol Pharmacol* **53**:923-934

Kuhmonen J, Sivenius J, Riekkinen PJ Sr, Kauppinen RA (1994) Decrease in brain choline-containing compounds following a short period of global ischemia in gerbils as detected by 1H NMR spectroscopy in vivo. *NMR in Biomed* 7:231-6

Kurland R, Newton C, Nir S, Papahadjopoulos D (1979) Specificity of Na^+ binding to phosphatidylserine vesicles from a ^{23}Na NMR relaxation rate study. *Biochim Biophys Acta* **551**:137-147

Kurland R, Ohki S, Nir S (1982) A phosphorus-31 NMR study of monovalent cation interactions with the negatively charged surface of phosphatidylserine vesicles. In Solution Behaviour of Surfactants, pp. 1443-1453. Plenum Press, New York.

Kushmerick MJ, Podolsky RJ (1969) Ionic mobility in muscle cells. *Science* **166**:1297-1298

Kushner M, Nencini P, Reivich M, Rango M, Jamieson D, Fazekas F, Zimmerman R, Chawluk J, Alavi A, Alves W (1990) Relation of hyperglycemia early in ischemic brain infarction to cerebral anatomy, metabolism, and clinical outcome. *Ann Neurol* **28**:129-135

Lane DP (1992) Cancer: p53, guardian of the genome. *Nature* **358**:15-16

Laptook AR, Corbett RJ, Arencibia-Mireles O, Ruley J, Garcia D (1994) The effects of systemic glucose concentration on brain metabolism following repeated brain ischemia. *Brain Res* **638**:78-84

Lawson JWR, Veech RL (1979) *J Biol Chem* **254**:6528-6537

LeMay DR, Gehua L, Zelenock GB, D'Alecy LG (1988) Insulin administration protects neurologic function in cerebral ischemia in rats. *Stroke* **19**:1411-1419

Lindman B, Soderman O, Wennerstrom H (1987) NMR studies of surfactant systems. In Surfactant Solutions: New Methods of Investigation, pp. 295-357. Marcel Dekker Inc., New York.

Ljunggren B, Schutz H, Siesjö BK (1974) Changes in energy state and acid-base parameters of the rat brain during complete compression ischemia. *Brain Res* **73**:277-289

London RE (1991) *Ann Rev Physiol* **53**:241-258

Longo R, Bampo A, Vidimari R, Magnaldi S, Giorgini A (1995) Absolute quantitation of brain 1H nuclear magnetic resonance spectra. Comparison of different approaches. *Investigative Radiology* **30**:199-203

Lowe SW, Ruley HE, Jacks T, Housman DE (1993) p53-dependent apoptosis modulates the cytotoxicity of anticancer agents. *Cell* **74**:957-967

Lundgren J, Cardell M, Wieloch T, Seisjö B (1990) Preischemic hyperglycemia and postischemic alteration of rat brain pyruvate dehydrogenase activity. *J Cereb Blood Flow Metab* **10**:536-541

Lyon RC, Pekar J, Moonen CTW, McLaughlin AC (1991) Double-quantum surface-coil NMR studies of sodium and potassium in the rat brain. *Magn Reson Med* **18**:80-92

Lyon RC, McLaughlin AC (1994) Double-quantum-filtered ^{23}Na NMR study of intracellular sodium in the perfused rat liver. *Biophys J* 67:369-376

Macri MA, Campanella R, Garreffa G, Occhigrossi M, De Luca F, Arrigoni Martelli E, Maraviglia B (1992) Partial cerebral ischemia assessed by "in vivo" 31P NMR spectroscopy in rats. *Magn Reson Imaging* **10**:769-772

Malloy CR, Buster DC, Castro MMCA, Geraldes CFGC, Jeffrey FM, Sherry AD (1990) Influence of global ischemia on intracellular sodium in the perfused rat heart. *Magn Reson Med* **15**:33-44

Manev H, Costa E, Wroblewski JT (1990) Abusive stimulation of excitatory amino acid receptors: a strategy to limit neurotoxicity. *FASEB J* **4**:2789-2797

Mantych GJ, James DE, Chung HD, Devaskar SU (1992) Cellular localization and characterization of Glut 3 glucose transporter isoform in human brain. *Endocrinology* **131**:1270-1278

Marks V, Dawson A (1965) Rapid stick method for determining blood glucose concentration. *Brit Med J* **1**:293

Marquardt DW (1963) An algorithm for least squares estimation of non linear parameters. *J Soc Ind Appl Math* **11**:431-441

Marsh WR, Anderson RE, Sundt TM (1986) Effect of hyperglycemia on brain pH levels in areas of focal incomplete cerebral ischemia in monkeys. *J Neurosurg* **65**:693-696

McIntosh TK, Vink R, Yamakami I, Faden AI (1989) Magnesium protects against neurological deficit after brain injury. *Brain Res* **482**:252-60

Medings JB, deSouza D, Goel M, Thiesen S (1990) Glucose transport and microvillus membrane physical properties along the crypt-villus axis of the rabbit. *J Clin Invest* **85**:1099-1107

Meldrum B, Evans M, Griffith T, Simon R (1985) Ischaemic brain damage; the role of excitatory activity and of calcium entry. *Br J Anaesth* **57**:44-46

Mellergard P, Bengtsson F, Smith ML, Riesenfeld V, Siesjö BK (1989) Time course of early brain edema following reversible forebrain ischemia in rats. *Stroke* **20**:1565-1570

Meyers RE, Yamaguchi S (1977) Nervous system effects of cardiac arrest in monkeys. *Arch Neurol* **34**:65-74

Michenfelder JD, Milde JH (1991) The relationship among canine brain temperature, metabolism, and function during hypothermia. *Anesthesiology* **75**:130-136

Miller BL (1991) A review of chemical issues in 1H NMR spectroscopy: N-acetyl-L-aspartate, creatine and choline. *NMR in Biomed* **4**:47-52

Moonen CTW, van Zijl PCM (1990) *J Magn Reson* **88**:28

Moriyoshi K, Masu M, Ishii T, Shigemoto R, Mizuno N, Nakanishi S (1991) Molecular cloning and characterization of the rat NMDA receptor. *Nature* **354**:31-37

Morris PG, Feeney J, Cox DWG, Bachelard HS (1985) ^{31}P-saturation-transfer nuclear-magnetic-resonance measurements of phosphocreatine turnover in guinea-pig brain slices. *Biochem J* **227**:777-782

Mrsulja BB, Djuricic BM, Cvejic V, Mrsulja BK, Abe K, Spatz M (1980) Biochemistry of experimental ischemic brain edema. *Adv Neurol* **28**:217-230

Murphy E, Freundenrich CC, Lieberman M (1991) *Ann Rev Physiol* **53**:273-287

Nadasy GL, Mela-Riker L, Reivich M, Kovach AG (1989) Parallel changes in brain tissue blood flow and mitochondrial function during and after 30 minutes of bilateral carotid arterial ischemia in the gerbil. *Acta Physioogica Hungarica* **74**:267-276

Nakai H, Yamamoto YL, Diksic M, Worsley KJ, Takara E (1988) Triple-tracer autoradiography demonstrates effects of hyperglycemiaon cerebral blood flow, pH, and glucose utilization in cerebral ischemia of rats. *Stroke* **19**:764-771

Nakao N, Itakura T, Yokote H, Nakai K, Komai N (1990) Effect of atrial natriuretic peptide on ischemic brain edema: changes in brain water and electrolytes. *Neurosurgery* **27**:39-43

Nakata N, Kato H, Liu Y, Kogure K (1992) Effects of pretreatment with sublethal ischemia on the extracellular glutamate concentrations during secondary ischemia in the gerbil hippocampus evaluated with intracerebral microdialysis. *Neurosci Lett* **138**:86-88

Nedergaard M (1987a) Transient focal ischemia in hyperglycemic rats is associated with increased cerebral infarction. *Brain Res* **408**:79-85

Nedergaard M, Diemer NH (1987b) Focal ischemia of the rat brain, with special reference to the influence of plasma glucose concentration. *Acta Neuropathol* **73**:131-137

Nilsson B, Norberg K, Nordstrom CH, Siesjö BK (1975) Rate of energy utilization in the cerebral cortex of rats. *Acta Physiol Scand* **93**:569-571

Norton WT, Podualo SE, Suzuki K (1966) Subacute sclerosing leukoencephalitis. II. Chemical studies including abnormal myelin and abnormal ganglioside pattern. *J Neuropathol Exp Neurol* **24**:582-597

Ogurno EA, Hearse DJ, Shillingford JP (1977) Creatine kinase isoenzymes: their separation and quantification. *Cardiobasc Res* **11**:94-102

Okawa M (1992) Effects of magnesium sulfate on brain damage by complete global brain ischemia. *Masui - Japanese Journal of Anesthesiology* **41**:341-55

Olsson T, Viitanen M, Asplund K, Eriksson S, Hägg E (1990) Prognosis after stroke in diabetic patients. A controlled prospective study. *Diabetol* **33**:244-249

Ordridge RJ, Connelly A, Lohman JAB (1986) *J Magn Reson* **66**:283

Padmanabhan S, Richey B, Anderson CF, Record MT (1988) Interaction of an N-methylated polyamine analogue, hexamethonium(+2), with NaDNA: quantitative ^{14}N and ^{23}Na NMR relaxation rate studies of the cation-exchange process. *Biochemistry* **27**:4367-4376

Papadopoulos SM, Chandler WF, Salamat MS, Topol EJ, Sackellares JC (1987) recombinant human tissue-type plasminogen activator therapy in acute thromboembolic stroke. *J Neurosurg* **67**:394-398

Pardridge, WM (1988) Recent advances in blood-brain barrier transport. *Ann Rev Pharmacol Toxicol* **28**:25

Pardridge, WM, Boado, RJ, Farrell, CR (1990) Brain-type glucose transporter (Glut 1) is selectively localized to the blood-brain barrier. *J Biol Chem* **265**:18035-40

Payne GS, Styles P (1991) Multiple-quantum-filtered ^{23}Na NMR spectroscopy in model systems. *J Magn Reson* **95**:253-266

Pekar J, Leigh JS Jr. (1986a) Detection of biexponential relaxation in sodium-23 facilitated by double-quantum filtering. *J Magn Reson* **69**:582-584

Pekar J, Renshaw PF, Leigh JS Jr. (1986b) Selective detection of intracellular sodium by coherence-transfer NMR. *J Magn Reson* **72**:159-161

Pekar J, Renshaw PF, Leigh JS Jr (1987) Selective detection of intracellular sodium by coherence-transfer NMR. *J Magn Reson* **72**:159-161

Petrasovits A, Nair C (1994) Epidemiology of stroke in Canada. *Health Rep* **6**:39-44

Petroff OAC, Prichard JW, Behar KL, Alger JR, den Hollander JA, Shulman RG (1985) Cerebral intracellular pH by ^{31}P nuclear magnetic resonance spectroscopy. *Neurology* **35**:781-788

Petroff OAC, Prichard JW, Ogino T, Shulman RG (1988) Proton magnetic resonance spectroscopic studies of agonal carbohydrate metabolism in rabbit brain. *Neurology* **38**:1569-1574

Pettegrew JW, Post JFM, Panchalinam K, Withers G, Woessner DE (1987) ^{7}Li NMR study of normal human erythrocytes. *J Magn Reson* **71**:504-519

Piantini U, Sorensen OW, Ernst RR (1982) Multiple quantum filters for elucidating NMR coupling networks. *J Magn Reson* **104**:6800-6801

Pike MM, Springer CS Jr. (1982) Aqueous shift reagents for high-resolution cationic nuclear magnetic resonance. *J Magn Reson* **57**:185-196

Pike MM, Yarmush DM, Balschi JA, Lenkinski RE, Springer CS Jr. (1983) Aqueous shift reagents for high resolution cationic nuclear magnetic resonance. 2. ^{25}Mg, ^{39}K, and ^{23}Na resonances shifted by chelidamate complexes of dysprosium (III) and thulium (III). *Inorg Chem* **22**:2388-2392

Pike MM, Frazer JC, Dedrick DF, Ingwall JS, Allen PD, Springer CS, Smith TW (1985) ^{23}Na and ^{39}K nuclear magnetic resonance studies of perfused rat hearts: discrimination of intra- and extracellular ions using a shift reagent. *Biophys J* **48**:159-173

Plum F (1983) What causes an infarction in ischemic brain? The Robert Wartenberg lecture. *Neurology* **33**:222-233

Prado R, Ginsberg MD, Dietrch WD, Watson BD, Busto R (1988) Hyperglycemia increases infarct size in collaterally perfused but not end-arterial vascular territories. *J Cereb Blood Flow Metab* **8**:186-192

Pulsinelli WA, Brierley JB (1979) A new model of bilateral hemispheric ischemia in the unanesthetized rat. *Stroke* **10**:267-272

Pulsinelli WA, Waldman S, Rawlinson D, Plum F (1982a) Moderate hyperglycemia augments ischemic damage: A neuropathological study in the rat. *Neurology* **32**:1239-1246

Pulsinelli WA, Levy DE, Duffy TE (1982b) Regional cerebral blood flow and flucose metabolism following transient forebrain ischemia. *Ann Neurol* **11**:499-509

Pulsinelli WA, Brierley JB, Plum F (1982c) Temporal profile of neuronal damage in a model of transient forebrain ischemia. *Ann Neurol* **11**:491-498

Pulsinelli WA, Lefy DE, Sigsbee B, Scherer P, Plum F (1983) Increased damage after stroke in patients with hyperglycemia with or without established diabetes mellitus. *Am J Med* **74**:540-544

Raju B, Murphy E, Levy LA, Hall RD, London RE (1989) *Am J Physiol C* **256**:540-548

Rehncrona S, Rosén I, Seisjö BK (1979) Recovery of brain mitochondrial function in the rat after complete and incomplete cerebral ischemia. *Stroke* **10**:437-446

Reuben J, Shporer M, Gabbay EJ (1975) The alkali ion-CNA interaction as reflected in the nuclear relaxation rates of ^{23}Na and ^{87}Rb. *Proc Natl Acad Sci USA* **72**:245-247

Roberts, Jr. EL, Sick TJ (1987) Recovery of synaptic transmission predicted from extracellular K^+ undershoots following brief anoxia in hippocampal slices. *Brain Res* **402**:178-181

Rooney WD, Springer, Jr. CS (1991a) A comprehensive approach to the analysis and interpretation of the resonances of spins 3/2 from living systems. *NMR Biomed* **4**:209-226

Rooney WD, Springer, Jr. CS (1991b) The molecular environment of intracellular sodium: ^{23}Na NMR relaxation. *NMR Biomed* **4**:227-245

Roucher P, Meric P, Correze JL, Mispelter J, Tiffon B, Lhoste JM, Seylaz J (1991) Metabolic effects of kynurenate during reversible forebrain ischemia studied by in vivo 31P-nuclear magnetic resonance spectroscopy. *Brain Res* **550**:54-60

Roux M, Bloom M (1990) Ca^{+2}, Mg^{+2}, Li^+, Na^+, and K^+ distributions in the headgroup region of binary membranes of phosphatidylcholine and phosphatidylserine as seen by deuterium NMR. *Biochemistry* **29**:7077-7089

Rubin LL, Philpott L, Brooks SF (1993) The cell cycle and cell death. *Curr Biol* **3**:391-394

Rudin M, Sauter A (1989) Dihydropyridine calcium antagonists reduce the consumption of high-energy phosphates in the rat brain. A study using combined ^{31}P/^{1}H magnetic resonance spectroscopy and ^{31}P saturation transfer. *J Pharm Exp Therapeutics* **251**:700-706

Sauter A, Rudin M (1993) Determination of creatine kinase kinetic parameters in rat brain by nmr magnetization transfer: correlation with brain function. *J Biol Chem* **268**:13166-13171

Sadiq F, Holtzclaw L, Chunder K, Muzzafar A, Devaskar S (1990) The ontogeny of the rabbit brain glucose transporter. *Endocrinology* **126**:2417-2424

Schienberg P (1965) Observations on cerebral carbohydrate metabolism in man. *Ann Intern Med* **62**:367-371

Schmidt-Kastner R, Freund TF (1991) Selective vulnerability of the hippocampus in brain ischemia. *Neuroscience* **40**:599-636

Schnall MD, Yoshizaki K, Chance B, Leigh JS, Jr (1988) Triple nuclear NMR studies of cerebral metabolism during generalized seizure. *Magn Reson Med* **6**:15-23

Segebarth CM, Baleriaux DF, Luyten PR, den Hollander JA (1990) *Magn Reson Med* **13**:62

Sharbrough, FW, Messick, JM Jr., Sundt, TM Jr. (1973) Correlation of continuous electroencephalograms with cerebral blood flow measurements during carotid endarterectomy. *Stroke* **4**:674-683

Sherry AD, Malloy CR, Jeffrey FMH, Cacheris WP, Geraldes FGC (1988) $Dy(DOTP)^{-5}$: a new, stable ^{23}Na shift reagent. *J Magn Reson* **76**:528-533

Shigeno T, Yamasaki Y, Kato G, Kusaka K, Mima T, Takakura K, Graham DI, Furukawa S (1990) Reduction of delayed neuronal death by inhibition of protein synthesis. *Neurosci Lett* **120**:117-119

Shigeno T, Mima T, Takakura K, Graham DI, Kato G, Hashimoto Y, Furukawa S (1991) Amelioration of delayed neuronal death in the hippocampus by nerve growth factor. *J Neurosci* **11**:2914-2919

Shinar H, Knubovets T, Eliav U, Navon G (1993) Sodium interaction with ordered structures in mammalian red blood cells detected by Na-23 double quantum NMR. *Biophys J* **64**:1273-1279

Shoubridge EA, Briggs RW, Radda GK (1982) ^{31}P nmr saturation transfer measurments of the steady state rates of creatine kinase and ATP synthetase in the rat brain. *FEBS Letters* **140**:288-292

Shozuhara H, Onodera H, Katoh-Semba R, Kato K, Yamasaki Y, Kogure K (1992) Temporal profiles of nerve growth factor b-subunit level in rat brain regions agter transient ischemia. *J Neurochem* **59**:175-180

Sick TJ, Rosenthal M, LaManna JC, Lutz PL (1982) Brain potassium ion homeostasis, anoxia, and metabolic inhibition in turtles and rats. *Am J Physiol* **243**:R281-R288

Siegel GJ, Agranoff BW, Albers RW, Molinoff PB (1994) Basic Neurochemistry, 5th ed., Chapter 31, pp 645-680, Raven Press, New York.

Siemkowicz E, Hansen AJ (1978) Clinical restitution following cerebral ischemia in hypo-, normo- and hyperglycemic rats. *Acta Neurol Scand* **58**:1-8

Siemkowicz E (1981a) Hyperglycemia in the reperfusion period hampers recover from cerebral ischemia. *Acta Neurol Scand* **64**:207-216

Siemkowicz E, Hansen AJ (1981b) Brain extracellular ion composition and EEG activity following 10 minutes ischemia in normo- and hyperglycemic rats. *Stroke* **12**:236-372

Siemkowicz E, Hansen AJ, Gjedde A (1982) Hyperglycemic ischemia of rat brain: The effect of post-ischemic insulin on metabolic rate. *Brain Res* **243**:386-390

Siemkowicz E (1985) The effect of glucose upon restitution after transient cerebral ischemia: A summary. *Acta Neurol Scand* **71**:417-427

Siesjö BK (1981) Cell damage in the brain: A speculative synthesis. *J Cereb Blood Flow Metab* **1**:155-185

Siesjö BK (1984) Historical overview: Calcium, ischemia, and death of brain cells. *Ann New York Acad Sciences* **522**:638-661

Siesjö B.K (1988) Acidosis and ischemic brain damage. *Neurochem Pathol* **9**:31-88

Siesjö BK, Agardh CD, Bengtsson F (1989) Free radicals and brain damage. *Cerebrovasc Brain Metab Rev* **1**:165-211

Siesjö BK (1992a) Pathophysiology and treatment of focal cerebral ischemia. Part II: Mechanisms of damage and treatment. *J Neurosurg* 77:337-354

Siesjö BK, Katsura K, Ekholm A (1992b)Tissue PCO_2 in brain ischemia related to lactate content in normo- and hypercapnic rats. *J Cereb Blood Flow Metab* **12**:270-280

Silver IA, Erecinska M (1992) Ion homeostasis in rat brain in vivo: intra- and extracellular [Ca^{+2}] and [H^{+}] in the hippocampus during recovery from short-term, transient ischemia. *J Cereb Blood Flow Metab* **12**:759-772

Sims NR, Pulsinelli WA (1987) Altered mitochondrial respiration in selecetively vulnerable brain subregions following transient forebrain ischemia in the rat. *J Neurochem* **49**:1367-1374

Smith M-L, Auer RN, Siesjö BK (1984) The density and distribution of ischemic brain injury in the rat following 2-10 min of forebrain ischemia. *Acta Neuropathol (Berl)* **64**:319-332

Smith M-L, von Hanwehr R, Seisjö BK (1986) Changes in extra- and intracellular pH in the brain during and following ischemia in hyperglycemic and in moderately hypoglycemic rats. *J Cereb Blood Flow Metab* **6**:574-583

Smith M-L, Kalimo H, Warner DS, Seisjö BK (1987) Glucose pretreatment preceding forebrain ischemia causes Substantia Nigra damage. *J Cereb Blood Flow Metab [Suppl. 1]* 7:S76

Sokoloff, L (1960) The metabolism of the central nervous system *in vivo*. In: Field, J, Magoun, HW, Hall, VE (eds.), Handbook of Physiology-Neurophysiology, v. 3, American Physiological Society, Washington, D.C., pp 1843-64

Spencer RGS, Horská A, Ferretti JA, Weiss GH (1993) Spillover and incomplete saturation in kinetic measurements. *J Magn Reson Ser B* **101**:294-296

Springer, Jr. CS (1987) Measurement of metal cation compartmentalization in tissue by high-resolution metal cation NMR. *Ann Rev Biophys Chem* **16**:375-389

Stevens A, Paschalis P, Schleich T (1992) Sodium-23 and potassium-39 nuclear magnetic resonance relaxation in eye lens. Examples of quadrupole ion magnetic relaxation in a crowded environment. *Biophys J* **61**:1061-1075

Stout RW (1989) Hyperglaecemia and stroke. *Quart J Med* **73**:997-1004

Strong AJ, Fairfield JE, Monteiro E, Kirby M, Hogg AR, Snape M, Ross-Field L (1990) Insulin protects cognitive function in experimental stroke. *J Neurol Neurosurg Psychiatry* **53**:847-853

Stys PK, Waxman SG, Ransome BR (1992) Ionic mechanisms of anoxic injury in mammalian CNS white matter: role of Na^+ channels and Na^+-Ca^{+2} exchanger. *J Neurosci* **12**:430-439

Sutherland GR, Peeling J, Lesiuk HJ, Brownstone RM, Rydzy M, Saunders JK, Geiger JD (1991) The effects of caffeine on ischemic neuronal injury as determined by magnetic resonance imaging and histopathology. *Neuroscience* **42**:171-182

Sutherland GR, Lesiuk H, Hazendonk P, Peeling J, Kozlowski P, Jazinski A, Saunders JK (1992a) Magnetic resonance imaging and ^{31}P spectroscopy study of the effect of temperature on ischemic brain injury. *Can J Neurol Sci* **19**:317-325

Sutherland GR, Peeling J, Sutherland E, Tyson R, Dai F, Kozlowski P, Saunders JK (1992b) Forebrain ischemia in diabetic and nondiabetic BB rats studied with ^{31}P magnetic resonance spectroscopy. *Diabetes* **41**:1328-1334

Tamura, A, Graham, DI, McCulloch, J (1981) Focal cerebral ischaemia in the rat: 2. Regional cerebral blood flow determined by 14C-iodoantipyrine autoradiography following middle cerebral artery occlusion. *J Cereb Blood Flow Metab* **1**:61-69

Thorens, B, Charron, MJ, Lodish, HF (1990) Molecular physiology of glucose transporters. *Diabetes Care* **13**:209

Triolo AJ, Osterholm JL, Alexander GM, Bell RD, Frazer GD (1990) Local cerebral glucose metabolism after global ischemia: treatment by ventriculocisternal perfusion with a fluorocarbon emulsion. *Neurosurgery* **26**:480-487

Tyson R, Peeling J, Sutherland G (1993) Metabolic changes associated with altering blood glycose levels in short duration forebrain ischemia. *Brain Res* **608**:288-298

Urenjak J, Williams SR, Gadian DG, Noble M (1993) Proton nuclear magnetic resonance spectroscopy unambiguously identifies different neural cell types. *J Neurosci* **13**:981-9

Vazquez-Cruz J, Marti-Vilalta JL, Ferrer I, Perez-Gallofre A, Folch J (1990) Progressing cerebral infarction in relation to plasma glucose in gerbils. *Stroke* **21**:1621-1624

Venables GS, Miller SA, Gibson G, Hardy JA, Strong AJ (1985) The effects of hyperglycaemia on changes during reperfusion following focal cerebral ischaemia in the cat. *J Neurol Neurosurg Psychiatry* **48**:663-669

Vink R (1991) *Magnes Trace Elem* **10**:1-10

Voet D, Voet JG (1990) Biochemistry, John Wiley & Sons, New York.

Vogelstein B, Kinzler KW (1992) p53 function and dysfunction. *Cell* **70**:523-526

Voll CL, Auer RN (1988) The effect of postischemic blood glucose levels on ischemic brain damage in the rat. *Ann Neurol* **24**:638-646

Voll CL, Whishaw IQ, Auer RN (1989) Postischemic insulin reduced spatial learning deficit following transient forebrain ischemia in rats. *Stroke* **20**:646-651

Voll CL, Auer RN (1991a) Insulin attenuates ischemic brain damage independent of its hypoglycemic effect. *J Cereb Blood Flow Metab* **11**:1006-1014

Voll CL, Auer RN (1991b) Postischemic seizures and necrotizing ischemic brain damage: Neuroprotective effects of postischemic diazepam and insulin. *Neurology* **41**:423-428

Wagner KR, Kleinholz M, de Courten-Meyers GM, Meyers RE (1992) Hyperglycemic versus normoglycemic stroke: topography of brain metabolites, intracellular pH, and infarct size. *J Cereb Blood Flow Metab* **12**:213-222

Wallimann T, Hemmer W (1994) Creatine kinase in non-muscle tissues and cells. *Mol Cell Biochem* **133**:193-220

Watson BD, Prado R, Dietrich WD, Busto R, Scheinberg P, Ginsberg MD (1985) Induction of reproducible brain infarction by photochemically initiated thrombosis. *Ann Neurol* **17**:497-504

Weinachter SN, Blavet N, O'Donnell RA, MacKenzie ET, Rapin JR (1990) Models of hypoxia and cerebral ischemia. *Pharmacopsychiatry* **23** Suppl 2:94-97

Welsh FA, Ginsberg MD, Rieder W, Budd WW (1980) Deleterious effect of glucose pretreatment on recovery from diffuse cerebral ischemia in the cat. *Stroke* **11**:355-363

Werner DW, Raizada MK, Mudd LM, Foyt HL, Simpson IA, Roberts Jr CT, LeRoith D (1989) Regulation of rat brain/Hep G2 glucose transporter gene expression by insulin and insulin-like growth factor-I in primary cultures of neuronal and glial cells. *Endocrinology* **125**:314-320

Widmer H, Abiko H, Faden AI, James TL, Weinstein PR (1992) Effects of hyperglycemia on the time course changes in energy metabolism and pH during global ischemia and reperfusion in rats: correlation of ^{1}H and ^{31}P NMR spectroscopy with fatty acid and excitatory amino acid levels. *J Cereb Blood Flow Metab* **12**:456-468

Williams GD, Palmer C, Roberts RL, Heitjan DF, Smith MB (1992) ^{31}P NMR spectroscopy of perinatal

hypoxic-ischemic brain damage: a model to evaluate neuroprotective drugs in immature rats. *NMR in Biomed* **5**:145-53

Williams GD, Mosher TJ, Smith MB (1993) Simultaneous determination of intracellular magnesium and pH from the three ^{31}P NMR chemical shifts of ATP. *Anal Biochem* **214**:458-467

Williams GD, Towfighi J, Smith MB (1994) Cerebral energy metabolism during hypoxia-ischemia correlates with brain damage: a ^{31}P NMR study in unanesthetized immature rats. *Neurosci Lett* **170**:31-34

Williams GD, Smith MB (1995) Application of the accurate assessment of intracellular magnesium and pH from the 31P shifts of ATP to cerebral hypoxia-ischemia in neonatal rat. *Magn Reson Med* **33**:853-857

Wimperis S, Wood B (1991) Triple-quantum sodium imaging. *J Magn Reson* **95**:428-436

Woo J, Lam CWK, Kay R, Wong AHY, Teoh R, Nicholls MG (1990) The influence of hyperglycemia and diabetes mellitus on immediate and 3-month morbidity and mortality after acute stroke. *Arch Neurol* **47**:1174-1177

Wozniak M, Rydzewski B, Baker SP, Raizada MK (1993) The cellular and physiological actions of insulin in the central nervous system. *Neurochem Int* **22**:1-10

Xie Y, Mies G, Hossmann KA (1989) Ischemic threshold of brain protein synthesis after unilatoral carotid artery occlusion in gerbils. *Stroke* **20**:620-626

Yamamoto K, Hayakawa T, Mogami H, Akai F, Yanagihara T (1990) Ultrastructural investigation of the CA1 region of the hippocampus after transient cerebral ischemia in gerbils. *Acta Neuropathol (Berlin)* **80**:487-492

Yamasaki Y, Matsuura N, Shozuhara H, Onodera H, Itoyama Y, Kogure K (1995) Interleukin-1 as a pathogenetic mediator of ischemic brain damage in rats. *Stroke* **26**:676-680

Yip PK, He YY, Hsu CY, Garg N, Marangos P, Hogan EL (1991) Effect of plasma glucose on infarct size in focal cerebral ischemia-reperfusion. *Neurology* **41**:899-905

Yorek MA, Stefani MR, Moore SA (1991) Acute and chronic exposure of mouse cerebral microvessel endothelial cells to increased concentration of glucose and galactose: effect on *myo*-inositol metabolism, PGE_2 synthesis, and Na^+/K^+-ATPase transport activity. *Metabolism* **40**:347-358

Yoshida S, Busto R, Martinez E, Scheinberg P, Ginsberg MD (1985) Regional brain energy metabolism after complete versus incomplete ischemia in the rat in the absence of severe lactic acidosis. *J Cereb Blood Flow Metab* **5**:490-501